

## ON THE INTERACTION BETWEEN EQUILIBRATION PROCESSES AND WET OR DRY DEPOSITION

SPYROS N. PANDIS and JOHN H. SEINFELD

Department of Chemical Engineering and Environmental Quality Laboratory, California Institute of Technology, Pasadena, CA 91125, U.S.A.

(First received 12 December 1989 and in final form 6 March 1990)

**Abstract**—Atmospheric equilibration processes between two phases with different deposition velocities have the potential to affect significantly the amount of total material deposited on the ground. The magnitude of the effects of the equilibration processes depends primarily on the ratio of the deposition velocities of the two phases, on the production/emission rate of the gas phase species, and on the initial distribution of species between the two phases. The deposition of a condensible species equilibrating between gas and aerosol phases can increase by as much as 20 times over that when equilibration processes are not present under appropriate conditions (very large aerosol particles, most of the material initially in the gas phase and high gas-phase production rate) or to decrease by as much as 15 times (very small aerosol particles, most of the material initially in the gas phase and high gas-phase production rate). In fog episodes, the deposition of a gaseous species with a Henry's Law constant between  $10^3$  and  $10^6$  M atm<sup>-1</sup> (e.g. SO<sub>2</sub> for pH between 4.5 and 7, H<sub>2</sub>O<sub>2</sub>, HCHO etc) can be enhanced by as much as a factor of 3 because of its transfer to the aqueous phase. For the NH<sub>3</sub>-HNO<sub>3</sub>-NH<sub>4</sub>NO<sub>3</sub> system the total deposition can be reduced by as much as a factor of 3 for typical conditions in a polluted atmosphere and small initial concentration of aerosol NH<sub>4</sub>NO<sub>3</sub> with NH<sub>3</sub> initially dominating HNO<sub>3</sub> in the gas phase. If an operator splitting scheme is used in a mathematical model both equilibration and removal processes should be included in the same operator or very small operator time steps (typically less than 1 min) will be necessary.

**Key word index:** Equilibration processes, phase partitioning, dry deposition, wet deposition, deposition velocity, acid deposition, numerical modeling.

### INTRODUCTION

Processes such as condensation of vapor on aerosol particles, dissolution of material in aqueous droplets, and evaporation of species from aerosol particles or droplets move in the direction of establishing and maintaining thermodynamic equilibrium between the gas and aerosol or gas and aqueous phases in the atmosphere. These equilibration processes change the species' distribution among the various phases present and transfer material between phases that often have very different deposition characteristics. It is reasonable to expect therefore that the equilibration processes may affect significantly the amounts of material deposited on the ground, either enhancing or suppressing the removal processes over those from gas-phase processes alone. The goal of this study is to investigate the effects of the equilibration processes on wet and dry deposition and furthermore to examine the accuracy of the currently used modelling approaches of these phenomena.

The importance of equilibration processes in interpreting vertical concentration profiles and turbulent fluxes of HNO<sub>3</sub>, NH<sub>3</sub> and NH<sub>4</sub>NO<sub>3</sub> near the surface of the Earth has been discussed by Brost *et al.* (1988). Bidleman (1988) suggested that the wet and dry deposition of organic compounds are controlled by their vapor-particle partitioning but his analysis was limited by experimental uncertainties and the lack of data

concerning semivolatile organic compounds. Stafford (1988) has recently criticized the independent modeling of gas and aerosol deposition, neglecting gas-aerosol transfer. He suggested that coupled, reversible reactions are the more realistic representation of deposition.

In the present work, three cases will be examined to obtain useful insight into the relationship between equilibration processes and deposition. The first case concerns a gas phase species A(g) that can be reversibly transferred to the aerosol phase as B(s) (Fig. 1a). In the second case the gas-phase species (e.g. HCHO, H<sub>2</sub>O<sub>2</sub>, O<sub>3</sub>) in the presence of droplets of liquid water content C is transferred reversibly to the aqueous-phase as B(aq) (Fig. 1b). Finally, in the third case two gases A(g) and B(g) react to give a volatile aerosol AB(s), and in general all three species have different deposition velocities. This case is typified by the system of NH<sub>3</sub>(g), HNO<sub>3</sub>(g), and NH<sub>4</sub>NO<sub>3</sub>(s).

We begin with the formulation of the governing differential equations that will be used to describe the system dynamics for the three representative cases. To reduce the large number of parameters involved in these equations and obtain valuable physical insight, the solutions of the systems of dimensionless differential equations will be presented in dimensionless form. Next, the effects of the equilibration processes on dry or wet deposition will be studied for various typical mass transfer rates, vapor, aqueous, and aero-

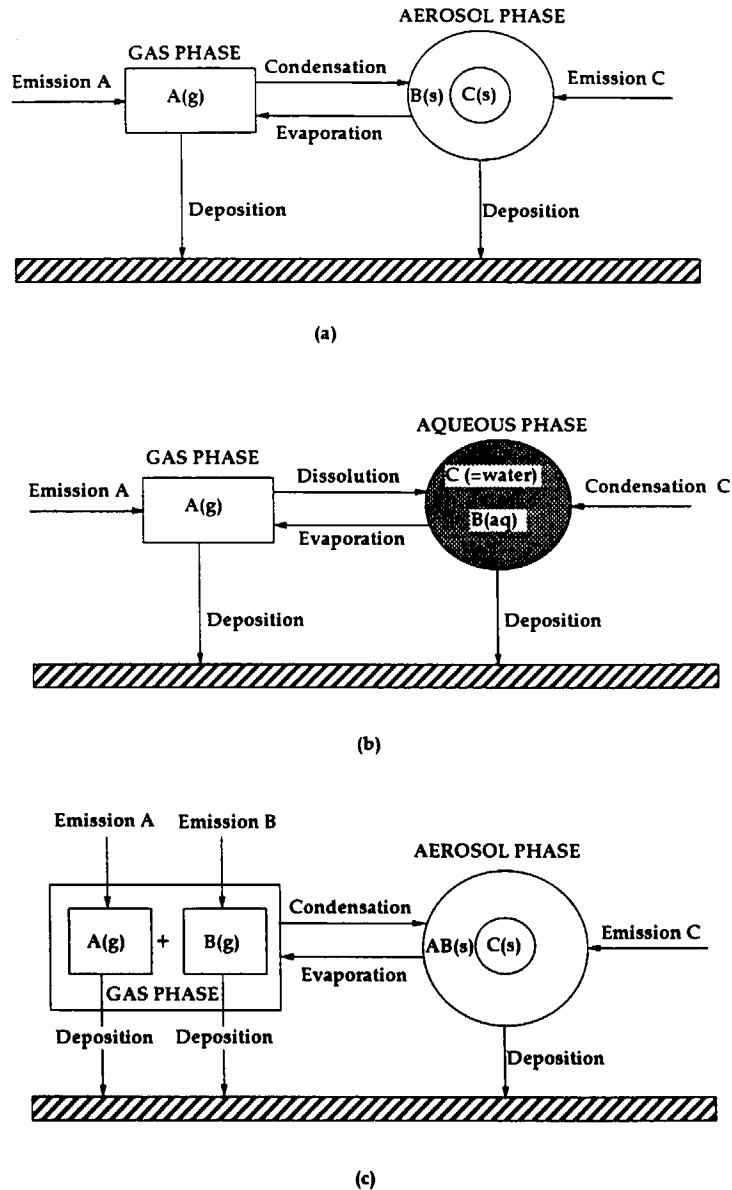


Fig. 1. Schematic representation of the multiphase systems studied. (a) Case 1:  $A(g) \rightleftharpoons B(s)$ . (b) Case 2:  $A(g) \rightleftharpoons B(aq)$ . (c) Case 3:  $A(g) + B(g) \rightleftharpoons AB(s)$ .

sol deposition velocities, emission and production rates, and initial gas and aerosol phase concentrations. Finally the accuracy of the currently employed modeling approaches will be discussed and suggestions for improvement will be presented.

**PROBLEM DESCRIPTION AND NUMERICAL MODEL FORMULATION**

We will consider interphase mass transfer processes taking place inside a homogeneous air parcel, the height of which coincides with the mixing height of the atmosphere and is assumed to remain constant. The

vapor phase is assumed to be initially in thermodynamic equilibrium with the aerosol or aqueous phase and at  $t=0$  the ground surface is added and the deposition starts. Due to the different rates of removal of the present phases and the emission or production of the vapor species the system deviates from thermodynamic equilibrium and mass is transferred from the one phase to the other in an attempt to reestablish equilibrium. This transfer of material from a slowly depositing phase to a rapidly depositing one or *vice versa* can enhance or suppress the removal processes under favorable conditions. Processes described in the models include the reversible mass transfer between

the phases present, the emission or production of the gas-phase species and the deposition of all species.

Case 1:  $A(g) \rightleftharpoons B(s)$

In Case 1 a condensable vapor species A(g) is reversibly transferred (condensation/evaporation) to the aerosol phase as B(s). We assume that the aerosol phase also contains non-volatile species C(s). The vapor species and the aerosol particles are deposited on the ground with different deposition velocities (Fig. 1a).

Let  $M_A$ ,  $M_B$ ,  $M_C$  be the mass concentrations of species A in the gas phase and of species B(s) and C(s) in the aerosol phase, respectively. Let  $S_A(t)$  and  $S_B(t)$  be the amounts of A(g) and B(s) that have been deposited on the ground up to the time  $t$ . For simplicity it is assumed that the aerosol particles are monodisperse (diameter  $d_p$ ),  $M_C \gg M_B$  at all times and that there is a source of C(s) particles balancing their deposition so that  $M_C$  and the number of particles can be considered constant with time. As a result of these assumptions the particle diameter is not influenced by the condensation/evaporation of A(g) and is assumed to be constant with time.

Within the air parcel  $M_A$ ,  $M_B$ ,  $S_A$  and  $S_B$  are governed by the following four ordinary differential equations (the aerosol mass concentration remains constant at  $M_C^0$ ):

$$\frac{dM_A}{dt} = -k_m M_C^0 (M_A - M_{eq}) - k_{da} M_A + E_A \quad (1)$$

$$\frac{dM_B}{dt} = k_m M_C^0 (M_A - M_{eq}) - k_{dc} M_B \quad (2)$$

$$\frac{dS_A}{dt} = k_{da} M_A \quad (3)$$

$$\frac{dS_B}{dt} = k_{dc} M_B \quad (4)$$

where  $k_m = 12D_A/(\rho_p d_p^2)$  is the constant for the mass transfer of A between the gas and aerosol phases for the continuum regime (the particle diameter is assumed to be large compared to the mean free path of the diffusing molecules), assuming unity accommodation coefficient (Seinfeld, 1986) and where  $D_A$  is the diffusion coefficient of A in the gas phase,  $\rho_p$  is the density of the aerosol particles,  $M_{eq}$  is the mass concentration of A(g) at equilibrium,  $k_{da}$ ,  $k_{dc}$  are the deposition rate constants for A(g) and the aerosol particles defined as the ratio of their deposition velocities to the mixing height  $H$ , and  $E_A$  is the emission or gas-phase production rate of the gas species A.

The following initial conditions are used:

$$M_A(0) = M_{eq} = M_A^0, \quad M_B(0) = M_B^0, \quad S_A(0) = 0, \quad S_B(0) = 0. \quad (5)$$

Non-dimensionalizing the above differential equations one gets

$$\frac{dm_A}{d\tau} = -\alpha(m_A - 1) - m_A + \delta \quad (6)$$

$$\frac{dm_B}{d\tau} = \alpha\beta(m_A - 1) - \gamma m_B \quad (7)$$

$$\frac{ds_A}{d\tau} = m_A \quad (8)$$

$$\frac{ds_B}{d\tau} = \gamma m_B \quad (9)$$

with initial conditions,  $m_A(0) = 1$ ,  $m_B(0) = 1$ ,  $s_A(0) = 0$ , and  $s_B(0) = 0$  where the dimensionless dependent variables are defined as,

$$m_A = \frac{M_A}{M_A^0}, \quad m_B = \frac{M_B}{M_B^0}, \quad s_A = \frac{S_A}{M_A^0}, \quad s_B = \frac{S_B}{M_B^0} \quad (10)$$

and the dimensionless parameters are,

$$\tau = tk_{da}, \quad \alpha = \frac{k_m M_C^0}{k_{da}}, \quad \beta = \frac{M_A^0}{M_B^0}, \quad \gamma = \frac{k_{dc}}{k_{da}}, \quad \delta = \frac{E_A}{k_{da} M_A^0}. \quad (11)$$

The dimensionless time has been defined relative to the characteristic time for vapor deposition,  $\alpha$  is the ratio of the evaporation rate to the vapor deposition rate,  $\beta$  is the ratio of the initial gas-phase concentration of A(g) to the corresponding concentration of B(s),  $\gamma$  is the ratio of the aerosol deposition velocity to the vapor deposition velocity, and  $\delta$  is the ratio of the emission rate of A to the initial vapor deposition rate.

Case 2:  $A(g) \rightleftharpoons B(aq)$

In Case 2 a vapor species A(g) is reversibly transferred to the aqueous phase consisting of droplets of liquid water C. The liquid water of the fog,  $M_C$  ( $\ell$  water/ $\ell$  air), is assumed to remain constant with time, applicable during the rapid growth period of the fog (Pandis and Seinfeld, 1989b). The fog is assumed to consist of monodisperse droplets of constant diameter  $d_p$  and to be spatially homogeneous. Let  $H$  be the constant height of the fog. The vapor species and the aqueous droplets are both deposited with different deposition velocities (Fig. 1b).

The main difference between Cases 1 and 2 is that in Case 2 the flux of A from the aqueous to the gas phase depends on its aqueous phase concentration, whereas in Case 1 the flux of A from the dry aerosol phase to the gas phase is independent of the quantity of A that exists in the aerosol particles as B(s). Let  $M_A$  now be the mass concentration of species A in the gas phase, and  $M_B$  its mass concentration in the aqueous phase. The equations that describe the evolution of the mass concentrations of A and B are (Pandis and Seinfeld, 1989a):

$$\frac{dM_A}{dt} = -k_m(M_C^0 M_A - K_H M_B) - k_{da} M_A + E_A \quad (12)$$

$$\frac{dM_B}{dt} = k_m(M_C^0 M_A - K_H M_B) - k_{dc} M_B \quad (13)$$

where  $k_m$  is the combined rate coefficient for gas-phase plus interfacial mass transport,  $K_H$  a numerical constant (no units) defined by  $K_H = 1/K_{Ha}RT$  with  $K_{Ha}$  the

effective Henry's Law constant of species A,  $R$  the ideal gas constant, and  $T$  the temperature (Pandis and Seinfeld, 1989a). The remainder of the symbols are the same as in Case 1. The deposited amounts  $S_A$  and  $S_B$  are described once more by Equations (3) and (4). Initially, as in Case 1, equilibrium is assumed between the two phases and from Henry's Law,  $M_A^0 = K_H M_B^0 / M_C^0$ .

To simplify the present problem we assume that the effective Henry's Law constant of the species remains constant with time. This is exactly true for species that do not dissociate upon dissolution (e.g.  $O_3$ ,  $NO_2$ ,  $HCHO$ ) and a very good assumption for species that weakly dissociate for the pH range of interest (1–8) like  $H_2O_2$ . To use the above assumption for species like  $SO_2$  with a strongly pH dependent solubility we have to assume that the pH of the aqueous droplets remains constant. By non-dimensionalizing Equations (12) and (13) one obtains, together with the Equations (8) and (9) that describe the dimensionless deposited amounts:

$$\frac{dm_A}{d\tau} = -\alpha(m_A - m_B) - m_A + \delta \quad (14)$$

$$\frac{dm_B}{d\tau} = \alpha \beta(m_A - m_B) - \gamma m_B \quad (15)$$

with the same initial conditions as in Case 1 and dimensionless dependent variables defined by Equation (10). The dimensionless parameters are the same as in Case 1 (Equation 11) except  $\beta$  that is defined as  $\beta = M_A^0 / M_B^0 = K_H / M_C^0$ . The parameter  $\beta$  physically represents the distribution ratio of A between the gas and aqueous phases at equilibrium.

Case 3:  $A(g) + B(g) \rightleftharpoons AB(s)$

In Case 3 two gas-phase species react to produce volatile aerosol  $AB(s)$  and all three species are deposited on the ground. The aerosol particles are assumed to consist of  $AB(s)$  with mass concentration  $M_{AB}$  and nonvolatile material that is not influenced by the above equilibration process and has mass concentration  $M_{nv}$ . Hence, the total aerosol concentration is  $M_{AB} + M_{nv}$  (Fig. 1c). Assuming that the reaction of A and B takes place on the surface of the aerosol particles and is mass transfer limited the differential equations of the model are

$$\frac{dM_A}{dt} = -k_m(M_{AB} + M_{nv})(M_A - M_{As}) - k_{da}M_A + E_A \quad (16)$$

$$\frac{dM_B}{dt} = -k_m(M_{AB} + M_{nv})(M_B - M_{Bs}) - k_{db}M_B + E_B \quad (17)$$

$$\frac{dM_{AB}}{dt} = k_m(M_{AB} + M_{nv})(M_A + M_B - M_{As} - M_{Bs}) - k_{ds}M_{AB} \quad (18)$$

$$\frac{dS_A}{dt} = k_{da}M_A \quad (19)$$

$$\frac{dS_B}{dt} = k_{db}M_B \quad (20)$$

$$\frac{dS_{AB}}{dt} = k_{ds}M_{AB} \quad (21)$$

Once more equilibrium is assumed initially between the gas species A and B and  $AB$  in the aerosol phase. At  $t=0$  the surface is introduced,

$$M_A(0) = M_A^0, M_B(0) = M_B^0 = M_{eq}^0 / M_A^0, M_{AB}(0) = M_{AB}^0 \quad (22)$$

$$S_A(0) = S_B(0) = S_{AB}(0) = 0. \quad (23)$$

The mass concentrations of  $A(g)$  and  $B(g)$  on the aerosol surface are calculated using the equality of the molar fluxes of A and B to the aerosol surface and the equilibrium condition  $M_{As}M_{Bs} = M_{eq}$ . Their values are

$$M_{As} = \frac{M_{eq}}{M_{Bs}}, M_{Bs} = 0.5 [M_B - \mu M_A + ((M_B - \mu M_A)^2 + 4\mu M_{eq})^{0.5}] \quad (24)$$

with  $\mu = \mu_B / \mu_A$  the ratio of the molecular weights of the two gases.

Non-dimensionalizing Equations (16)–(21) one gets

$$\frac{dm_A}{d\tau} = -\sigma_1(m_A - m_{As})(1 + \sigma_2 m_{AB}) - m_A + \sigma_5 \quad (25)$$

$$\frac{dm_B}{d\tau} = -\sigma_1 \left( m_B - \frac{m_B}{\sigma_7} \right) (1 + \sigma_2 m_{AB}) - \sigma_3 m_B + \frac{\sigma_5 \sigma_6}{\sigma_7} \quad (26)$$

$$\frac{dm_{AB}}{d\tau} = \sigma_1 \sigma_8 (1 + \sigma_2 m_{AB})(m_A + \sigma_7 m_B - m_{As} - m_{Bs}) - \sigma_4 m_{AB} \quad (27)$$

$$\frac{ds_A}{d\tau} = m_A \quad (28)$$

$$\frac{ds_B}{d\tau} = \sigma_3 m_B \quad (29)$$

$$\frac{ds_{AB}}{d\tau} = \sigma_4 m_{AB} \quad (30)$$

with initial conditions

$$m_A(0) = 1, m_B(0) = 1, m_{AB}(0) = 1, s_A(0) = 0, s_B(0) = 0, s_{AB}(0) = 0 \quad (31)$$

where the dimensionless dependent variables are defined as

$$m_A = \frac{M_A}{M_A^0}, m_B = \frac{M_B}{M_B^0}, m_{AB} = \frac{M_{AB}}{M_{AB}^0}, s_A = \frac{S_A}{M_A^0}, s_B = \frac{S_B}{M_B^0}, s_{AB} = \frac{S_{AB}}{M_{AB}^0} \quad (32)$$

and the dimensionless parameters are

$$\begin{aligned} \tau &= tk_{da}, \quad \sigma_1 = \frac{k_m M_{nv}}{k_{da}}, \quad \sigma_2 = \frac{M_{AB}^0}{M_{nv}}, \quad \sigma_3 = \frac{k_{db}}{k_{da}}, \\ \sigma_4 &= \frac{k_{ds}}{k_{da}}, \quad \sigma_5 = \frac{E_A}{k_{da} M_A^0}, \quad \sigma_6 = \frac{E_B}{E_A}, \\ \sigma_7 &= \frac{M_{eq}}{M_A^0} = \frac{M_B^0}{M_A^0}, \quad \sigma_8 = \frac{M_A^0}{M_{AB}^0}. \end{aligned} \quad (33)$$

The dimensionless time has been once more defined relative to the characteristic time for vapor deposition,  $\sigma_1$  is the ratio of the mass transfer rate to the gas-phase deposition rate,  $\sigma_2$  is the ratio of the initial aerosol concentration of AB to the corresponding concentration of the rest of the aerosol species,  $\sigma_3$  is the ratio of the deposition velocities of the two gas-phase species,  $\sigma_4$  is the ratio of the aerosol deposition velocity to the deposition velocity of A(g),  $\sigma_5$  is the ratio of the emission (or gas-phase chemical reactions) of A to its initial deposition rate,  $\sigma_6$  is the ratio of the emission rates of A and B,  $\sigma_7$  is the ratio of the initial gas phase concentrations of A and B, and finally  $\sigma_8$  is the ratio of the initial concentrations of gas species A and aerosol of AB.

#### SOLUTION OF THE MODEL EQUATIONS

##### Case 1

The solutions of Equations (6)–(9) with the corresponding initial conditions are

$$m_A = m_A^s + (1 - m_A^s) e^{-(1+\alpha)\tau} \quad (34)$$

$$m_B = m_B^s + \frac{\alpha\beta(1-\delta)}{(1+\alpha)(\gamma-1-\alpha)} e^{-(1+\alpha)\tau} + P e^{-\gamma\tau} \quad (35)$$

$$s_A = m_A^s \tau + \frac{1-\delta}{(1+\alpha)^2} (1 - e^{-(1+\alpha)\tau}) \quad (36)$$

$$\begin{aligned} s_B &= \gamma m_B^s \tau + \frac{\alpha\beta\gamma(1-\delta)}{(\gamma-1-\alpha)(1+\alpha)^2} (1 - e^{-(1+\alpha)\tau}) \\ &+ P(1 - e^{-\gamma\tau}) \end{aligned} \quad (37)$$

where

$$P = 1 + \frac{\alpha\beta(\delta-1)}{1+\alpha} \left[ \frac{1}{\gamma-1-\alpha} - \frac{1}{\gamma} \right] \quad (38)$$

and

$$m_A^s = \frac{\alpha + \delta}{1 + \alpha}, \quad m_B^s = \frac{\alpha\beta(\delta-1)}{\gamma(1+\alpha)}. \quad (39)$$

In the above formulas  $m_A^s$  and  $m_B^s$  are the steady-state values of  $m_A$  and  $m_B$  in Equations (6) and (7). These steady-states are nonnegative and therefore physically significant only if  $\delta \geq 1$ . Note that for  $\alpha=0$  the above equations give us the solution of the deposition problem if one neglects the equilibration processes between the two phases. Such quantities are

noted using a (\*):

$$\begin{aligned} m_A^* &= \delta + (1-\delta)e^{-\tau} & m_B^* &= e^{-\gamma\tau} \\ s_A^* &= \delta\tau + (1-\delta)(1-e^{-\tau}) & s_B^* &= 1 - e^{-\gamma\tau}. \end{aligned} \quad (40)$$

##### Case 2

The solutions of Equations (14), (15), (8) and (9) with the corresponding initial conditions are

$$m_A = Q e^{\lambda_1 \tau} + W e^{\lambda_2 \tau} + m_A^s \quad (41)$$

$$m_B = Q \frac{1+\alpha+\lambda_1}{\alpha} e^{\lambda_1 \tau} + W \frac{1+\alpha+\lambda_2}{\alpha} e^{\lambda_2 \tau} + m_B^s \quad (42)$$

$$s_A = m_A^s \tau - \frac{Q}{\lambda_1} (1 - e^{\lambda_1 \tau}) - \frac{W}{\lambda_2} (1 - e^{\lambda_2 \tau}) \quad (43)$$

$$\begin{aligned} s_B &= \gamma m_B^s \tau - \frac{\gamma Q (1 + \alpha + \lambda_1)}{\alpha \lambda_1} (1 - e^{\lambda_1 \tau}) \\ &- \frac{\gamma W (1 + \alpha + \lambda_2)}{\alpha \lambda_2} (1 - e^{\lambda_2 \tau}) \end{aligned} \quad (44)$$

with  $\lambda_1$  and  $\lambda_2$  the eigenvalues of the system given by

$$\begin{aligned} \lambda_{1,2} &= -\frac{1}{2} \left[ (1 + \alpha + \alpha\beta + \gamma) \pm \left( (1 + \alpha \right. \right. \\ &\left. \left. - \alpha\beta - \gamma)^2 + 4\alpha^2\beta \right)^{\frac{1}{2}} \right] \end{aligned} \quad (45)$$

and with  $m_A^s$  and  $m_B^s$  the steady-state values of  $m_A$  and  $m_B$ ,

$$m_A^s = \frac{\delta(\alpha\beta + \gamma)}{\alpha\beta + \alpha\gamma + \gamma}, \quad m_B^s = \frac{\delta\alpha\beta}{\alpha\beta + \alpha\gamma + \gamma} \quad (46)$$

and

$$Q = \frac{1 + \lambda_2 - m_A^s(1 + \alpha + \lambda_2) + \alpha m_B^s}{\lambda_2 - \lambda_1} \quad (47)$$

$$W = \frac{1 + \lambda_1 - m_A^s(1 + \alpha + \lambda_1) + \alpha m_B^s}{\lambda_2 - \lambda_1}. \quad (48)$$

If one neglects the equilibration processes between the two phases the corresponding variables are given by Equations (40).

##### Case 3

The system of ordinary Equations (25)–(30) with initial conditions given by Equation (31) is solved numerically using a standard Gear routine.

Neglecting the gas-aerosol phase equilibration processes is equivalent to setting  $\sigma_1=0$  in Equations (25)–(30). The corresponding solutions of this simplified system are denoted by using a (\*) and are:

$$m_A^* = \sigma_5 + (1 - \sigma_5) e^{-\tau} \quad m_B^* = \frac{\sigma_5 \sigma_6}{\sigma_3 \sigma_7} + \left( 1 - \frac{\sigma_5 \sigma_6}{\sigma_3 \sigma_7} \right) e^{-\sigma_3 \tau}$$

$$m_{AB}^* = e^{-\sigma_4 \tau} \quad s_A^* = \sigma_5 \tau + (1 - \sigma_5)(1 - e^{-\tau})$$

$$s_B^* = \frac{\sigma_5 \sigma_6}{\sigma_3 \sigma_7} \tau + \left( 1 - \frac{\sigma_5 \sigma_6}{\sigma_3 \sigma_7} \right) (1 - e^{-\sigma_3 \tau})$$

$$s_{AB}^* = 1 - e^{-\sigma_4 \tau}. \quad (49)$$

## THE DEPOSITION RATIO

A simple way of assessing the effects of the equilibration processes on wet or dry deposition is to compare the predictions of the full models described above with those of the corresponding models where the equilibration processes are neglected. To facilitate this comparison we define the deposition ratio at the time  $t$ ,  $DR(t)$ , as the ratio of the total species mass that has been deposited since  $t=0$  in gas, aerosol and aqueous forms, when the equilibration processes are taken into account, to the same quantity when the equilibration processes have been neglected. Values of the deposition ratio close to unity mean that the equilibration processes do not affect significantly the deposition of species. Values of the deposition ratio larger than one correspond to deposition enhancement by the equilibration processes while values smaller than one represent deposition suppression.

Using the above definition for the deposition ratio one obtains for the three cases presented above:

$$DR_1(t) = DR_2(t) = \frac{\beta s_A + s_B}{\beta s_A^* + s_B^*}$$

$$DR_3(t) = \frac{\sigma_8 s_A + \sigma_7 \sigma_8 s_B + s_{AB}}{\sigma_8 s_A^* + \sigma_7 \sigma_8 s_B^* + s_{AB}^*} \quad (50)$$

The deposition ratio is a function of time and due to the initial assumed equilibrium state in all the above three cases,  $DR(0)=1$ . This can be easily shown because the mass transfer terms in all the differential equations vanish at  $t=0$  and the equations for both approaches to the deposition problem are the same. The behavior of  $DR$  as  $t \rightarrow \infty$  depends on whether emissions of material are occurring. If no emissions of material enter the system it is clear that for both approaches all the initially present material will be eventually deposited on the ground and therefore  $DR(\infty)=1$ . The cases with vapor emissions present will be examined independently below.

In order to facilitate comparisons it is useful to define a specific time  $t^*$  at which all the comparisons will be made. In direct analogy to the half life of a species, we define, for Cases 1 and 2,  $t^*$  as the time at which the total deposited mass of A (in both gas and aerosol or gas and aqueous forms) equals half the initially present mass of A. Therefore when there are no emissions of A,  $t^*$  equals the half life of A. For Case 3 at time  $t^*$  the total deposited mass of A, B and AB equals half their initially present mass. Henceforth all the results will refer to the time  $t^*$  unless specifically stated.

## EFFECTS OF EQUILIBRATION PROCESSES ON DRY AND WET DEPOSITION

## Case 1

The model developed for Case 1 is applicable, for example, to secondary organic condensible species. Possible examples include nitro-cresol from the gas-

phase photooxidation of toluene, glutaric and adipic acid from the photooxidation of cyclopentene and cyclohexene. Species C then corresponds to the remainder of the material found in the aerosol phase.

Relatively little is known about the vapor pressures of organic species that are found in secondary organic aerosols. For the purposes of this study the range of  $5 \times 10^{-6}$  to  $5 \times 10^{-5}$  Pa (Stern *et al.*, 1987; Tao and McMurry, 1989) will be investigated. This range corresponds to values of  $M_{eq}$  between 0.3 and  $3 \mu\text{g m}^{-3}$ . The mass of condensible organics has been predicted to vary roughly from zero to  $10 \mu\text{g m}^{-3}$  (Pilinis and Seinfeld, 1988). Average particle mass concentrations range from  $20 \mu\text{g m}^{-3}$  in clean air to values up to  $200 \mu\text{g m}^{-3}$ . A value of  $80 \mu\text{g m}^{-3}$  representative of a polluted urban atmosphere will be used for our calculations. The deposition velocity of aerosol particles depends on particle diameter, wind speed, atmospheric stability, and surface characteristics. It varies roughly from  $0.003 \text{ cm s}^{-1}$  for particles of  $0.5 \mu\text{m}$  diameter to  $10 \text{ cm s}^{-1}$  for the  $10 \mu\text{m}$  particles (McMahon and Denison, 1979; National Center for Atmospheric Research, 1982; Wesely and Shannon, 1984) and for a mixing height varying between 100 and 2000 m the aerosol deposition constant  $k_{dc}$  is in the range between  $10^{-8}$  and  $10^{-3} \text{ s}^{-1}$ . There is little information available on the dry deposition velocities of condensible organic vapors so, based on reported values for species like PAN (McRae and Russel, 1984), we assume a range of  $0.1 - 0.5 \text{ cm s}^{-1}$ , corresponding to a vapor deposition rate constant  $k_{da}$  between  $5 \times 10^{-7}$  and  $5 \times 10^{-5} \text{ s}^{-1}$ . The mass transfer constant  $k_m$  varies from  $10^{-6} \text{ m}^3 \text{ s}^{-1} \mu\text{g}^{-1}$  for  $10 \mu\text{m}$  diameter particles to  $10^{-2} \text{ m}^3 \text{ s}^{-1} \mu\text{g}^{-1}$  for  $0.1 \mu\text{m}$  particles. The source of these condensible organics in the atmosphere is the gas-phase photooxidation of their parent hydrocarbons. The source rate  $E_A$  can be estimated from the average concentrations of the primary organic precursors and the corresponding rate constants to be between  $\leq 0.001 \mu\text{g m}^{-3} \text{ s}^{-1}$ .

Using the above information one can derive the range of the dimensionless variables of our model applicable to condensible organics. They are approximately:

$$2 \leq \alpha \leq 2 \times 10^6, \quad 0.01 \leq \beta, \quad 10^{-3} \leq \gamma \leq 10^3,$$

$$0 \leq \delta \leq 3 \times 10^3.$$

The first case discussed is for rapid mass transfer between the gas and aerosol phases,  $\alpha=1000$ . The deposition ratios are presented in Fig. 2 as a function of  $\beta$  and  $\gamma$ . When no source of the organic species A is present ( $\delta=0$ ), and because the system starts from equilibrium, the gas-phase concentration of A cannot exceed its saturation value. Therefore in this case A does not condense at any time to the aerosol phase and the particles evaporate in an attempt to maintain equilibrium. This non-symmetry in the system is depicted in Fig. 2a and for  $\gamma \geq 1$  (deposition velocity of the particles exceeds the deposition velocity of the

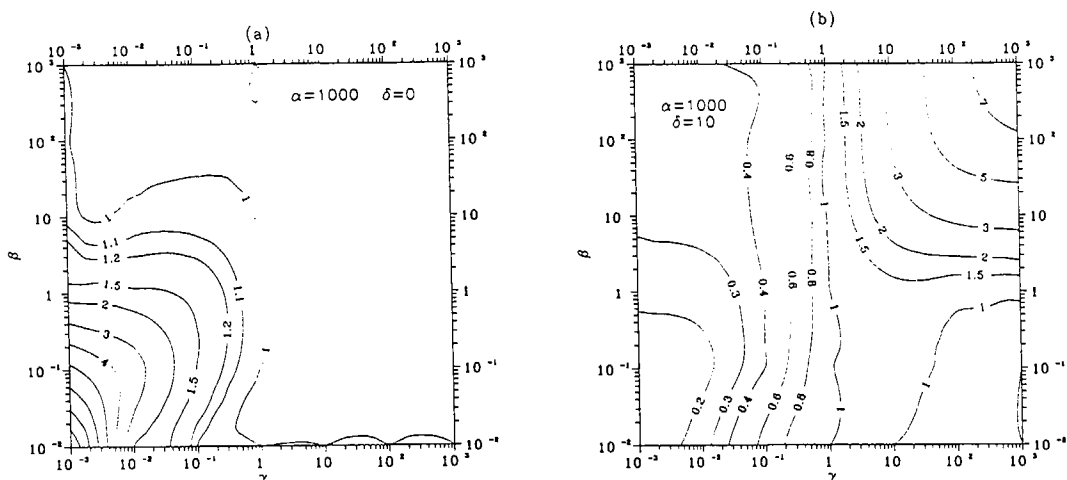


Fig. 2. Deposition ratio  $DR_1(t^*)$  (total deposition with equilibration processes over deposition without) as a function of the initial species distribution  $\beta$  and the ratio of the deposition velocities  $\gamma$  for rapid mass transfer ( $\alpha = 1000$ ) and two production-emission rates of A(g)  $\delta$ . (a)  $\delta = 0$ : No emission; (b)  $\delta = 10$ : strong emission source.

vapor) the equilibration process does not significantly affect the deposition. The material in the aerosol phase is preferentially deposited on the ground and only small quantities are transferred to the gas phase. On the contrary when  $\gamma < 1$  (deposition velocity of particles is less than that of the vapor) the equilibration processes can become very important depending on the relative quantities of the initial concentrations. As the gas-phase material is rapidly deposited, the material in the slowly deposited aerosol phase evaporates in an effort to maintain equilibrium. This transfer of material from the slowly depositing phase to the rapidly depositing phase enhances significantly the total deposition, and the larger the difference in the deposition velocities of the two phases the larger the enhancement. Additionally the significant enhancement is observed only when the initial concentration of the organic in the aerosol phase exceeds its initial gas-phase concentration ( $\beta < 1$ ). If the initial mass of A exceeds significantly the aerosol mass ( $\beta \gg 1$ ) the transfer of relatively small quantities of A from the aerosol to the gas phase and their subsequent rapid deposition does not affect the total amount of A deposited. When  $\beta = 0.01$  and  $\gamma = 0.001$  the equilibration processes result in a ninefold increase of the total deposition.

If the organic condensible species A is produced in the gas phase much slower than it is deposited ( $\delta = 0.1$ ) the behavior of the system is qualitatively the same as in the case of  $\delta = 0$ . The main effect of this small source of A is the reduction of the deposition enhancement observed for  $\gamma < 1$  and  $\beta < 1$ , because of the increase of the mass of A in the gas-phase. Under optimum conditions ( $\beta = 0.01$ ,  $\gamma = 0.001$ ) the enhancement of deposition is fivefold

When the gas-phase production rate of A equals its deposition rate ( $\delta = 1$ ) the gas-phase concentration of

A remains constant and equal to its equilibrium value. Hence, no transfer of mass takes place between the two phases and the equilibration processes do not play any role. In this case,  $DR_1(t) = 1$ , for all  $t$ .

If the gas phase production rate exceeds the deposition rate ( $\delta = 10$ ), the gas phase becomes supersaturated in A and condensation of A to the aerosol phase takes place. If the vapor deposits faster than the aerosol phase ( $\gamma < 0.1$ ) this transfer of A causes significant reduction of the total deposition (Fig. 1b). This reduction is more pronounced for organics with low vapor pressures or high initial aerosol concentration of the organic and it can be as much as eightfold. On the contrary if the aerosol particles deposit faster than the vapor itself, the condensation of vapor results in a significant enhancement of total deposition if the mass of A in the gas phase exceeds the corresponding mass in the aerosol phase ( $\beta > 1$ ).

A further increase of the production rate of A compared to its vapor deposition rate ( $\delta = 100$ ) results in the same qualitative features as the case with  $\delta = 10$ . Quantitatively this increased production rate enhances the significance of the equilibration processes. Under the appropriate conditions the total deposition rate decreases 50 times ( $\beta = 0.1$ ,  $\gamma = 0.001$ ) or increases 48 times ( $\beta = 1000$ ,  $\gamma = 1000$ ).

The effects of the rate constant of mass transfer can be studied by comparing Fig. 2b with Fig. 3. A decrease of the parameter  $\alpha$  (due to low total aerosol loading or larger average particle diameter, etc) by two orders of magnitude does not change the qualitative behavior of the system but decreases the importance of the equilibration processes. For example, for  $\delta = 0$  the maximum deposition enhancement is reduced from 9 ( $\alpha = 1000$ ) to 8.4, for  $\delta = 10$  from 7.7 to 3.2 (Fig. 3) and for  $\delta = 100$  from 48 to 6.

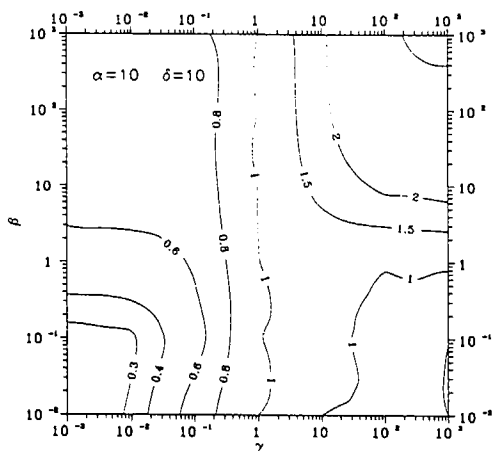


Fig. 3. Deposition ratio  $DR_1(t^*)$  (total deposition with equilibration processes over deposition without) as a function of the initial species distribution  $\beta$  and the ratio of the deposition velocities  $\gamma$  for slow mass transfer ( $\alpha = 10$ ) and strong emission source of A(g) ( $\delta = 10$ ).

#### Case 2

The model developed for Case 2 can be applied to species that do not dissociate upon dissolution in water like  $O_3$ ,  $NO_2$ ,  $NO$ ,  $HCHO$  and  $PAN$  or dissociate weakly in the pH range of interest (from 1 to 8) like  $H_2O_2$ . Several important pollutants like  $SO_2$ ,  $HNO_3$ , etc. dissociate upon dissolution and therefore their solubility depends on the droplets' pH. To apply the same model to these species one must assume that the pH is not affected by the dissolution of species A and neglect aqueous phase reactions.

The liquid water content of a fog has been found to vary between  $0.05$  and  $0.5 \text{ g m}^{-3}$  that corresponds to values of  $M_0^0$  between  $5 \times 10^{-8}$  and  $5 \times 10^{-7}$  ( $\ell$  water/ $\ell$  air) (Seinfeld, 1986). The effective Henry's Law constant  $K_H$  ranges from  $2 \times 10^{-3} \text{ M atm}^{-1}$  for species like  $NO$  (Schwartz and White, 1981) to  $10^{16} \text{ M atm}^{-1}$  for  $HCl$  for  $pH = 7$ . Because of the assumptions outlined above the range of pH around 7 where strong acids like  $HNO_3$  and  $HCl$  have such a large solubility that they cause a dramatic pH decrease will be omitted from this discussion. Therefore this study concentrates on a range of  $K_H$  from  $5 \times 10^{-8}$  to 5 and to a corresponding range of  $\beta$  from  $0.1$  to  $10^8$ .

The typical diameter of a fog droplet varies between  $10$  and  $40 \mu\text{m}$  corresponding to mass transfer constants  $k_m$  between  $10^6 \text{ s}^{-1}$  and  $7 \times 10^4$ . The gas-phase deposition velocity is between  $0.1$  and  $1 \text{ cm s}^{-1}$  and, assuming a fog height of  $100 \text{ m}$ , the gas phase deposition rate constant  $k_{da}$  is between  $10^{-5}$  and  $10^{-4} \text{ s}^{-1}$  and the dimensionless variable  $\alpha$  is  $30 \leq \alpha \leq 5 \times 10^4$ .

Experimental data provided by Dollard and Unsworth (1983) suggest that during fog episodes the turbulent droplet flux to a grass surface is  $1.8 \pm 0.9$  times the droplet sedimentation rate for wind speeds  $3\text{--}4 \text{ m s}^{-1}$ . At wind speeds less than  $2 \text{ m s}^{-1}$ , typical of

radiation fog episodes, their measurements showed that the total droplet deposition rate was almost equal to the droplet sedimentation rate. Based on the above data, the droplet deposition velocity varies roughly between  $0.3$  and  $3 \text{ cm s}^{-1}$  resulting in  $k_{db}$  values between  $3 \times 10^{-5}$  and  $5 \times 10^{-4}$  and  $\gamma$  values in the range  $0.3 \leq \gamma \leq 50$ .

The case examined here is for a typical mass transfer rate ( $d_p = 20 \mu\text{m}$ ),  $\alpha = 1500$ , with gas-phase sources of A ranging from nonexistent ( $\delta = 0$ ) to strong ( $\delta = 100$ ). The calculated values of the deposition ratio  $DR_2$  for  $t^*$  are shown in Fig. 4. If there are no sources of A in the gas phase ( $\delta = 0$ ) then the equilibration processes affect significantly (more than 20%) the total deposition of A over a relatively small range of the dimensionless parameters  $\beta$  and  $\gamma$ , namely when  $\gamma > 7$  and  $1 < \beta < 100$ . Therefore the fog droplets should deposit seven times faster than the vapor species before a maximum 20% increase in total deposition occurs. When the deposition velocity of the aqueous phase becomes 50 times larger than the corresponding vapor deposition velocity, the deposition is enhanced 2.5 times by the equilibration processes. If the deposition velocities of the two phases are sufficiently different, the solubility of A in the aqueous phase determines the importance of the equilibration processes. The maximum influence is observed for values of  $\beta$  around 10 that correspond to effective Henry's Law constants from around  $8 \times 10^3 \text{ M atm}^{-1}$  for dense fogs (liquid water content  $0.5 \text{ g m}^{-3}$ ) to  $8 \times 10^4 \text{ M atm}^{-1}$  for light fogs (liquid water content  $0.05 \text{ g m}^{-3}$ ).

In Case 2 the emission/production rate of A influences the deposition ratio considerably less than in Case 1. This is mainly due to the fact that the aqueous phase has a limited A dissolution capacity, while unlimited amounts of A can condense on the dry aerosol phase. The extent of these effects can be realized by comparing Figs 4a and 4b. For a strong source of A in the gas phase ( $\delta = 100$ ) the maximum deposition enhancement is threefold. An extra interesting region appears when the deposition velocity of the droplets is less than half of the vapor deposition velocity. Then for very soluble species (Henry's Law constant  $10^6 - 10^7 \text{ M atm}^{-1}$ ) the equilibration processes cause a reduction of the total deposition by as much as a factor of 2.

In conclusion, the deposition of species with very low solubilities like  $O_3$ ,  $NO_2$ ,  $NO$  and  $PAN$  for which  $\beta > 10^4$  is generally not affected by their transfer to the aqueous phase. The deposition of highly soluble species like  $HNO_3$  and  $HCl$  for which  $\beta < 0.1$  will be affected only if their gas-phase deposition velocity exceeds the fog droplet deposition velocity. In that case the total deposition will decrease significantly in the presence of the fog. The deposition of species with small solubilities like  $CH_3OH$  ( $K_{Hi} = 220 \text{ M atm}^{-1}$ ) will be enhanced slightly (around 15–20%) under optimum conditions. Finally the deposition of species that have solubilities in the optimum range, ( $10^3 - 10^6 \text{ M atm}^{-1}$ ) like  $SO_2$  (for  $4.5 \leq pH \leq 7$ ),  $H_2O_2$  ( $pH$

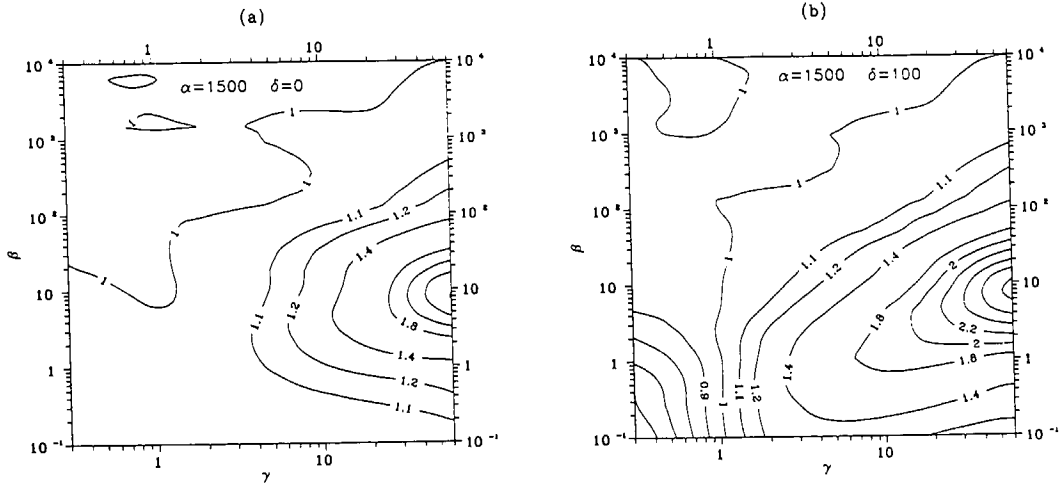


Fig. 4. Deposition ratio  $DR_2(t^*)$  (total deposition with equilibration processes over deposition without) as a function of the initial species distribution  $\beta$  and the ratio of the deposition velocities  $\gamma$  for typical mass transfer ( $\alpha = 1500$ ) and (a)  $\delta = 0$ : zero A(g) emission/production rate; (b)  $\delta = 100$ : very high A(g) emission/production rate.

independent),  $\text{HNO}_2$  ( $4.8 \leq \text{pH} \leq 7$ ),  $\text{HCHO}$  (pH independent), and  $\text{HCOOH}$  ( $2 \leq \text{pH} \leq 6.5$ ) can be enhanced by as much as 3 times by equilibration processes.

### Case 3

The most important example of a system corresponding to Case 3 is that of  $\text{NH}_3$ ,  $\text{HNO}_3$  and  $\text{NH}_4\text{NO}_3$  particles, and therefore the dimensionless parameters  $\sigma_1 - \sigma_8$  will be chosen to correspond to the conditions encountered relevant to that system under polluted urban conditions. Let A denote  $\text{NH}_3$  and B the  $\text{HNO}_3$  vapor. Gas-phase concentrations of  $\text{NH}_3$  vary from  $0.5$  to  $20 \mu\text{g m}^{-3}$  (Seinfeld, 1986), the equilibrium constant of ammonium nitrate at 298 K is  $49.8 \mu\text{g}^2 \text{m}^{-6}$  (Stelson and Seinfeld, 1982) and measurements of Russel and Cass (1984) indicate concentrations of  $\text{NH}_4\text{NO}_3$  in the Los Angeles basin from  $5$  to  $50 \mu\text{g m}^{-3}$ . An average mixing height of  $600 \text{ m}$  is assumed. For this mixing height ammonia emissions calculations of Russel and Cass (1986) for the LA basin and of Jacob (1985) for San Joaquin Valley, CA suggest an average value of  $5 \times 10^{-5} \mu\text{g m}^{-3} \text{s}^{-1}$ . A nitric acid vapor production rate of  $8 \times 10^{-4} \mu\text{g m}^{-3} \text{s}^{-1}$  is assumed corresponding to an  $\text{NO}_2$  concentration of  $100 \text{ ppb}$  and an OH concentration of  $10^{-5} \text{ ppb}$ . The deposition velocities of  $\text{NH}_3$  and  $\text{HNO}_3$  are assumed equal to  $1 \text{ cm s}^{-1}$  and the aerosol particle deposition velocities vary between  $0.005 \text{ cm s}^{-1}$  and  $5 \text{ cm s}^{-1}$ .

In the base case the averages of the above ranges of parameters are used and assuming a particle diameter of  $1 \mu\text{m}$  the following values of the dimensionless parameters are obtained:

$$\begin{aligned} \sigma_1 &= 250, & \sigma_2 &= 0.2, & \sigma_3 &= 1, & \sigma_4 &= 0.01, \\ \sigma_5 &= 1.5, & \sigma_6 &= 15. \end{aligned}$$

$\sigma_7$  is allowed to vary between  $0.1$  and  $1000$  while  $\sigma_8$  varies between  $0.01$  and  $100$ . The sensitivity of the results to the above chosen values of  $\sigma_1 - \sigma_6$  will also be examined.

The calculated values of the deposition ratio for  $t = t^*$  are presented in Fig. 5 as a function of  $\sigma_7$  and  $\sigma_8$  for the base case. The results indicate that there are three regions of behavior. The first region is for  $\sigma_7 > 20$  where for all values of  $\sigma_8$  of interest the equilibration processes do not affect significantly the total deposition. In this region the initial concentration of nitric acid exceeds the initial concentration of ammonia, and nitric acid is deposited faster than it is produced. At the same time the ammonia emission rate exceeds its deposition rate. Therefore the ammonia concentration increases and the equilibrium is maintained without significant evaporation of the aerosol ammonium

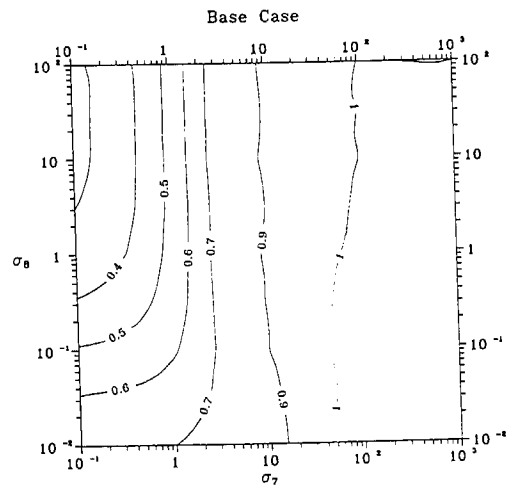


Fig. 5. Deposition ratio  $DR_3(t^*)$  for the base case.

nitrate. Most of the material deposited for this region is nitric acid vapor. The second region extends roughly between  $\sigma_7 = 20$  and  $\sigma_7 = 2$ . The deposition ratio drops from 0.95 to 0.75 and does not depend on the initial ammonium nitrate concentration. In this region the emission rates for both ammonia and nitric acid exceed their corresponding initial deposition rates and therefore they are both transferred to the aerosol phase and ammonium nitrate is formed. This transfer of material from a rapidly depositing phase to a slowly depositing one causes a decrease of the total deposition. In this second region the nitric acid deposition also dominates and therefore changes in the initial ammonium nitrate concentration affect the amount of aerosol deposition but have minimal effects on the nitric acid-dominated total deposition. Finally in the third region for  $\sigma_7 < 2$ , the deposition ratio varies between 0.75 and 0.3 and the initial ammonium nitrate concentration is important. The smaller the initial ammonium nitrate concentration the more the entire process changes by the transfer of material from the gas phase to the aerosol phase and the smaller the deposition ratio.

In conclusion, in the base case, the equilibration processes are found to affect the deposition the most when both ammonia and nitric acid production rates exceed their initial deposition rates and most of the material exists initially in the gas phase primarily as ammonia.

#### *Effect of the relative deposition velocities of the gas species*

In the base case discussed the two gas-phase species were assumed to have the same deposition velocity ( $\sigma_3 = 1$ ). The sensitivity of the model results to this value has been determined by examining the cases of  $\sigma_3 = 0.5$  and  $\sigma_3 = 2$ . In both cases this variation of the relative deposition velocity of the gas species caused by only small changes in the values of the deposition ratio in Fig. 5. Namely if the deposition velocity of  $\text{HNO}_3$  is half the deposition velocity of  $\text{NH}_3$  ( $\sigma_3 = 0.5$ ) then the minimum value of the deposition ratio in Fig. 5 (for  $\sigma_7 = 0.1$ ,  $\sigma_8 = 1000$ ) increases from 0.28 to 0.31. If the deposition velocity of  $\text{HNO}_3$  is twice the deposition velocity of  $\text{NH}_3$  ( $\sigma_3 = 2$ ) the same minimum value decreases from 0.28 to 0.24. Thus as long as the deposition velocities of the two gases do not differ significantly, the exact value of the parameter  $\sigma_3$  does not affect the deposition ratio by more than 15%. In the discussion that follows we will assume that both gas-phase species have the same deposition velocity and we will refer to that value as the 'gas-phase deposition velocity'.

#### *Effect of the relative deposition velocities of the gas and aerosol phases*

The effects of the aerosol deposition velocity on the deposition ratio can be studied by varying the parameter  $\sigma_4$  (Fig. 6). A tenfold increase of the aerosol

deposition velocity compared to its base value ( $\sigma_4$  increases from 0.01 to 0.1) has only minor effects on the deposition ratio. The base case deposition ratio surface moves slightly upwards. For example its minimum value increases from 0.28 to 0.33 while its value for  $\sigma_7 = 0.1$  and  $\sigma_8 = 0.01$  increases from 0.68 to 0.81. If the aerosol deposition velocity increases further approaching the velocity of the gas phase ( $\sigma_4 = 0.5$ ) the effects of the equilibration processes on the total deposition decrease, and the deposition ratio surface approaches the plane  $DR_3 = 1$  (Fig. 6a). If the deposition velocities of the two phases are the same, the transfer of mass between the two phases has no effect on the total mass deposited and the deposition ratio is 1 everywhere.

The behavior of the system changes drastically when the parameter  $\sigma_4$  exceeds unity. Ammonia and nitric acid are still produced faster than they deposit, so they are transferred to the aerosol phase enhancing in this way the total deposition. This enhancement is maximized once more for high ammonia concentrations and small initial concentrations of ammonium nitrate and for  $\sigma_4 = 2$  it can be as much as 60%. These effects are magnified when the aerosol deposition velocity increases further and for  $\sigma_4 = 10$  the total deposition increases by as much as 4.5 times (Fig. 6b).

#### *Effects of the emission/production rates of the gas-phase species*

The effects of the gas-phase sources of ammonia and nitric acid have been investigated by varying the parameters  $\sigma_5$  and  $\sigma_6$ . A change in  $\sigma_5$  can be viewed as change of both emission/production rates  $E_A$  and  $E_B$  by equal percentages, keeping all the deposition rates constant. For no gas-phase sources ( $\sigma_5 = 0$ ) the deposition ratio exhibits a maximum value of 4.2 (Fig. 7a). This maximum value is observed for roughly equal initial mass concentrations of ammonia and nitric acid and an initial ammonium nitrate concentration almost three times smaller. This peak is due to the fact that both  $DR_3(t^*, \sigma_7)$  for a constant  $\sigma_8$  and  $DR_3(t^*, \sigma_8)$  for a constant  $\sigma_7$  have maxima. If initially one of the two gases is in much higher concentration than the other, for example  $M_{\text{HNO}_3}^0 \gg M_{\text{NH}_3}^0$ , then the deviations from equilibrium created by the depositional losses can be suppressed by the evaporation of only small quantities of ammonium nitrate. On the contrary, as the two initial concentrations approach each other, a small depositional loss causes a larger ammonium nitrate evaporation, and more material is transferred from the aerosol to the gas phase enhancing the total deposition.

For an emission rate of  $\text{NH}_3$  that is initially slower than its deposition ( $\sigma_5 = 0.3$ ) there are two interesting regions (Fig. 7b). If  $\sigma_7 < 1$ , then nitric acid is produced fast enough so that its concentration increase compensates for the ammonia concentration decline and material condenses to the aerosol phase, slowing down the total deposition rate by as much as a factor

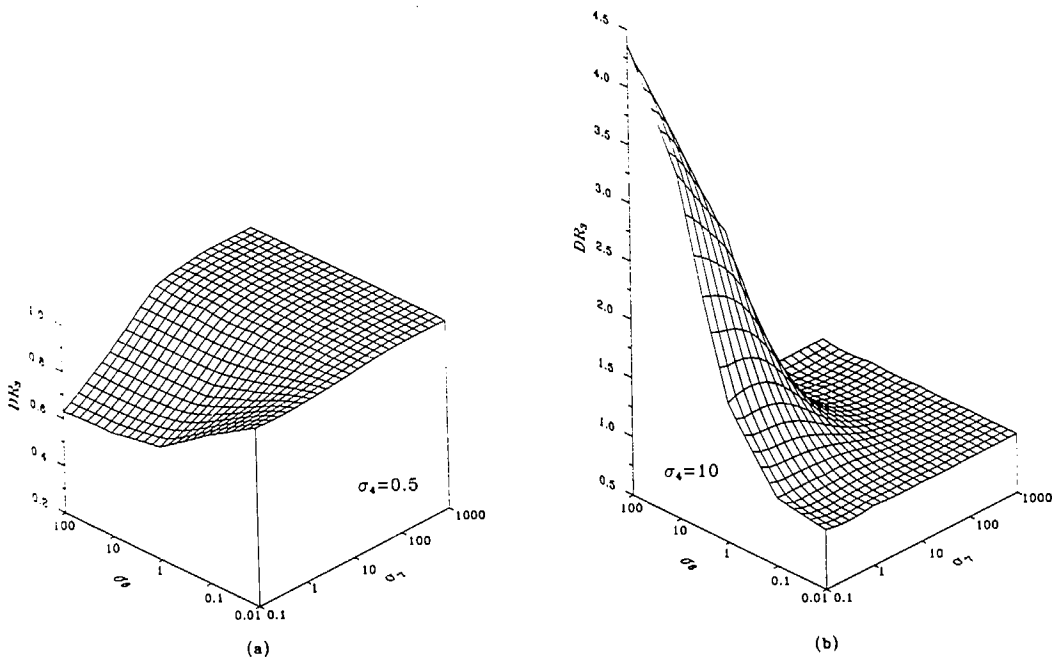


Fig. 6. Effect of the ratio of the aerosol and gas-phase deposition velocities on the deposition ratio  $DR_3(t^*)$ .  
(a)  $\sigma_4 = 0.5$ . (b)  $\sigma_4 = 10$ .

of 3. In the second region where  $2 < \sigma_7 < 100$ ,  $\sigma_8 < 0.2$ , the gas-phase production is not able to compensate for the depositional losses and ammonium nitrate evaporates trying to maintain equilibrium, enhancing total deposition by as much as 50%.

An increase of  $\sigma_5$  to 1.5 corresponds to the base case discussed previously. A further increase to  $\sigma_5 = 15$  (Fig. 7c) causes additional reduction of the total deposition as the strong sources of ammonia and nitric acid cause high supersaturations and rapid condensation to the slow depositing aerosol phase. For almost all conditions of interest total deposition is slowed down by as much as 2.3 times.

The effect of the variation of the nitric acid production rate keeping all other variables constant has been examined by varying the parameter  $\sigma_6$ . For no sources of nitric acid,  $\sigma_6 = 0$ , the increase of the ammonia concentration compensates for the decrease of nitric acid concentration unless  $0.5 < \sigma_7 < 50$ ,  $\sigma_8 < 0.1$  (Fig. 8a). In this region ammonia emissions are not sufficient for the equilibrium maintenance and evaporation of the ammonium nitrate is necessary. The total deposition is enhanced by as much as 2 times. An increase of the nitric acid production (Fig. 8b) causes the appearance of the two familiar regions with maximum enhancement 45% and maximum reduction 2.7 times. As  $\sigma_6$  increases to 15 the enhancement region disappears (see base case). For very high nitric acid production rates the total deposition decreases by as much as 35% (Fig. 8c).

#### MONODISPERSE VS POLYDISPERSE CONDENSED PHASE

A major assumption in the three models presented is the monodispersity of the aerosol or aqueous phase. Atmospheric aerosols sizes range roughly from  $0.01 \mu\text{m}$  to  $10 \mu\text{m}$ , and fog or cloud droplets range from a few  $\mu\text{m}$  to a few hundred  $\mu\text{m}$  and their distributions are usually far from monodisperse. All the above models can easily be extended to account for polydispersity of the condensed phases by discretizing the continuous aerosol or droplet distribution into  $n$  size sections.

Nondimensionalization of the resulting system of  $n + 3$  equations suggests that the solutions depend on  $3n + 1$  dimensionless parameters, the initial mass fraction of species B in section  $i$ ,  $x_i = M_{B_0}^i / \sum_i M_{B_0}^i$ , the initial partitioning of the species between gas and aerosol phases,  $\beta = M_A^0 / \sum_i M_{B_0}^i$ , the ratios of deposition constants of sections  $i$  to the gas-phase deposition constant,  $\gamma_i = k_{dc}^i / k_{da}$ , the ratio  $\delta$  of the emission rate of A to the initial vapor deposition rate, and the ratios of the mass transfer rates of section  $i$  to the vapor deposition rate,  $\alpha_i = k_m^i M_C^i / k_{da}$ .

Because of the large number of parameters involved in the model a thorough investigation of the importance of the equilibration processes on the  $(3n + 1)$  dimensional parameter space is beyond the scope of the present work. In the case of a polydisperse aerosol one can obtain a rough estimate of the importance of the equilibration processes on deposition by treating

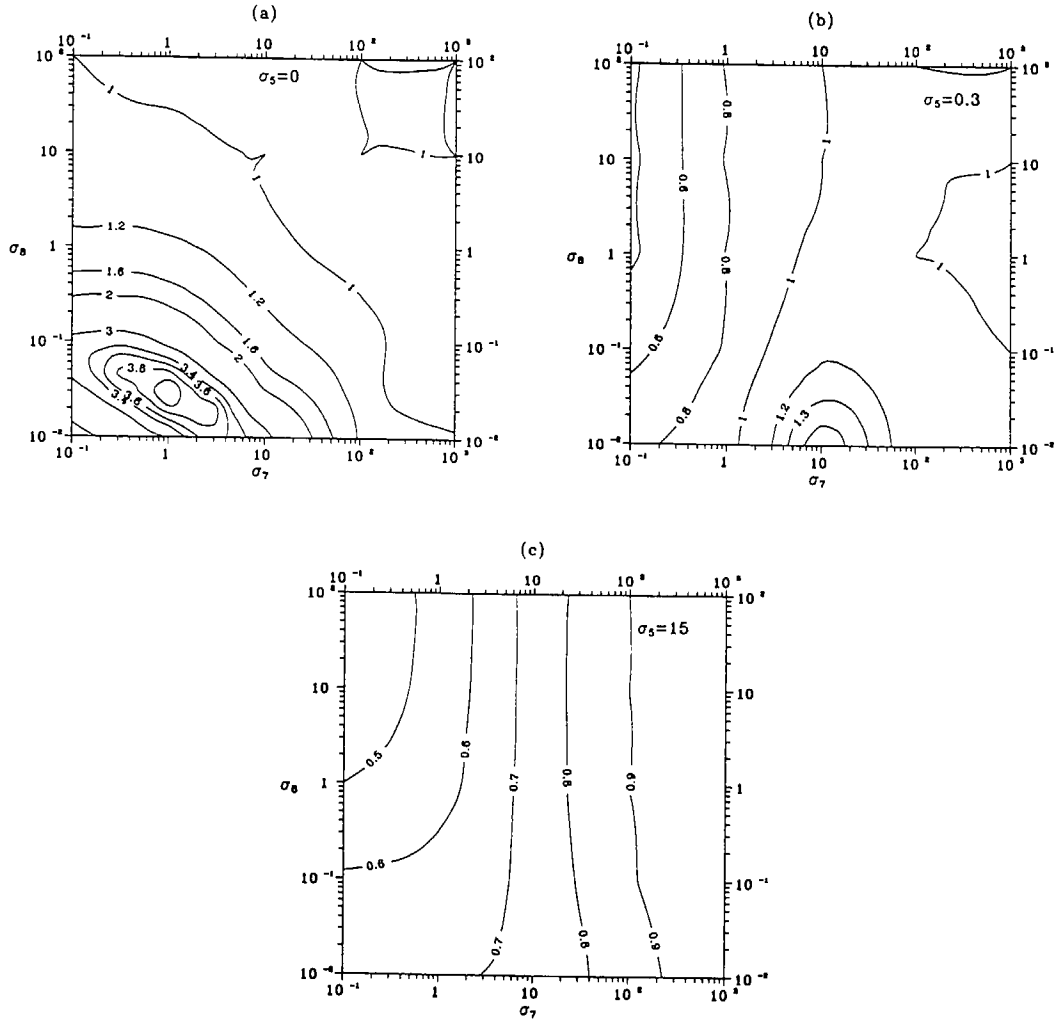


Fig. 7. Effect of the ratio of the gas-phase source rates to the gas-phase deposition rate on the deposition ratio  $DR_3(t^*)$ . (a)  $\sigma_5 = 0$ . (b)  $\sigma_5 = 0.3$ . (c)  $\sigma_5 = 15$ .

the aerosol as monodisperse and using for Case 1

$$M_B = \sum_{i=1}^n M_B^i, \quad M_C^0 = \sum_{i=1}^n M_C^i, \quad k_m = \frac{\sum_{i=1}^n k_m^i M_C^i}{M_C^0},$$

$$k_{dc} = \sum_{i=1}^n x_i k_{dc}^i.$$

The inaccuracy of the above treatment arises in calculating an average aerosol deposition velocity using as weighting factors the initial fractions  $x_i$ . The distribution of B over the aerosol size spectrum usually changes with time due to mass transfer and deposition and the average deposition velocity follows this change. An accurate solution can only be obtained by actually solving the system of differential equations and comparing with the solution if one neglects equilibration processes.

The models for Cases 2 and 3 can be similarly extended to describe a polydisperse aerosol or droplet

phase. A treatment of Case 2 with a full fog droplet spectrum has been presented by Pandis *et al.* (1990).

#### IMPLICATIONS FOR MATHEMATICAL MODELING

The values of the deposition ratio presented up to this point can be interpreted as the errors introduced in deposition calculations by completely neglecting equilibration processes. The first point suggested by this work is that the equilibration processes between different phases should be included in all mathematical models attempting to predict deposition. The problem that should be addressed next is how should these processes be modelled.

The common practice in gas-aerosol or gas-aqueous phase models has been the splitting of the whole problem into subproblems that are solved sequentially. In this method, called operator splitting, there is usually one operator describing the processes

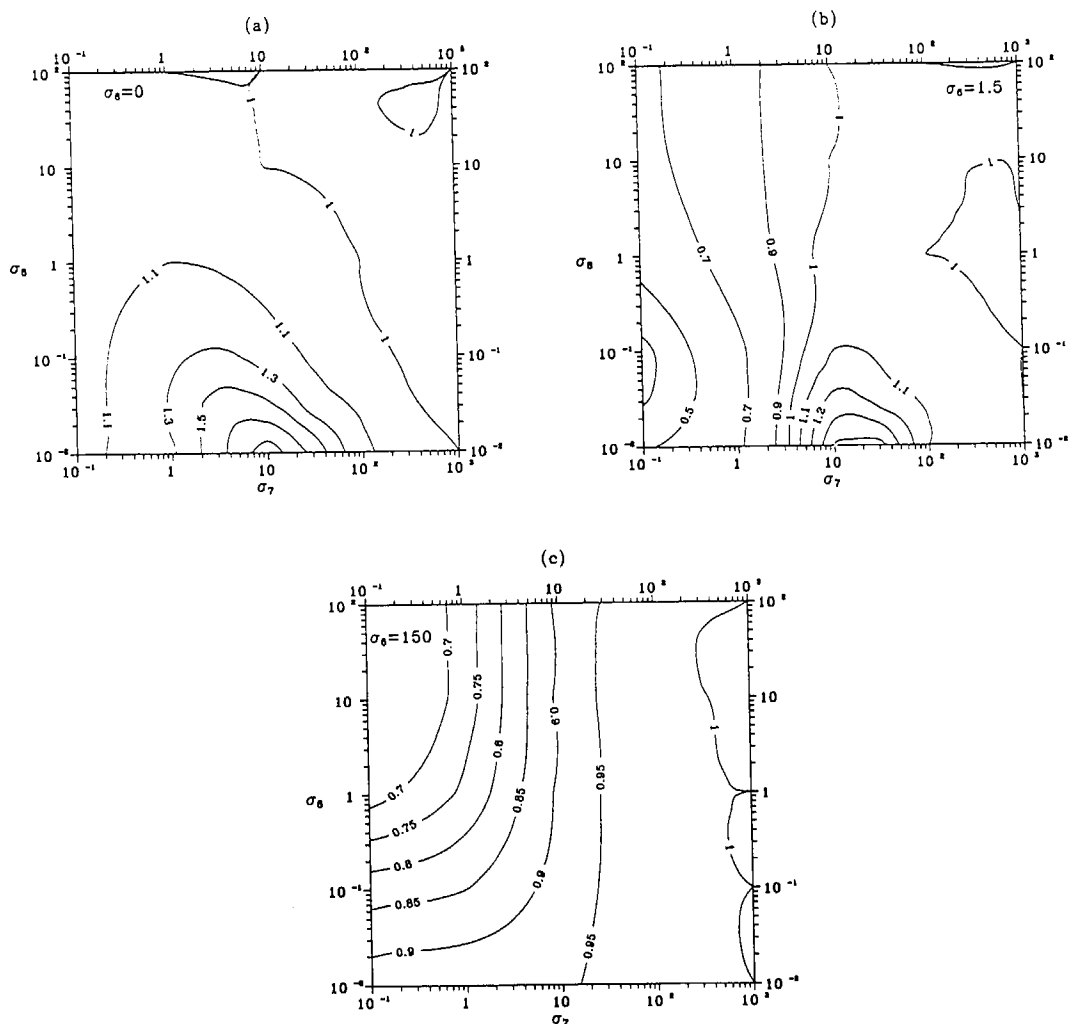


Fig. 8. Effect of the ratio of the nitric acid production rate on the deposition ratio  $DR_3(t^*)$ . (a)  $\sigma_6 = 0$ . (b)  $\sigma_6 = 1.5$ . (c)  $\sigma_6 = 150$ .

in each phase. For example in an Eulerian photochemical gas-aerosol model Pilinis and Seinfeld (1988) used the following operator scheme to calculate the variable vector  $F_i$  at time  $t + 2h$  is

$$F_i^{(t+2h)} = A_i(2h)A_{th}(2h)A_d(2h) \\ \times A_x(h)A_y(h)A_{zc}(2h)A_y(h)A_x(h)F_i^{(t)}$$

where  $A_x$ ,  $A_y$ ,  $A_{zc}$  are the x-transport, y-transport, z-transport and gas-phase chemistry operators, respectively, while  $A_i$ ,  $A_{th}$ ,  $A_d$  are the operators for the intersectional movement of the aerosol particles, the aerosol thermodynamics and dynamics, respectively. In this model the gas and aerosol deposition have been included in the z-transport and gas-phase chemistry operator while the equilibration processes have been included in the thermodynamics operator. The operator step  $2h$  used was 10 min.

The separation of the equilibration processes and the deposition into different operators is expected to

introduce errors in the calculations when the operator time step used is not sufficiently small. To investigate the magnitude of these errors we have compared the models developed in this study with the corresponding operator splitting schemes.

For Case 1 we have chosen the point  $\alpha = 1000$ ,  $\beta = 1$ ,  $\gamma = 0.01$ ,  $\delta = 100$  for which neglect of the equilibration processes would cause an overprediction of total deposition by 16 times (Fig. 2d). Selecting  $M_{eq} = 1 \mu\text{g m}^{-3}$  and gas deposition velocity  $0.5 \text{ cm s}^{-1}$  we find that the smallest time scale in the problem is the emission time scale equal to 17 min. The errors introduced by the operator splitting scheme are shown in Fig. 9. For a time step of 10 min the error is almost a 100% deposition overprediction. Timesteps less than 2 min should be used to avoid errors more than 10%.

For Case 3 the base case with  $\sigma_7 = 0.1$ ,  $\sigma_8 = 100$  has been examined. Complete omission of the equilibration processes results in an overprediction of the total deposition by a factor of 3.6 (Fig. 5). The results of the

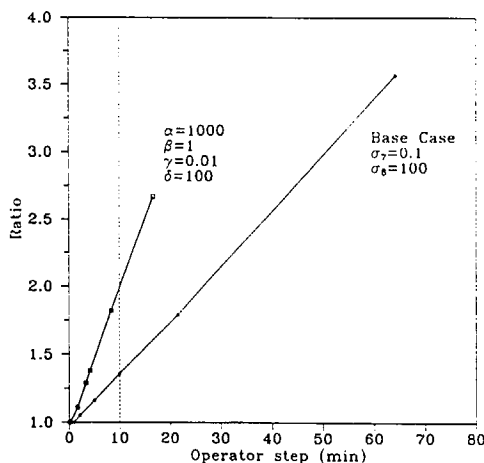


Fig. 9. Ratio of the total deposited mass as calculated by the operator splitting scheme over the full solution as a function of the operator time step.

corresponding operator splitting scheme are depicted in Fig. 9 for  $k_{da} = 10^{-4} \text{ s}^{-1}$ . The smallest time scale of the problem is the production of  $\text{HNO}_3$  at 1 min. The performance of the operator splitting scheme is better but it still overpredicts total deposition by 40% for a time step of 10 min.

In conclusion, when equilibration processes significantly affect deposition one should try to include both processes in the same numerical operator. If this is not possible then one should be prepared to use very small time steps in the operator splitting scheme to avoid the above described errors.

#### CONCLUSIONS

The study of three idealized problems has demonstrated that equilibration processes between two atmospheric phases that are removed with different rates can significantly influence the amount of material deposited on the ground and the residence times of material in the atmosphere. The larger the difference of deposition velocities between the two phases the more the equilibration processes affect the removal processes. If the two phases have the same deposition velocities, the equilibration processes just alter the material distribution between the two phases without affecting the total deposition.

The role of the equilibration processes is enhanced under conditions that cause large deviations from the system equilibrium state resulting in transfer of material between the two phases. The emission or gas-phase production of a vapor is the factor examined in this study. High emission or production rates cause supersaturations in the gas phase and material transfer to the aerosol phase. On the contrary, the absence of gas-phase sources causes subsaturation and evaporation of material from the aerosol or aqueous-phase.

The initial conditions of the system determine the relative magnitude of the material transferred between the two phases compared to the total system mass determining thus indirectly the importance of the equilibration processes.

In all cases examined the equilibration processes were able to enhance or suppress significantly the removal processes and therefore should not be neglected in deposition calculations. Furthermore our analysis demonstrates that if an operator splitting scheme is used in a mathematical model both equilibration and removal processes should be included in the same operator or very small operator steps (typically less than 1 min) will be necessary.

*Acknowledgement*—This work was supported by State of California Air Resources Board Agreement A932-054

#### REFERENCES

- Bidleman T. F. (1988) Wet and dry deposition of organic compounds are controlled by their vapor-particle partitioning. *Envir. Sci. Technol.* **22**, 361–367.
- Brost R. A., Delany A. C. and Heubert B. J. (1988) Numerical modeling of concentrations and fluxes of  $\text{HNO}_3$ ,  $\text{NH}_3$  and  $\text{NH}_4\text{NO}_3$  near the surface. *J. geophys. Res.* **93**, 7137–7152.
- Dollard G. J. and Unsworth M. H. (1983) Field measurements of turbulent fluxes of wind-driven fog drops to a grass surface. *Atmospheric Environment* **17**, 775–780.
- Jacob D. J. (1985) The origins of inorganic acidity in fogs. Ph. D. Thesis, California Institute of Technology, Pasadena, CA.
- McMahon T. A. and Denison P. J. (1979) Empirical atmospheric deposition parameters—a survey. *Atmospheric Environment* **13**, 571–585.
- McRae G. J. and A. G. Russel (1984) Dry deposition of nitrogen-containing species. In *Deposition Both Wet and Dry* (edited by B. B. Hicks), pp. 153–193. Acid Precipitation Series. Butterworth, Boston.
- National Center for Atmospheric Research (1982) *Regional Acid Deposition Models and Physical Processes*. Boulder, CO.
- Pandis S. N. and Seinfeld J. H. (1989a) Sensitivity analysis of a chemical mechanism for aqueous-phase atmospheric chemistry. *J. geophys. Res.* **94**, 1105–1126.
- Pandis S. N. and Seinfeld J. H. (1989b) Mathematical modeling of acid deposition due to radiation fog. *J. geophys. Res.* **94**, 12,911–12,923.
- Pandis S. N., Seinfeld J. H. and C. Pilinis (1990) The smog-fog-smog cycle and acid deposition. *J. geophys. Res.* (in press).
- Pilinis C. and Seinfeld J. H. (1988) Development and evaluation of an eulerian photochemical gas-aerosol model. *Atmospheric Environment* **22**, 1985–2001.
- Russel A. G. and Cass G. R. (1984) Acquisition of regional air quality model validation data for nitrate, sulfate, ammonium ion and their precursors. *Atmospheric Environment* **18**, 1815–1827.
- Russel A. G. and Cass G. R. (1986) Verification of a mathematical model for aerosol nitrate and nitric acid formation and its use for control measure evaluation. *Atmospheric Environment* **20**, 2011–2025.
- Schwartz S. E. and White W. H. (1981) Solubility equilibrium of the nitrogen oxides and oxyacids in dilute aqueous solution. *Adv. Envir. Sci. Eng.* **4**, 1–45.
- Seinfeld J. H. (1986) *Atmospheric Chemistry and Physics of Air Pollution*. John Wiley, New York.
- Stern J. E., Flagan R. C., Grosjean D. and Seinfeld J. H. (1987) Aerosol formation and growth in atmospheric aromatic

Equilibrium processes and wet or dry deposition

- hydrocarbon photooxidation. *Envir. Sci. Technol.* **21**, 1224-1231.
- Stafford M. A. (1988) The effects of partitioning between gas and aerosol phases on the dry deposition of acidity. Paper presented at American Chemical Society Meeting, Toronto, 5-11 June.
- Stelson A. W. and Seinfeld J. H. (1982) Relative humidity and temperature dependence of the ammonium nitrate dissociation constant. *Atmospheric Environment* **16**, 983-993.
- Tao Y. and McMurry P. H. (1989) Vapor pressures and surface free-energies of C14-C18 monocarboxylic acids and C5-dicarboxylic and C6-dicarboxylic acids. *Envir. Sci. Technol.* **23**, 1519-1523.
- Wesely M. L. and Shannon J. D. (1984) Improved estimates of sulfate dry deposition in Eastern North America. *Envir. Progress* **3**, 78-81.

## SECOND-GENERATION INORGANIC AEROSOL MODEL

ANTHONY S. WEXLER\*

Department of Mechanical Engineering and Environmental Quality Laboratory, California Institute of Technology, Pasadena, CA 91125, U.S.A.

and

JOHN H. SEINFELD

Department of Chemical Engineering, California Institute of Technology, Pasadena, CA 91125, U.S.A.

(First received 20 July 1990 and in final form 19 February 1991)

**Abstract**—Accurate prediction of the size distribution of the inorganic components of atmospheric aerosols must account for both the thermodynamic properties of the aerosol particles and transport between the gas and aerosol phases. For volatile inorganic species the transport rate is governed by the particle surface partial pressures which, in turn, is determined by the phase state and composition of the aerosol. We develop a model of the temporal composition of atmospheric aerosol particles based on their transport and thermodynamic properties. Included in the model is an improved theory of the temperature and composition dependence of deliquescence. Components of the model are tested against measurements of activity coefficients in single- and multicomponent aqueous solutions and general agreement is found. Aerosol water predictions are significantly higher under conditions of low relative humidity due to the improved theory of deliquescence.

**Key word index:** Deliquescence, efflorescence, water activity, atmospheric aerosols, thermodynamic equilibrium.

### INTRODUCTION

Traditionally the mass, composition, and size distribution of the volatile inorganics in atmospheric aerosol have been predicted assuming local thermodynamic equilibrium between the aerosol and gas phases (Russell *et al.*, 1983, 1986, 1988; Bassett and Seinfeld, 1983, 1984; Pilinis and Seinfeld, 1987, 1988). Atmospheric measurements by Allen *et al.* (1989) demonstrate that under certain ambient conditions the volatile inorganics are not in equilibrium with the aerosol, and in a recent paper, we show that (1) the characteristic time scales for equilibration between the gas and aerosol phases may be too long for the equilibrium assumption to hold, in agreement with the observations of Allen; and (2) under typical atmospheric conditions both transport and thermodynamic considerations determine the size distribution of volatile inorganics (Wexler and Seinfeld, 1990).

Inorganic salts comprise 25–50% of atmospheric fine aerosol mass (Gray *et al.*, 1986; Heintzenberg, 1989). The concentration of the aerosol inorganics, together with the ambient relative humidity (r.h.), determine the aerosol water content, which, in turn, is a significant portion of the total aerosol mass under conditions of higher ambient r.h. The remaining aerosol mass is generally composed of primary and sec-

ondary condensed organics and primary elemental carbon.

Since mass transport influences the total aerosol mass and its size distribution, a model has been developed that simulates both the thermodynamics of the aerosol and the transport between the gas and aerosol phases. It will be referred to as the aerosol inorganics model (AIM). Ultimately AIM will be coupled to trajectory and grid based air quality models. In this paper we describe the model, test components of the model by comparing predictions with fundamental thermodynamic data, and compare the equilibrium predictions of AIM to those of other models. In the first section of this paper, we present the fundamental relationships that govern the transport and aerosol thermodynamics and in the second section we describe the numerical methods and algorithms used to solve these governing equations. In the third section we derive some useful relationships that describe the deliquescence properties of atmospheric aerosols. We then compare the thermodynamic predictions of the model to fundamental thermodynamic data and finally we compare the equilibrium predictions of AIM to those of equilibrium models.

### TRANSPORT TO AND THERMODYNAMICS OF AEROSOL PARTICLES

In this section we present the equations that govern transport between the gas and aerosol phases and the

\*Current address: Department of Mechanical Engineering at the University of Delaware, Newark, DE 19716, U.S.A.

phase state and composition of the aerosol. The predominant inorganic components of atmospheric aerosol in the 1  $\mu\text{m}$  size range and smaller are sodium, ammonium, chloride, nitrate, and sulfate. Sodium chloride is found close to the ocean in aerosol particles that are formed from sea spray, and all sodium can be assumed to remain in the aerosol phase. The chloride initially associated with NaCl can be displaced by strong acids and may evaporate or condense as HCl. Ammonia is present in virtually all terrestrial air masses and condenses on aerosol particles where it neutralizes aerosol acidity.  $\text{HNO}_3$  is formed by gas-phase oxidation of primary  $\text{NO}_x$  emissions and moves to the aerosol phase to equilibrate the gas and aerosol phases. Sulfate is formed by gas-phase oxidation of  $\text{SO}_2$  and is transported to the aerosol phase, where it remains due to its low vapor pressure. Given this list of constituents the aerosol may be comprised of an aqueous solution of  $\text{Na}^+$ ,  $\text{NH}_4^+$ ,  $\text{NO}_3^-$ ,  $\text{Cl}^-$ , and  $\text{SO}_4^{2-}$  and solid salt phases of pure NaCl,  $\text{NaNO}_3$ ,  $\text{Na}_2\text{SO}_4$ ,  $\text{NaHSO}_4$ ,  $\text{NH}_4\text{Cl}$ ,  $\text{NH}_4\text{NO}_3$ ,  $(\text{NH}_4)_2\text{SO}_4$ ,  $\text{NH}_4\text{HSO}_4$ , and  $(\text{NH}_4)_3\text{H}(\text{SO}_4)_2$ .

The rate of change of the mass,  $M_i$ , of species  $i$  in aerosol particles of radius  $R_p$  at time  $t$  due to diffusion and surface accommodation of the corresponding vapor-phase species is given by:

$$\frac{dM_i}{dt} = \frac{4\pi ND_i R_p}{\beta + 1} (C_{i,\infty} - C_{i,e}), \quad (1)$$

where  $D_i$  is the gas-phase molecular diffusivity of species  $i$ ,  $N$  is the number concentration of particles,  $C_{i,\infty}$  is the ambient gas-phase concentration of species  $i$ , and  $C_{i,e}$  is the equilibrium gas-phase concentration at the particle surface (Wexler and Seinfeld, 1990). Imperfect accommodation on the particle surface is accounted for by  $\beta = D_i/\alpha_i c_i R_p$ , where  $\alpha_i$  is the surface accommodation coefficient of species  $i$  and  $c_i$  is the molecular velocity of species  $i$ .

The surface equilibrium concentration,  $C_{i,e}$ , depends on the composition and phase state of the aerosol. The particles consist of an aqueous phase at high r.h., one or more solid phases at low r.h., and both aqueous and solid phases at intermediate r.h. We will assume that if the aerosol consists of more than one phase, these phases are in thermodynamic equilibrium; the system is closed with respect to the total quantity of available inorganic components; and the Gibbs free energy is at the global minimum. Furthermore, one can assume that water is in equilibrium between the aerosol and gas phases, such that the activity of water in the aerosol phase is equal to the relative humidity. Once the equilibrium composition of the aerosol is determined, the surface equilibrium gas-phase concentrations of the volatile species can be deduced from appropriate equilibrium constants.

The phase composition of the aerosol is determined by minimizing the Gibbs free energy of the aerosol system. The change in Gibbs free energy,  $dG$ , due to changes in composition of the solid,  $dn_{s,i}$ , and aqueous,  $dn_{t,i}$ , phases is given by:

$$dG = \sum_i \mu_{s,i} dn_{s,i} + \sum_i \mu_{t,i} dn_{t,i}, \quad (2)$$

where  $\mu_{s,i}$  and  $\mu_{t,i}$  are the chemical potentials of the species in these phases. The chemical potential of the solid phases is the standard free energy of formation,  $\mu_{s,i}^\circ$ . The chemical potential of the ionic species is:

$$\mu_{t,i} = \mu_{t,i}^\circ + RT \ln a_i, \quad (3)$$

where  $\mu_{t,i}^\circ$  is the standard free energy of formation of ion  $i$  in solution,  $R$  is the gas constant,  $T$  is the ambient temperature, and  $a_i$  is the activity of ion  $i$ . This activity is a function of the composition of the aerosol aqueous phase. The free energies of formation of the solid, ionic, and gaseous species are calculated from (Bassett and Seinfeld, 1983)

$$\begin{aligned} \frac{\mu^\circ}{RT} = & \frac{\Delta G_f^\circ}{RT_0} + \frac{\Delta H_f^\circ}{RT_0} \left( \frac{T_0}{T} - 1 \right) \\ & - \frac{\Delta C_p}{R} \left( \frac{T_0}{T} - 1 - \ln \frac{T_0}{T} \right), \quad (4) \end{aligned}$$

where the values of the standard free energy of formation,  $\Delta G_f^\circ$ , enthalpy,  $\Delta H_f^\circ$ , and heat capacity,  $C_p$ , for the species of interest here are given in Tables 1, 2, and 3.

What remains in the evaluation of Equation (3) is calculation of the activity,  $a_i$ . The current literature does not provide an exact means for calculating the thermodynamic properties of the concentrated aqueous solutions, so empirical or semi-empirical methods must be employed. In polluted urban environments, ammonium nitrate is frequently the dominant inorganic electrolyte and at STP ammonium nitrate is in equilibrium with its solid phase at a concentration of over 25 M. Models of multicomponent electrolyte solutions of, for instance, Pitzer (1979) or Chen *et al.* (1982, 1986) are limited to ionic strengths below 6 M. Due to the exponential variation of these correlations with ionic strength, above 6 M the predictions of these models often do not agree well with experimental data (Zematis *et al.*, 1986). More recently, relations have been developed that hold at higher ionic strengths (Pitzer, 1986; Haghtalab and Vera, 1988; Liu *et al.*, 1989), but correlations for multicomponent systems of the type that occur in atmospheric aerosols have yet to be developed. The empirical correlations of Kusik and Meissner (1978) have been chosen for use here since these relations are well behaved at high ionic strengths, correlations for most of the individual components of atmospheric aerosol are available in the literature, and the model does not require correlations for multicomponent solutions. The notable exception here is sulfuric acid, which is poorly dealt with by all of these electrolyte models (Zematis *et al.*, 1986). In a subsequent section, the ability of the Kusik and Meissner model to predict the activity coefficients of multicomponent electrolyte solutions will be compared with experimental data for systems relevant to atmospheric aerosols.

The mass of water in the aerosol aqueous phase is

Table 1. Thermodynamic properties of solids relevant to atmospheric aerosols

Solid	$\Delta H_f^\circ$ kJ mol <sup>-1</sup>	$\Delta G_f^\circ$ kJ mol <sup>-1</sup>	$C_p^\circ$ J mol <sup>-1</sup> K <sup>-1</sup>
NaCl	-411.153	-384.138	50.50
NaNO <sub>3</sub>	-467.85	-367.00	92.88
NaHSO <sub>4</sub>	-1125.5	-992.8	85§
Na <sub>2</sub> SO <sub>4</sub>	-1387.08	-1270.16	128.20
NH <sub>4</sub> Cl	-314.43	-202.87	84.1
NH <sub>4</sub> NO <sub>3</sub>	-365.57	-183.87	139.3
NH <sub>4</sub> HSO <sub>4</sub>	-1026.96	-823*	127.5†
(NH <sub>4</sub> ) <sub>2</sub> SO <sub>4</sub>	-1180.85	-901.67	187.49
(NH <sub>4</sub> ) <sub>3</sub> H(SO <sub>4</sub> ) <sub>2</sub>	-1730*	-2207*	315‡

Source: Wagman *et al.* (1982) unless otherwise indicated:

\* Bassett and Seinfeld (1983);

† Karapet'yants and Karapet'yants (1970);

‡ Sum of  $C_p^\circ$  for (NH<sub>4</sub>)<sub>2</sub>SO<sub>4</sub> and NH<sub>4</sub>HSO<sub>4</sub>;

§ Estimated from  $C_p^\circ(\text{NH}_4\text{HSO}_4)/C_p^\circ(\text{Na}_2\text{SO}_4)/C_p^\circ((\text{NH}_4)_2\text{SO}_4)$ .

dependent on the composition of this phase and the ambient r.h., such that the activity of water in the aerosol phase is equal to the r.h. The ZSR relationship (Zdanovskii, 1948; Stokes and Robinson, 1966) has been used to predict the water content of atmospheric aerosols (Hanel and Zankl, 1979; Cohen *et al.*, 1987; Pilinis and Seinfeld, 1987):

$$W = \sum_i \frac{\hat{M}_i}{m_{i,0}(\text{r.h.})}, \quad (5)$$

where  $W$  is the mass of water in the aerosol in kg of water per m<sup>3</sup> of air,  $\hat{M}_i$  is the number of moles of electrolyte  $i$  per m<sup>3</sup> of air, and  $m_{i,0}$  is the molality (mol kg<sup>-1</sup>) of a single-component aqueous solution of electrolyte  $i$  that has a water activity r.h.

Equations (1)–(5) form a system of equations that describe the time evolution of the mass of inorganic species in the aerosol phase. In the following section we describe a method for solving these equations.

#### INTEGRATING TRANSPORT AND MINIMIZING GIBBS FREE ENERGY

##### Transport

Since Equation (1) will ultimately be included in a grid-based model of urban atmospheric aerosols, its integration must be done economically. A number of numerical integrators have been considered for use in predicting the temporal concentrations of atmospheric pollutants and the hybrid integrator has been determined to be economical and accurate (McRae *et al.*, 1982). The hybrid integrator (Young and Boris, 1977) was developed for integrating chemical kinetics in reacting flows. AIM employs a recent update of this code, available in Young (1980) and Young (1983), to integrate Equation (1). Under typical urban atmospheric conditions, the code conserves mass and maintains positivity, but under conditions of low r.h., when the aerosol water content is small, a large number of evaluations of the right-hand side of Equation

Table 2. Thermodynamic properties of ions in solutions relevant to atmospheric aerosols

Ion	$\Delta H_f^\circ$ kJ mol <sup>-1</sup>	$\Delta G_f^\circ$ kJ mol <sup>-1</sup>	$C_p^\circ$ J mol <sup>-1</sup> K <sup>-1</sup>
H <sup>+</sup>	0	0	0
Na <sup>+</sup>	-240.12	-261.905	46.4
NH <sub>4</sub> <sup>+</sup>	-132.51	-79.31	79.9
NO <sub>3</sub> <sup>-</sup>	-205.0	-108.74	-86.6
Cl <sup>-</sup>	-167.159	-131.228	-136.4
SO <sub>4</sub> <sup>2-</sup>	-909.27	-744.53	-293.0
HSO <sub>4</sub> <sup>-</sup>	-887.34	-755.91	-84.0

Source: Wagman *et al.* (1982) except NO<sub>3</sub><sup>-</sup> which is in error in this source. The equivalent HNO<sub>3</sub>(aq) data was used instead.

Table 3. Thermodynamic properties of the gas-phase components of atmospheric aerosols

Gas	$\Delta H_f^\circ$ kJ mol <sup>-1</sup>	$\Delta G_f^\circ$ kJ mol <sup>-1</sup>	$C_p^\circ$ J mol <sup>-1</sup> K <sup>-1</sup>
HCl	-92.307	-95.299	29.12
HNO <sub>3</sub>	-135.06	-74.72	53.35
NH <sub>3</sub>	-46.11	-16.45	35.06

Source: Wagman *et al.* (1982).

(1) may be required. This occurs because the surface partial pressures of NH<sub>3</sub>, HCl, and HNO<sub>3</sub> are governed by the pH of the aerosol and at low r.h., the solute concentrations are high, so that small changes in hydrogen ion content result in large changes in pH and consequently difficult integration conditions.

##### Thermodynamics

The equilibrium composition of the aerosol is calculated by directly minimizing the Gibbs free energy, subject to the constraints that the water activity is fixed at the r.h. and the total inorganic aerosol mass is conserved. The minimization algorithm is described in this section.

In the minimization procedure employed in AIM, the independent variables are the number of moles of each of the solid phases and the dependent variable is the Gibbs free energy. Initially, the aerosol is assumed to be completely aqueous. If one or more of the ions listed previously do not appear in the solution in significant quantities, the corresponding solid phases of these salts cannot exist and are therefore eliminated from consideration. In addition, if the r.h. is above the deliquescence point for a solid phase, this solid phase cannot exist. (This is proved in the next section.) If both of these criteria eliminate all solid phases from consideration, the aerosol exists as an aqueous solution and the water content is simply calculated from Equation (5).

If one or more solid phases may exist, the number of moles of these phases that minimizes the Gibbs free energy is calculated as follows. The number of moles in each of the solid phases,  $s$ , is initially zero. The gradient of the Gibbs free energy,  $\nabla G(s)$ , with respect to the number of moles of each solid is evaluated at the current phase composition and the negative of this gradient is followed until a minimum is found. The gradient direction comes from Equation (2) by taking the differential with respect to  $n_{s,j}$ :

$$\begin{aligned} \frac{\partial G}{\partial n_{s,j}} &= \mu_{s,j} - \sum_i v_{i,j} \mu_{i,i} \\ &= \mu_{s,j}^0 - \sum_i v_{i,j} (\mu_{i,i}^0 + RT \ln a_i), \end{aligned} \quad (6)$$

where the values of  $v_{i,j} = -\partial n_{i,i} / \partial n_{s,j}$ , the stoichiometry of the solid phases in terms of their ionic components, are given in Table 4. The mass of water, obtained from Equation (5), is used to calculate the molalities of the aqueous-phase components, which are then used in the Kusik and Meissner model to calculate the activities,  $a_i$ .

This minimization is subject to two classes of linear constraints: both the number of moles of each solid phase and the number of moles of each ion in the aqueous phase must be non-negative. The constrained gradient direction,  $\nabla_c G(s)$ , is calculated by the method of Russell (1970).

Changing the phase composition of the aerosol by moving in the  $-\nabla_c G$  direction will eventually encounter one of the constraints. The line segment from

the current value of  $s$  to the constraint is given by  $s - \eta \nabla_c G(s)$ , where  $0 \leq \eta \leq \eta_{\max}$ , and  $\eta_{\max}$  is the value of  $\eta$  where the first constraint is encountered. A binary search is performed along this line segment to find the zero of:

$$\nabla_c G(s) \cdot \nabla G \{s - \eta \nabla_c G(s)\}.$$

The value of  $\eta$  at this zero,  $\eta_0$ , defines a new estimate of the phase composition,  $s \leftarrow s - \eta_0 \nabla_c G(s)$ .

Under conditions of low ambient relative humidity many if not all of the salts may precipitate. If reciprocal salt pairs form, such as NaCl and  $\text{NH}_4\text{NO}_3$ , and  $\text{NH}_4\text{Cl}$  and  $\text{NaNO}_3$ , the Gibbs free energy of the solid phases can be further minimized, without altering the composition of the aqueous phase, by shifting the composition from one salt pair to the other. Typically the Gibbs free energy of the solid phases is minimized when one of the reciprocal salts is no longer present. Minimizing the Gibbs free energy of the solid phases is a linear programming problem with two kinds of constraints, inequality constraints such that the moles in each solid phase are non-negative and equality constraints such that the total number of moles of each ion is conserved in the solid phases.

Thus the Gibbs free energy minimization involves two steps. The first is a non-linear constrained minimization that moves material between the aqueous phase and one or more solid phases. The second step is a linear constrained minimization that moves material between reciprocal solid phases. These two minimization steps result in a new estimate of  $s$ . If this new estimate is sufficiently close to the previous value of  $s$ , convergence is assumed. Otherwise, a new gradient is calculated at the current value of  $s$  and the procedure is repeated until convergence is achieved.

The algorithm described here assumes that salt precipitates can be eliminated from consideration if the ambient r.h. is above the deliquescence relative humidity (DRH) of the salt. In the following section we prove that this is a valid assumption and then derive an expression for the temperature dependence of the deliquescence point.

#### DELIQUESCENCE AND EFFLORESCENCE

The Gibbs free energy minimization algorithm employs the assumption that a salt will not precipitate at r.h. above its deliquescence point, where here the deliquescence point (DRH) at a given temperature is defined as the water activity of a single electrolyte solution that is in equilibrium with its salt precipitate. In general, the water activity at which a precipitate is in equilibrium with an electrolyte solution is dependent on its temperature and composition. In this section we will prove that the deliquescence point of a salt in equilibrium with a multicomponent solution always occurs at a relative humidity lower than its deliquescence point in a single-component solution.

Table 4. Solid stoichiometry in terms of the ionic components

Solids	Na <sup>+</sup>	NH <sub>4</sub> <sup>+</sup>	H <sup>+</sup>	Cl <sup>-</sup>	NO <sub>3</sub> <sup>-</sup>	SO <sub>4</sub> <sup>2-</sup>
NaCl	1	0	0	1	0	0
NaNO <sub>3</sub>	1	0	0	0	1	0
NaHSO <sub>4</sub>	1	0	1	0	0	1
Na <sub>2</sub> SO <sub>4</sub>	2	0	0	0	0	1
NH <sub>4</sub> Cl	0	1	0	1	0	0
NH <sub>4</sub> NO <sub>3</sub>	0	1	0	0	1	0
NH <sub>4</sub> HSO <sub>4</sub>	0	1	1	0	0	1
(NH <sub>4</sub> ) <sub>2</sub> SO <sub>4</sub>	0	2	0	0	0	1
(NH <sub>4</sub> ) <sub>3</sub> H(SO <sub>4</sub> ) <sub>2</sub>	0	3	1	0	0	2

We will then derive an expression for the temperature dependence of the deliquescence point of a single electrolyte solution.

#### Variation of DRH with composition

Let us consider two electrolytes in a solution exposed to the atmosphere. The solution and the atmosphere are in equilibrium with respect to water when the ambient r.h. is equal to the water activity in solution. Under conditions of sufficiently low r.h., one of the electrolytes may form a salt precipitate that is in equilibrium with its ions in solution. At still lower r.h., both electrolytes will exist in the solid phase. Let us define the r.h. where one of the electrolytes is in equilibrium with its solid phase as the DRH for this electrolyte. This DRH is a function of the relative mole fractions of the two electrolytes.

That the DRH of one electrolyte is lowered by the addition of another electrolyte is a conclusion of the Gibbs–Duhem equation, which for a solution of two electrolytes (1 and 2) in water (w) at constant temperature and pressure is:

$$n_1 d\mu_1 + n_2 d\mu_2 + n_w d\mu_w = 0. \quad (7)$$

Let us assume that initially electrolyte 1 is in equilibrium with solid salt 1 in a solution that does not yet contain electrolyte 2. As electrolyte 2 is added to the solution, the chemical potential of electrolyte 1 does not change, because it is in equilibrium with its solid phase. Thus  $d\mu_1 \equiv 0$  and Equation (7) becomes:

$$n_2 d\mu_2 + n_w d\mu_w = 0. \quad (8)$$

The chemical potentials of electrolyte 2 and water can be expressed in terms of their activities by:

$$\mu_i = \mu_i^\circ + RT \ln a_i, \quad (9)$$

where  $\mu_i^\circ$  is the chemical potential of species  $i$  under standard conditions and  $a_i$  is the activity of species  $i$  in the solution. By combining Equations (8) and (9) and noting that  $n_2/n_w = M_w m_2/1000$  and  $d\mu_i^\circ \equiv 0$  gives:

$$m_2 d \ln a_2 + \frac{1000}{M_w} d \ln a_w = 0, \quad (10)$$

where  $m_2$  is the molality of species 2 and  $M_w$  is the molecular weight of water. Integrating this expression from  $m_2' = 0$  to  $m_2 = m_2$  gives:

$$\ln \frac{a_w(m_2)}{a_w(0)} = - \frac{M_w}{1000} \int_0^{m_2} \frac{m_2'}{a_2} \frac{da_2}{dm_2'} dm_2'. \quad (11)$$

Although the integrand of Equation (11) is difficult to evaluate for these highly concentrated solutions, it is sufficient to show that the integrand is greater than zero to demonstrate that the DRH of one electrolyte is lowered by the addition of a second electrolyte. The solutes that are being considered here behave like most strong electrolytes. At low ionic strengths their activity coefficient,  $\gamma$ , decreases with increasing concentration according to Debye–Huckel theory. At intermediate ionic strengths their activity coefficient

levels-out, and at high ionic strengths it increases with concentration. Solutions that are in equilibrium with the solid phases typical of atmospheric aerosols have high ionic strength, so  $d\gamma_2/dm_2 > 0$  and thus  $da_2/dm_2 > 0$ . Even at low ionic strength where Debye–Huckel theory applies the decrease in  $\gamma_2$  with increasing concentration is not enough to cause  $a_2$  to decrease with increasing concentration. That the water activity is at a minimum at the mutual solubility point has been stated without proof in previous work (Kirgintsev and Trushnikova, 1968) and substantiating data for atmospherically relevant salt pairs are given in Table 5.

Since the integrand is greater than zero, the activity of water (which is equivalent to the DRH of solute 1 since the solution is in equilibrium with the solid phase of electrolyte 1) decreases as electrolyte 2 is added to the system until the solid phase of salt 2 forms. Adding more electrolyte 2 to the solution beyond this point increases the amount of salt in the solid phase, but does not change the composition of the solution. For solutions with more than two electrolytes, a similar analysis can be used to prove that the DRH of a salt in a multicomponent solution is always lower than its DRH in solution alone.

Evaluation of Equation (11) is complicated because there is no rigorous theory for the activity of an electrolyte in a solution saturated with another electrolyte, so we will assume that the electrolyte activities obey a generalized Harned's rule (Harned and Owen, 1958, p. 600):

$$\gamma_2(m_2) = \gamma_2(0) \exp(\alpha_2 m_2), \quad (12)$$

where  $\gamma_2$  is the activity coefficient of electrolyte 2 at molality  $m_2$  and  $\alpha_2$  is an arbitrary constant determined from data.

For a simple binary mixture of two uni-univalent electrolytes  $a = \gamma^2 m_{\text{cation}} m_{\text{anion}}$ . If we consider, for example, the system  $\text{NH}_4\text{NO}_3\text{--NH}_4\text{Cl--H}_2\text{O}$ , then  $a_{\text{NH}_4\text{NO}_3} = \gamma_{\text{NH}_4\text{NO}_3}^2 m_{\text{NH}_4^+} m_{\text{NO}_3^-}$  and  $a_{\text{NH}_4\text{Cl}} = \gamma_{\text{NH}_4\text{Cl}}^2 m_{\text{NH}_4^+} m_{\text{Cl}^-}$ , which for this system is  $a_{\text{NH}_4\text{NO}_3} = \gamma_{\text{NH}_4\text{NO}_3}^2$

Table 5. Deliquescence relative humidity at mutual solubility point at 303 K

Compounds	MDRH	DRH <sub>1</sub>	DRH <sub>2</sub>
$\text{NH}_4\text{NO}_3 + \text{NaCl}$	42.2*	59.4	75.2
$\text{NH}_4\text{NO}_3 + \text{NaNO}_3$	46.3	59.4	72.4
$\text{NH}_4\text{NO}_3 + \text{NH}_4\text{Cl}$	51.4	59.4	77.4
$\text{NaNO}_3 + \text{NH}_4\text{Cl}$	51.9*	72.4	77.2
$\text{NH}_4\text{NO}_3 + (\text{NH}_4)_2\text{SO}_4$	62.3	59.4	79.2
$\text{NaNO}_3 + \text{NaCl}$	67.6	72.4	75.2
$\text{NaCl} + \text{NH}_4\text{Cl}$	68.8	75.2	77.2
$\text{NH}_4\text{Cl} + (\text{NH}_4)_2\text{SO}_4$	71.3	77.2	79.2

Note: DRH<sub>1</sub> corresponds to the first salt in the compound; DRH<sub>2</sub> corresponds to the second.

Source: Adams and Merz (1929) for all single and mutual DRH values except for the MDRH values indicated.

\* The stable solids are  $\text{NaNO}_3$  and  $\text{NH}_4\text{Cl}$  at this temperature. Source: Merz *et al.* (1933).

$(m_{\text{NH}_4\text{NO}_3} + m_{\text{NH}_4\text{Cl}})m_{\text{NH}_4\text{NO}_3}$  and  $a_{\text{NH}_4\text{Cl}} = \gamma_{\text{NH}_4\text{Cl}}^2(m_{\text{NH}_4\text{NO}_3} + m_{\text{NH}_4\text{Cl}})m_{\text{NH}_4\text{Cl}}$ . Using these expressions and Equation (12) we can integrate Equation (11) and evaluate the constants  $\alpha_{\text{NH}_4\text{NO}_3} = -0.028$  and  $\alpha_{\text{NH}_4\text{Cl}} = 0.051$  from the solubility data of Prutton *et al.* (1935) and the water activity data at saturation of Adams and Merz (1929) (see Table 5). The resulting approximate solution to Equation (11) for the system saturated with  $\text{NH}_4\text{Cl}$  is:

$$\frac{a_w(m_{\text{NH}_4\text{NO}_3})}{0.774} = \exp \left[ -\frac{18}{1000} \{ 2m_{\text{NH}_4\text{NO}_3} - 0.028m_{\text{NH}_4\text{NO}_3}^2 + m_{\text{NH}_4\text{Cl}} \ln(1 - X_{\text{NH}_4\text{NO}_3}) \} \right], \quad (13)$$

and for the system saturated with  $\text{NH}_4\text{NO}_3$  it is:

$$\frac{a_w(m_{\text{NH}_4\text{Cl}})}{0.594} = \exp \left[ -\frac{18}{1000} (2m_{\text{NH}_4\text{Cl}} + 0.051m_{\text{NH}_4\text{Cl}}^2 + m_{\text{NH}_4\text{NO}_3} \ln X_{\text{NH}_4\text{NO}_3}) \right], \quad (14)$$

where  $X_{\text{NH}_4\text{NO}_3} \equiv m_{\text{NH}_4\text{NO}_3} / (m_{\text{NH}_4\text{NO}_3} + m_{\text{NH}_4\text{Cl}})$  is the solute relative mole fraction. By evaluating Equations (13) and (14) at the molalities determined by Prutton *et al.* (1935) we can plot the water activity at saturation as a function of  $X_{\text{NH}_4\text{NO}_3}$ . This curve is displayed in Fig. 1.

When  $X_{\text{NH}_4\text{NO}_3}$  is 0, the aerosol contains  $\text{NH}_4\text{Cl}$  and water, and the solution deliquesces at 77.4% r.h. If  $\text{NH}_4\text{NO}_3$  is added to the solution, the DRH de-

creases along curve 1 until a precipitate of  $\text{NH}_4\text{NO}_3$  forms at  $X_{\text{NH}_4\text{NO}_3} = 0.811$ . The solution in equilibrium with precipitates of both  $\text{NH}_4\text{Cl}$  and  $\text{NH}_4\text{NO}_3$  has the mutual deliquescence relative humidity, MDRH, of 51.4%. Likewise, when  $X_{\text{NH}_4\text{NO}_3}$  is 1, the aerosol contains  $\text{NH}_4\text{NO}_3$  and water, and the solution deliquesces at 59.4%. If  $\text{NH}_4\text{Cl}$  is added to the solution, the DRH follows curve 2 until the precipitate of  $\text{NH}_4\text{Cl}$  forms at  $X_{\text{NH}_4\text{NO}_3} = 0.811$ .

In region a of Fig. 1, the ambient r.h. is above both deliquescence points, and the salts are completely dissolved. In region b, the ambient r.h. is between the deliquescence points of the two electrolytes. The mixture is in solution for combinations of composition and r.h. to the right of line 1, whereas the mixture exists as solid  $\text{NH}_4\text{Cl}$  in equilibrium with a solution of both electrolytes to the left of line 1. In region c, the ambient r.h. is below the deliquescence points for both electrolytes, but the Gibbs free energy of the system is not necessarily minimized by the aerosol particle becoming a solid. Instead the mixture exists as a solution between lines 1 and 2. To the left of line 1 the mixture exists as  $\text{NH}_4\text{Cl}(s)$  in equilibrium with a solution of both electrolytes, whereas to the right of line 2 the mixture exists as  $\text{NH}_4\text{NO}_3(s)$  in equilibrium with a solution of both electrolytes. Finally, in region d the ambient r.h. is below the MDRH and the mixture is composed of  $\text{NH}_4\text{NO}_3(s)$  and  $\text{NH}_4\text{Cl}(s)$ .

Let us now examine what transpires as a particle of given composition is exposed to decreasing r.h. Starting at say 80% r.h. and  $X_{\text{NH}_4\text{NO}_3} = 0.4$ , the particle is aqueous. As the r.h. drops the solution becomes more concentrated until at about 70% r.h.  $\text{NH}_4\text{Cl}(s)$  forms. Further decreases in r.h. result in precipitation of additional  $\text{NH}_4\text{Cl}(s)$  such that  $X_{\text{NH}_4\text{NO}_3}$  in the aqueous phase follows curve 1. Finally at an r.h. of 51.4%

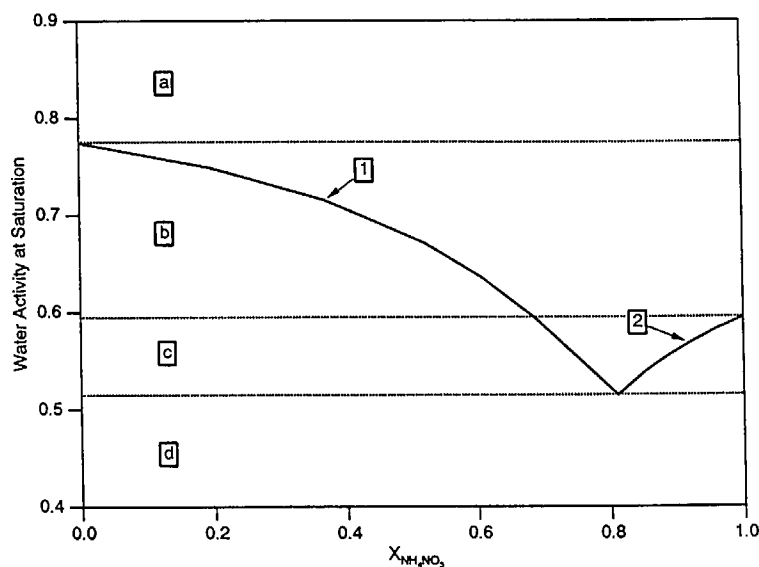


Fig. 1. Water activity at saturation of an aqueous solution of  $\text{NH}_4\text{NO}_3$  and  $\text{NH}_4\text{Cl}$ .

the aqueous phase reaches  $X_{\text{NH}_4\text{NO}_3} = 0.811$  and  $\text{NH}_4\text{NO}_3(\text{s})$  forms. Further decreases in r.h. cause the aerosol to abruptly effloresce.

It has been assumed that as an aerosol particle is dissolved during exposure to steadily increasing r.h., the  $\text{H}_2\text{O}$  mass of the aerosol will experience step increases at each of the single-component deliquescence points (e.g. Rood *et al.*, 1987; Pilinis *et al.*, 1989). A consequence of deliquescence point lowering in multicomponent solutions is that the theory does not allow step changes in aerosol  $\text{H}_2\text{O}$  mass as the ambient r.h. is raised or lowered; there is at most one step and this step corresponds to the mutual deliquescence point of the solution. For r.h. below the MDRH, the aerosol is dry. Just above the MDRH, the aerosol consists of one or more solids in equilibrium with a highly concentrated solution that contains the dissolved components of these solids. This is the only step change. Further increases in r.h. cause more of the solid phases to dissolve until finally one by one the solid phases each disappear. The r.h. where a given solid completely dissolves corresponds to its DRH in the multicomponent solution, but does not correspond to a step change in the aerosol mass. Instead a plot of aerosol mass vs relative humidity would exhibit abrupt changes in slope at these DRH points (Winkler, 1973, 1988). Abrupt changes in aerosol mass may occur due to nucleation events or hysteresis effects, but equilibrium thermodynamics does not predict them.

Thus, the assumption that a salt will not precipitate at relative humidities above its single electrolyte deliquescence point is valid for electrolytes that do not precipitate as double salts or solid solutions. In the next section we will explore how these single electrolyte deliquescence points vary with temperature.

#### Variation of DRH with temperature

The DRH for a single electrolyte in solution can increase, decrease, or remain constant as the temperature of the solution and the surrounding gas is varied (O'Brien, 1948). The temperature dependence of DRH has been explored for  $\text{NH}_4\text{NO}_3$  (Stelson and Seinfeld, 1982) and  $\text{NH}_4\text{Cl}$  (Pio and Harrison, 1987), who both showed a significant decrease in DRH with increasing temperature. In this section we will derive an expression for the variation of DRH with temperature and, for atmospherically relevant electrolytes, compare this variation to the existing experimental evidence.

Consider a single-component aqueous electrolyte solution in equilibrium with both water vapor and the crystalline form of the electrolyte. Denbigh (1981, Equation 7-11, p. 218) derives an expression for the variation of water vapor pressure with temperature for such a system:

$$\frac{d \ln p_s}{dT} = \frac{\Delta H}{RT^2}, \quad (15)$$

where  $p_s$  is the water vapor pressure over the solution,  $\Delta H = L_{w,s} + (M_w/1000) m_s L_s$  is the change in enthalpy of the system when 1 mol of water is evaporated and a corresponding  $(M_w/1000) m_s$  mol of solute are fused,  $m_s$  is the molality of the solute at saturation,  $L_{w,s}$  is the latent heat of vaporization of water at molality  $m_s$ , and  $L_s$  is the latent heat of fusion of the electrolyte from saturated solution at molality  $m_s$ .

The variation of water vapor pressure over pure water with temperature is given by the Clausius-Clapeyron equation (Denbigh, 1981, Equation 6-11, p. 200):

$$\frac{d \ln p_p}{dT} = \frac{L_{w,p}}{RT^2}, \quad (16)$$

where  $p_p$  is the water vapor pressure over pure water and  $L_{w,p}$  is the latent heat of vaporization of pure water. For sufficiently low vapor pressures such as exist under typical atmospheric conditions, the water activity,  $a_w$ , can be expressed in terms of the water vapor pressure over solution,  $p_s$ , and the water vapor pressure over pure water,  $p_p$ , by  $a_w = p_s/p_p$ . Differentiating the logarithm of this expression with respect to temperature gives:

$$\frac{d \ln a_w}{dT} = \frac{d \ln p_s}{dT} - \frac{d \ln p_p}{dT}. \quad (17)$$

Combining Equations (15)–(17) yields an expression for the variation in water activity with temperature in an electrolyte solution in equilibrium with the crystalline phase of the salt:

$$\frac{d \ln a_w}{dT} = \frac{L_{w,s} - L_{w,p} + \frac{M_w}{1000} m_s L_s}{RT^2}. \quad (18)$$

If we now assume that the molality and latent heats are relatively constant over small excursions in ambient temperature, this equation can be integrated to yield:

$$\ln \frac{a_w(T)}{a_w(T_0)} = -\frac{L_{w,s} - L_{w,p} + \frac{M_w}{1000} m_s L_s}{R} \left( \frac{1}{T} - \frac{1}{T_0} \right) \quad (20)$$

where  $T_0$  is the temperature at which the water activity is known and is typically 298.15 K. If we further assume that the latent heat of vaporization of water is not significantly affected by the presence of the solute then  $L_{w,s} - L_{w,p} \ll (M_w/1000) m_s L_s$  and:

$$\ln \frac{a_w(T)}{a_w(T_0)} = -\frac{M_w}{1000} m_s \frac{L_s}{R} \left( \frac{1}{T} - \frac{1}{T_0} \right). \quad (20)$$

Robinson and Stokes (1959) have measured the water activity in saturated solutions of  $\text{NaCl}$ ,  $\text{NaNO}_3$ ,  $\text{NH}_4\text{Cl}$ ,  $\text{NH}_4\text{NO}_3$ , and  $(\text{NH}_4)_2\text{SO}_4$  at 298.15 K. Using the activity and thermodynamic data of Table 6, Equation (20) can be evaluated for each

electrolyte:

$$(\text{NaCl}) \quad \ln \frac{a_w(T)}{0.7528} = 25 \left( \frac{1}{T} - \frac{1}{298.15} \right); \quad (21)$$

$$(\text{NaNO}_3) \quad \ln \frac{a_w(T)}{0.7379} = 304 \left( \frac{1}{T} - \frac{1}{298.15} \right); \quad (22)$$

$$(\text{NH}_4\text{Cl}) \quad \ln \frac{a_w(T)}{0.7710} = 239 \left( \frac{1}{T} - \frac{1}{298.15} \right); \quad (23)$$

$$(\text{NH}_4\text{NO}_3) \quad \ln \frac{a_w(T)}{0.6183} = 852 \left( \frac{1}{T} - \frac{1}{298.15} \right); \quad (24)$$

$$((\text{NH}_4)_2\text{SO}_4) \quad \ln \frac{a_w(T)}{0.7997} = 80 \left( \frac{1}{T} - \frac{1}{298.15} \right). \quad (25)$$

Stelson and Seinfeld (1982), using a least squares regression, obtained 856 for the slope in Equation (24) from data in Dingemans (1941). With a lack of other information, their hypothesis for the temperature dependence of the DRH for  $\text{NH}_4\text{NO}_3$  implied that this dependence was the same for all electrolytes, which we now see is not the case as evidenced by Equations (21)–(25). Pio and Harrison (1987) present data that imply a linear relationship between DRH and temperature for  $\text{NH}_4\text{Cl}$ , but the slope of their curve ( $da_w/dT = 2.02 \times 10^{-3} \text{ K}^{-1}$ ) is in excellent agreement with the slope of Equation (23) at 298 K ( $da_w/dT = 2.09 \times 10^{-3} \text{ K}^{-1}$ ).

A few important assumptions were used to derive Equations (20)–(25). First we assumed that the latent heat of vaporization of water is not changed significantly by the presence of the solute. Second, we extrapolated the enthalpy data of Wagman *et al.* (1982) to saturation molalities. Third, we assumed that the molality at saturation,  $m_s$ , does not change significantly over the range of temperatures of atmospheric relevance. And finally we assumed that over this range of temperature and molality the latent heat of fusion of the salt,  $L_s$ , does not change significantly. To investigate the validity of Equations (21)–(25), they are

compared to experimental data in Figs 2–6. The data are from measurements of water vapor pressure or r.h. over saturated salt solutions. Since the solution and the vapor are in equilibrium, the r.h. and water activity are identical. The agreement between the data and the equations is generally within  $\pm 1\%$  r.h. Thus Equations (20)–(25) accurately represent the temperature dependence of DRH in the range 283–313 K and the available enthalpy data (Wagman *et al.*, 1982) can be extrapolated to obtain enthalpy data at saturation without introducing substantial error.

#### Sodium sulfate

Sodium sulfate, a constituent of atmospheric aerosols, is not included here because the data in Wagman *et al.* (1982) are not as accurate as for the electrolytes listed above (see Wagman *et al.*, 1982, pp. 2–16) and the predicted temperature dependence does not agree with the available data. Enough information is available about sodium sulfate at least to give a semi-quantitative picture of its deliquescence behaviour. At 298 K and r.h. below about 81% (Baxter and Lansing, 1920; Wilson, 1921), sodium sulfate exists as  $\text{Na}_2\text{SO}_4(\text{s})$ . At 81% r.h.,  $\text{Na}_2\text{SO}_4$  and  $\text{Na}_2\text{SO}_4 \cdot 10\text{H}_2\text{O}$  are in equilibrium. Between 81% and a higher r.h. (e.g. 86%, Leopold and Johnston, 1927; 97%, Csontos, 1956) that we will call  $\text{DRH}_{10}$ ,  $\text{Na}_2\text{SO}_4 \cdot 10\text{H}_2\text{O}(\text{s})$  is the stable species although metastable  $\text{Na}_2\text{SO}_4(\text{s})$  has often been observed (e.g. Leopold and Johnston, 1927). At  $\text{DRH}_{10}$ ,  $\text{Na}_2\text{SO}_4 \cdot 10\text{H}_2\text{O}(\text{s})$  is in equilibrium with its aqueous solution and above  $\text{DRH}_{10}$  only the aqueous solution exists.

Below about 305 K, sodium sulfate has, in effect, two deliquescence points. The first occurs where the anhydrous and decahydrate salts are in equilibrium. The second occurs where the decahydrate salt and aqueous solution are in equilibrium. A triple point occurs at about 305 K where all three stable forms, anhydrous, decahydrate, and aqueous solution, exist

Table 6. Data at 298.16 K for calculating temperature dependence of deliquescence relative humidity

Species	DRH*	$\Delta H_{\text{cr}}\dagger$ kJ mol <sup>-1</sup>	$\Delta H_{\text{aq}}\ddagger$ kJ mol <sup>-1</sup>	$m_s$ mol kg <sup>-1</sup>	$\frac{M_w}{1000} \frac{L_s}{R}$ K
NaCl	0.7528	-411.153	-409.3	6.144§	-25
NaNO <sub>3</sub>	0.7379	-467.85	-454.9	10.830§	-304
NH <sub>4</sub> Cl	0.7710	-314.43	-299.5	7.405§	-239
NH <sub>4</sub> NO <sub>3</sub>	0.6183	-365.56	-350.4	25.954§	-852
(NH <sub>4</sub> ) <sub>2</sub> SO <sub>4</sub>	0.7997	-1180.85	-1174.5	5.843	-80

Symbols:  $\Delta H_{\text{cr}}$  is the standard heat of formation of the crystalline phase and  $\Delta H_{\text{aq}}$  is the standard heat of formation of the species in aqueous solution at molality  $m_s$ .  $L_s = \Delta H_{\text{cr}} - \Delta H_{\text{aq}}$  is the latent heat of fusion for the salt from a saturated solution,  $R$  is the gas constant, and  $M_w$  is the molecular weight of water.

Sources:

\* Robinson and Stokes (1959);

† Wagman *et al.* (1982);

‡ extrapolated from Wagman *et al.* (1982);

§ Hamer and Wu (1972);

|| Wishaw and Stokes (1954).

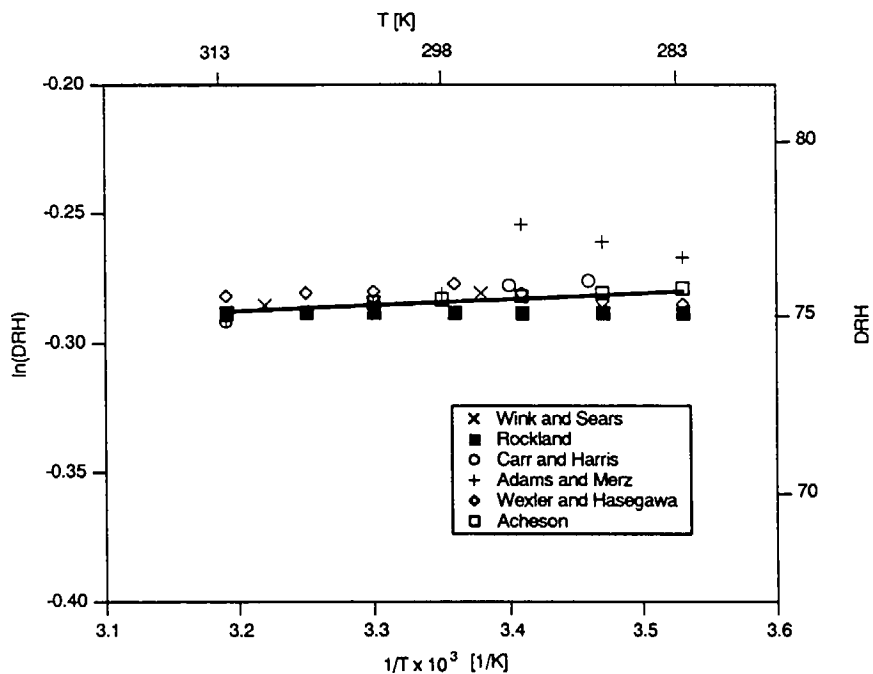


Fig. 2. Temperature dependence of DRH for NaCl.

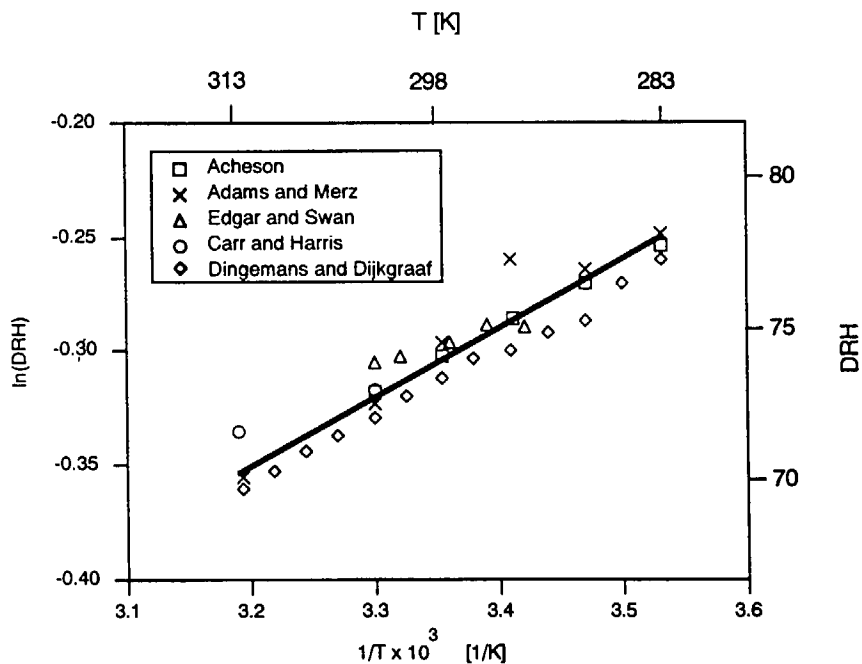


Fig. 3. Temperature dependence of DRH for NaNO<sub>3</sub>.

in mutual equilibrium. Above the triple point temperature, there is one deliquescence point where the anhydrous salt and aqueous solutions are in equilibrium and the decahydrate form is no longer stable.

Other sulfates of ammonium and sodium have been

observed in the atmosphere, but due to lack of sufficient data, analysis of their deliquescence properties as a function temperature will not be attempted. The solubility diagram for the ammonium sulfates at 303 K is available in Tang *et al.* (1978), and the

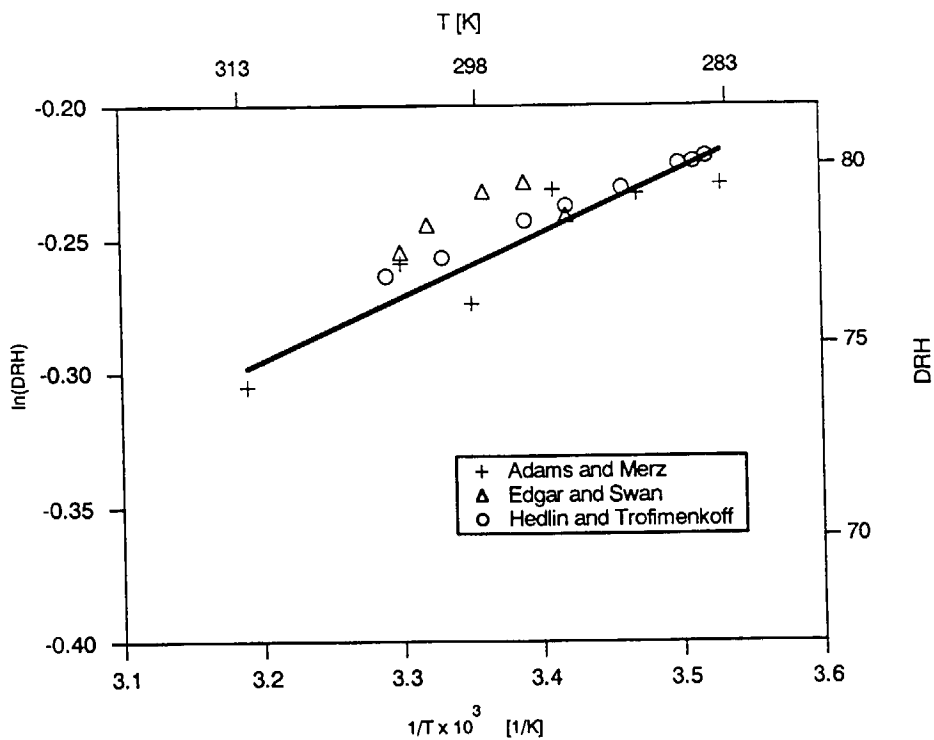
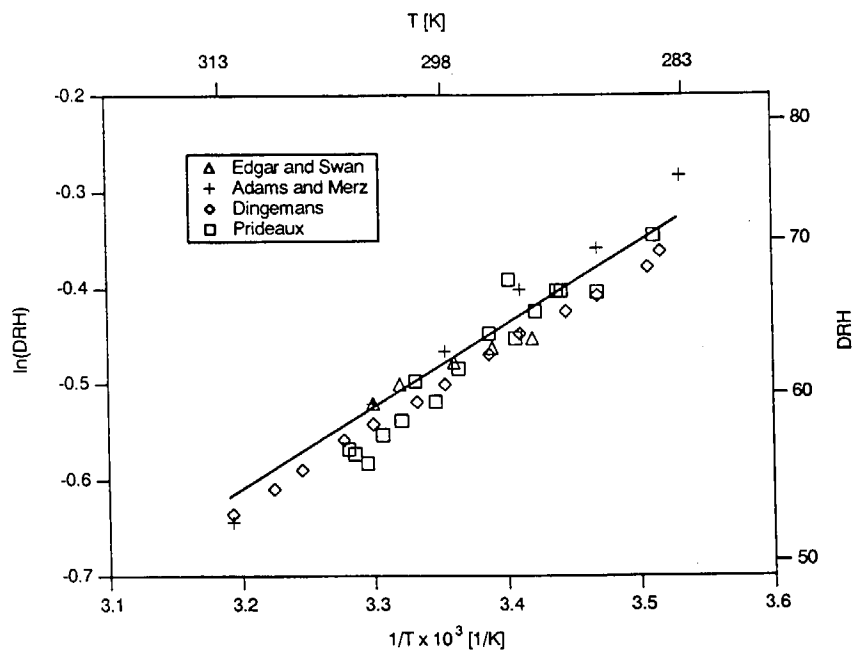


Fig. 4. Temperature dependence of DRH for  $\text{NH}_4\text{Cl}$ .



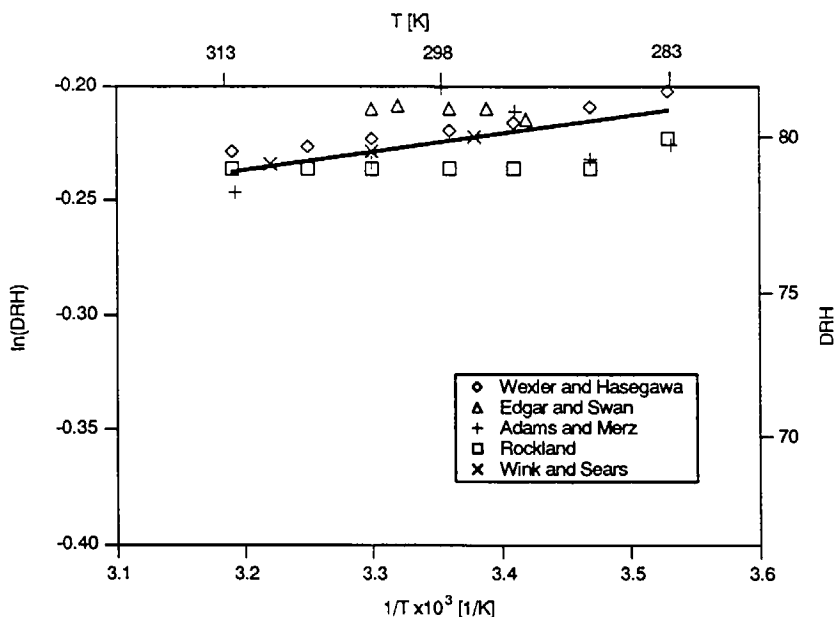


Fig. 6. Temperature dependence of DRH for  $(\text{NH}_4)_2\text{SO}_4$ .

corresponding diagram for sodium sulfates and their hydrates at 298 K is available in Gmelins, supplement 3 (1966).

#### Modelling implications

Previous models of the inorganic components of atmospheric aerosol (MARS: Saxena *et al.*, 1986; SEQUILIB: Pilinis and Seinfeld, 1987) have assumed, first, that the deliquescence point does not significantly vary with temperature, and second, that the aerosol is a solid below the lowest DRH of the aerosol electrolytes. The first assumption may result in serious over- or underprediction of the water content of the aerosol at temperatures other than 298 K. This is especially important for common aerosol species such as  $\text{NH}_4\text{NO}_3$ ,  $\text{NH}_4\text{Cl}$ , and  $\text{NaNO}_3$ , each of whose DRH has a significant temperature dependence. In this section, we have presented a consistent theory that accurately predicts the temperature variation of five salts of atmospheric relevance as evidenced by a large body of independent experimental data. AIM employs Equations (21)–(25) to assess the temperature dependence of each of these deliquescence points. The deliquescence points of other salts are assumed to be constant.

As a result of the second assumption noted above, the computer codes SEQUILIB and MARS predict a dry aerosol at r.h. significantly above the actual deliquescence point of the mixture. In a subsequent section we compare the predictions of AIM and SEQUILIB under typical atmospheric conditions.

#### COMPARISON OF PREDICTED AND MEASURED ACTIVITIES

In AIM, the activity coefficients of the solutes are predicted by the method of Kusik and Meissner (1978) and the aerosol water content is predicted by the ZSR method (Zdanovskii, 1948; Stokes and Robinson, 1966). Both of these methods are empirical in nature and their accuracy has not been established for the mix of solutes found in atmospheric aerosol particles. In this section, the components of the model that predict the thermodynamic properties of aerosol aqueous solutions will be compared to fundamental data.

#### Single-solute activity coefficients

The Meissner electrolyte activity model is a so-called single parameter model and Kusik and Meissner (1978) report recommended values for this parameter that agree with the available activity data ( $\text{NaNO}_3$ : Wu and Hamer, 1980;  $(\text{NH}_4)_2\text{SO}_4$ : Wishaw and Stokes, 1954;  $\text{Na}_2\text{SO}_4$ : Goldberg, 1981;  $\text{NaCl}$ ,  $\text{NH}_4\text{Cl}$ , and  $\text{NH}_4\text{NO}_3$ : Hamer and Wu, 1972) to within about 10% over the range of 1 M to saturation. For  $\text{HCl}$  and  $\text{HNO}_3$  we use parameter values of 6.0 and 2.6, respectively, so that the model fits the data over a wider range of ionic strengths, 1–16 M. For  $\text{H}_2\text{SO}_4$ , no parameter value is supplied and we chose 0.7 as a best fit. For these acids, Figs 7–9 compare the activity coefficients predicted by the model and the reported data ( $\text{HCl}$  and  $\text{HNO}_3$ : Hamer and Wu, 1972;  $\text{H}_2\text{SO}_4$ : Staples, 1981). The agreement between pre-

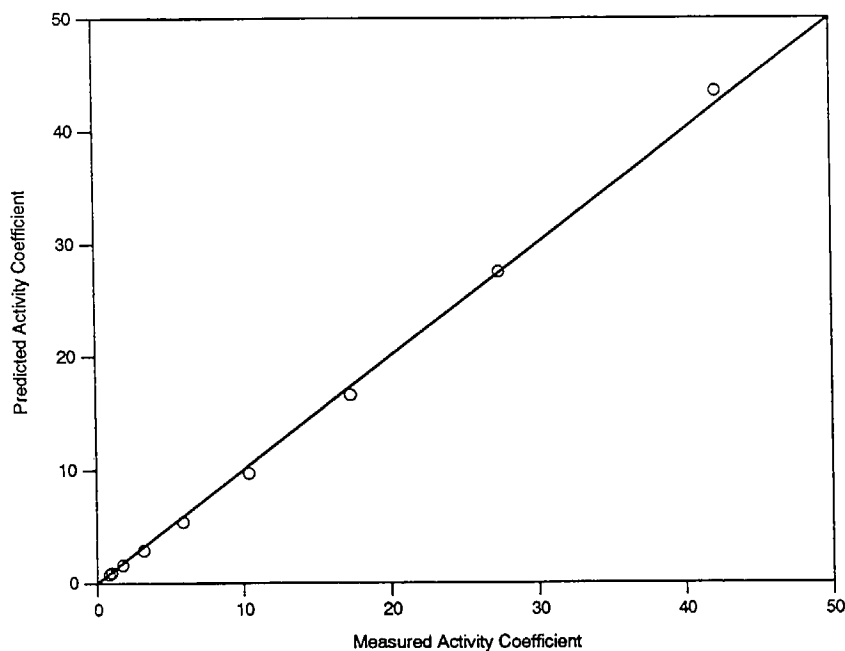


Fig. 7. Predicted vs measured activity coefficient for HCl.

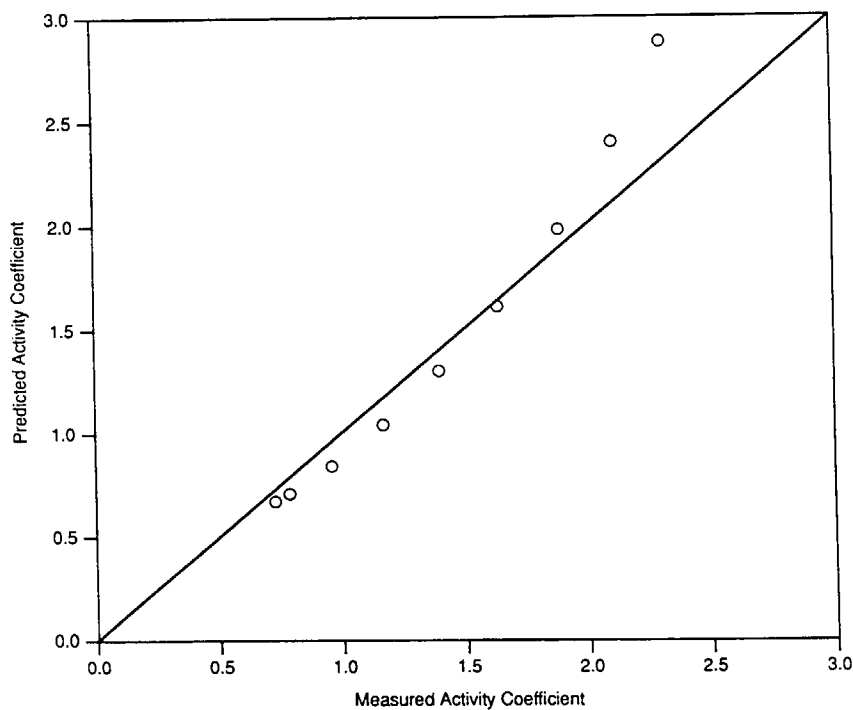


Fig. 8. Predicted vs measured activity coefficient for HNO<sub>3</sub>.

dictions and measurements is good except for H<sub>2</sub>SO<sub>4</sub>, as has been previously addressed (Meissner and Pappas, 1973; Zemaitis *et al.*, 1986).

What is the impact of errors in the prediction of the H<sub>2</sub>SO<sub>4</sub> activity coefficient? The activity coefficient of H<sub>2</sub>SO<sub>4</sub> is used to calculate the activity coefficients of

NaHSO<sub>4</sub>, NH<sub>4</sub>HSO<sub>4</sub>, and (NH<sub>4</sub>)<sub>3</sub>H(SO<sub>4</sub>)<sub>2</sub>:

$$\gamma_{\text{NaHSO}_4} = \sqrt{\gamma_{\text{Na}_2\text{SO}_4} \gamma_{\text{H}_2\text{SO}_4}}$$

$$\gamma_{\text{NH}_4\text{HSO}_4} = \sqrt{\gamma_{(\text{NH}_4)_2\text{SO}_4} \gamma_{\text{H}_2\text{SO}_4}}$$

$$\gamma_{(\text{NH}_4)_3\text{H}(\text{SO}_4)_2} = (\gamma_{(\text{NH}_4)_2\text{SO}_4}^3 \gamma_{\text{H}_2\text{SO}_4})^{1/4}$$

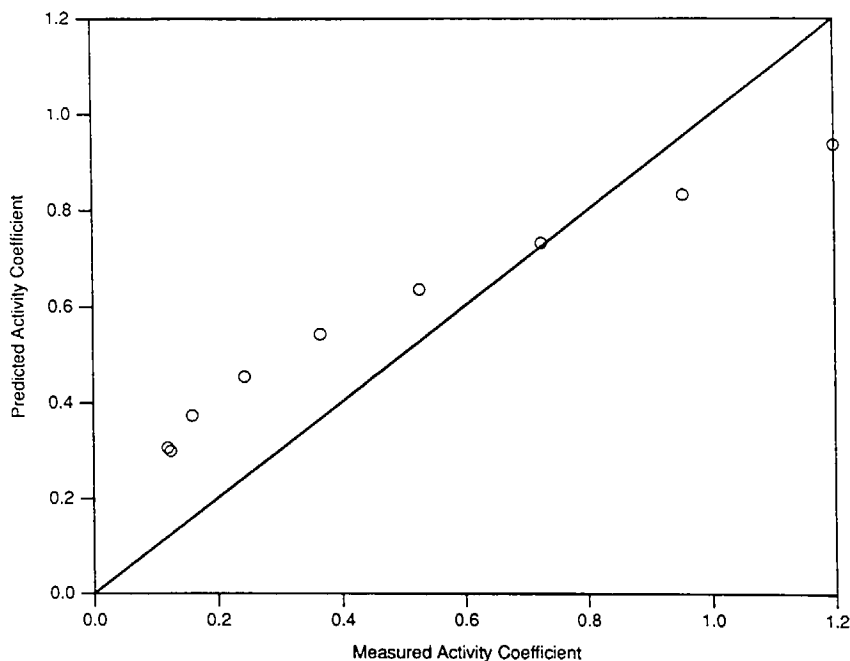


Fig. 9. Predicted vs measured activity coefficient for  $\text{H}_2\text{SO}_4$ .

which are then used to establish equilibrium between the aqueous phase and these three solid phases. Inaccuracies in the activity coefficients result in a maldistribution of these species between the solid and aqueous phases. For  $\text{NH}_4\text{HSO}_4$  and  $(\text{NH}_4)_3\text{H}(\text{SO}_4)_2$  this maldistribution will result in altered  $\text{NH}_4^+$  concentrations in the aqueous phase and therefore altered predictions of the surface gas-phase concentrations or gas-aerosol phase distribution of ammonia. The ability of any of the existing strong electrolyte activity models to predict the activity of complexing electrolytes, such as  $\text{H}_2\text{SO}_4$ , is limited (Zemaitis *et al.*, 1986). Since the square root or fourth root of  $\gamma_{\text{H}_2\text{SO}_4}$  is used in the calculation of the activities of  $\text{NaHSO}_4$ ,  $\text{NH}_4\text{HSO}_4$ , and  $(\text{NH}_4)_3\text{H}(\text{SO}_4)_2$ , the impact of any inaccuracy is substantially reduced.

#### Multiple-solute activity coefficients

There is a large body of experimental data on the activity coefficients of multi-component aqueous solutions (Harned and Robinson, 1968), but unfortunately, there are limited data on the systems of relevance here. Data are available for aqueous solutions of  $\text{NaCl-NaNO}_3$  (Lanier, 1965; Bezboruah *et al.*, 1970),  $\text{NaCl-HCl}$  (Lietzke *et al.*, 1965),  $\text{NaCl-Na}_2\text{SO}_4$  (Wu *et al.*, 1968; Lanier, 1965; Butler *et al.*, 1967),  $\text{HCl-NH}_4\text{Cl}$  (Robinson *et al.*, 1974), and  $\text{Na}_2\text{SO}_4\text{-H}_2\text{SO}_4$  (Akerlof, 1926). For the first four systems the predicted and measured activity coefficients agree to within 6%. For the fifth system the values differ by a nearly constant factor of two, not an unexpected result considering the poor fit for single component sulfate solutions.

The ZSR relationship, given in Equation (5), requires single component water activity data as a function of molality. These data are entered into AIM and SEQUILIB in tabular form for each electrolyte (Pilin and Seinfeld, 1987) and so for single electrolyte solutions, the model and data agree by definition. For multicomponent solutions, water activity has been measured in aqueous solutions of  $\text{NaCl-NH}_4\text{Cl}$  (Kirgintsev and Luk'yanov, 1963),  $\text{NaCl-NaNO}_3$  (Kirgintsev and Luk'yanov, 1964; Bezboruah *et al.*, 1970),  $\text{NaNO}_3\text{-NH}_4\text{NO}_3$  (Kirgintsev and Luk'yanov, 1965),  $\text{NaCl-(NH}_4)_2\text{SO}_4$  (Cohen *et al.*, 1987), and  $\text{NaCl-Na}_2\text{SO}_4$  (Wu *et al.*, 1968). All of these data are predicted to within a few per cent by the ZSR model, even for the supersaturated solutions of Cohen *et al.* (1987). Stokes (1948) has measured the water activity of  $\text{NaHSO}_4$  solutions, which are equivalent to the equimolar solution  $\text{Na}_2\text{SO}_4\text{-H}_2\text{SO}_4$ . Figure 10 shows the predicted and measured molalities as a function of water activity. At high water activities corresponding to dilute solutions, the molalities are in agreement. As the water activity decreases, the predictions and measurements deviate. At  $a_w = 0.765$ , the deviation in the two values has reached about 25%. This deviation is due to the formation of the bisulfate ion at the higher concentrations.

With the exception of solutions that contain  $\text{H}_2\text{SO}_4$ , the Kusik and Meissner and ZSR models accurately predict the activity of the solutes and the mass of water. In typical urban aerosols, sulfate is mostly neutralized by sodium and ammonium, and under these conditions the sulfate activities will be accurately predicted. Aerosol pH is usually lowest immedi-

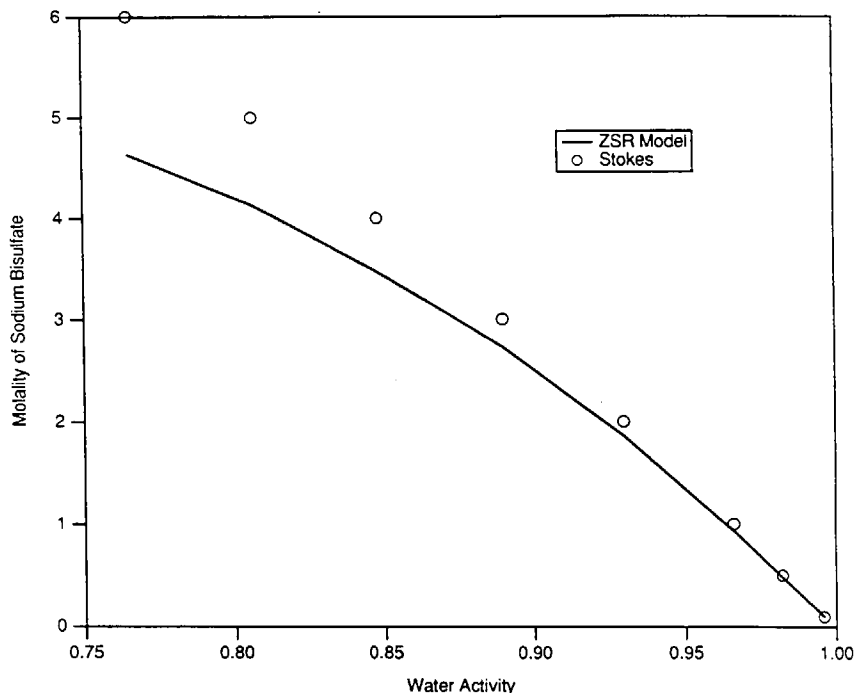


Fig. 10. Predicted and measured  $\text{NaHSO}_4$  concentration as a function of water activity.

ately after a fog. In Los Angeles post-fog conditions (Jacob *et al.*, 1985), aerosols are composed primarily of ammonium, nitrate, and sulfate. The low pH results in rapid evaporation of nitric acid and neutralization of the sulfate by ammonia. Thus we expect that any large  $\text{H}_2\text{SO}_4$  concentrations will be rapidly neutralized by ammonium and that inaccuracies in sulfate activity will have only a transient effect on the overall predictions of aerosol composition. The model is least accurate under atmospheric conditions with a large generation of sulfate and insufficient aerosol sodium or ammonium to neutralize this sulfate.

#### COMPARISON OF EQUILIBRIUM MODELS

AIM consists of two components: the thermodynamic portion and the transport portion. In this section the thermodynamic portion of the code is tested by running AIM until equilibrium is attained between the aerosol and gas phases. Pilinis and Seinfeld (1987) compared their SEQUILIB model to the predictions of EQUIL (Bassett and Seinfeld, 1983) and MARS (Saxena *et al.*, 1986) and found general agreement. EQUIL is an early aerosol equilibrium model that only includes ammonium, nitrate, and sulfate. MARS considers these same components, but is faster than EQUIL because it divides the composition and r.h. space up into regions. In each region, fewer phases need to be considered so less computing is performed to minimize the Gibbs free energy. SEQUILIB

uses the same approach as MARS, but in addition, sodium and chloride are considered. In this section the SEQUILIB model will be compared to AIM.

Table 7 reproduces the results of the conditions examined in Table 7 of Pilinis and Seinfeld (1987). At the lowest r.h. there is substantial disagreement between the two models. At 46% r.h. both models predict the aerosol to be composed of  $\text{NH}_4\text{NO}_3(\text{s})$  and  $(\text{NH}_4)_2\text{SO}_4(\text{s})$ . The disagreement between the models is due to a difference in the equilibrium constant for the reaction  $\text{NH}_4\text{NO}_3(\text{s}) \rightleftharpoons \text{NH}_3(\text{g}) + \text{HNO}_3(\text{g})$ . SEQUILIB uses the free energy of formation data from Parker *et al.* (1976), JANAF (1971), and Wagman *et al.* (1968) to obtain an equilibrium constant of 30  $\text{ppb}^2$ . AIM uses the more recent and self-consistent data contained in Tables 1-3 (Wagman *et al.*, 1982) to obtain an equilibrium constant of 58  $\text{ppb}^2$ . This factor of two difference in equilibrium constants results in AIM predicting much higher gas-phase concentrations of  $\text{NH}_3$  and  $\text{HNO}_3$  and correspondingly lower aerosol-phase concentrations of  $\text{NH}_4\text{NO}_3$ .

At 298 K, the deliquescence point of  $\text{NH}_4\text{NO}_3$  occurs at 62% r.h. For ambient r.h. of 51, 56 and 61%, SEQUILIB assumes that the aerosol is composed of  $\text{NH}_4\text{NO}_3(\text{s})$  and  $(\text{NH}_4)_2\text{SO}_4(\text{s})$ , but as we have shown, the r.h. of deliquescence of a salt is lowered in multicomponent solutions. At 51% r.h. AIM predicts that the aerosol is composed of a solid phase,  $(\text{NH}_4)_2\text{SO}_4(\text{s})$ , in equilibrium with an aqueous phase containing  $\text{NH}_4^+$ ,  $\text{NO}_3^-$ , and  $\text{SO}_4^{2-}$ , whereas at 56 and 61% AIM predicts the aerosol to be composed of a

Table 7. Aerosol model predictions of  $\text{NO}_3^-$ ,  $\text{NH}_4^+$ , and  $\text{H}_2\text{O}$  for  $T=298\text{ K}$ ,  $10\ \mu\text{g m}^{-3}\ \text{H}_2\text{SO}_4$ ,  $10\ \mu\text{g m}^{-3}\ \text{NH}_3$ , and  $30\ \mu\text{g m}^{-3}\ \text{HNO}_3$ 

r.h. %	AIM			SEQUILIB		
	$\text{NH}_4^+$ $\mu\text{g m}^{-3}$	$\text{NO}_3^-$ $\mu\text{g m}^{-3}$	$\text{H}_2\text{O}$ $\mu\text{g m}^{-3}$	$\text{NH}_4^+$ $\mu\text{g m}^{-3}$	$\text{NO}_3^-$ $\mu\text{g m}^{-3}$	$\text{H}_2\text{O}$ $\mu\text{g m}^{-3}$
46	5.9	7.6	0	7.4	12.9	0
51	6.0	7.9	8	7.4	12.9	0
56	6.5	9.7	11	7.4	12.9	0
61	7.0	11.4	15	7.4	12.9	0
66	7.4	13.0	20	7.8	14.0	19
71	7.8	14.3	25	8.2	15.5	26
76	8.2	15.6	34	8.6	16.8	35
81	8.5	17.5	47	9.0	18.3	49
86	8.9	19.4	71	9.4	19.7	73
91	9.6	20.6	129	9.8	21.2	124

single aqueous phase. That the two models differ in their prediction of the aerosol mass of ammonium and nitrate is primarily due to differences in the free energies of formation used by each model, but the difference in water mass is due to the incorrect assumption in SEQUILIB that each salt deliquesces at its individual DRH. At these three relative humidities, SEQUILIB predicts a dry aerosol, whereas AIM predicts a water content of 8, 11 and  $15\ \mu\text{g m}^{-3}$ , a significant portion of the total aerosol mass.

At relative humidities above 61% both models predict the aerosol to be composed of a single aqueous phase. Both models use similar thermodynamic properties to represent the aqueous phase so the agreement is excellent.

SEQUILIB employs two classes of assumption that we improve upon in AIM. The first is that the aerosol is composed solely of solid phases at r.h. below the lowest single-solute deliquescence point of the species in the aerosol. As we have proven previously and shown here, the deliquescence point is lowered for multicomponent solutions. Table 5 lists values of MDRH at 303 K for a number of salt pairs of atmospheric interest and all MDRH values, except that for  $\text{NH}_4\text{NO}_3$ - $(\text{NH}_4)_2\text{SO}_4$ , are significantly below each single electrolyte value.

When two electrolytes combine to precipitate a double salt, there are two mutual deliquescence relative humidities—one when the double salt and the first single salt are in equilibrium with solution, and the other when the double salt and the second single salt are in equilibrium with solution. This seemingly more complicated picture reduces to Fig. 1 if one of the electrolytes is considered to be the double salt and the other electrolyte is the single salt that exists in solid form. In the experiments of Adams and Merz (1929), some amount of  $(\text{NH}_4)_2\text{SO}_4$ (s) and  $\text{NH}_4\text{NO}_3$ (s) were combined with a small portion of water. This mixture was allowed to equilibrate and the resulting vapor pressure of water was measured. Adams and Merz hypothesized that the double salt  $(\text{NH}_4)_2\text{SO}_4$ - $2\text{NH}_4\text{NO}_3$  is formed by this mixture.

The DRH for  $(\text{NH}_4)_2\text{SO}_4$ - $2\text{NH}_4\text{NO}_3$  is 56.4% (Tang, 1980), which is significantly below the r.h. measured by Adams and Merz.

There are a number of possible explanations for this anomaly. That the system may not have reached equilibrium seems to be the most likely since solid-solid phase changes can be extremely slow. Another possibility is that a double salt such as  $(\text{NH}_4)_2\text{SO}_4$ - $3\text{NH}_4\text{NO}_3$  was formed (Tani *et al.*, 1983) which may have a higher DRH than that measured over the mixture. In this case, the  $\text{NH}_4\text{NO}_3$ (s) would have to have been completely transformed into the double salt to not violate Equation (11).

As can be seen in Table 5 for binary solutions, the MDRH values may be substantially lower than the single electrolyte DRH values. For solutions containing more components, the MDRH values are predicted to be even lower. For AIM to predict the MDRH values accurately, the ZSR water content model and Meissner solute activity model must be accurate for multicomponent solutions at ionic strengths exceeding 25 M (the solubility of  $\text{NH}_4\text{NO}_3$ ). At these high ionic strengths, uncertainties in both models do not permit the accurate prediction of MDRH values. Nevertheless, there is a range of relative humidities where AIM correctly predicts an aqueous aerosol and the previous equilibrium models erroneously predict a dry one.

## CONCLUSIONS

We have developed a model of the inorganic components of atmospheric aerosols, AIM. This model assumes that the components of the aerosol are in internal phase equilibrium and that the water activity of the aerosol is in equilibrium with the ambient relative humidity. Since the time constants for equilibration of the gas and aerosol phases may be large, equilibrium is not assumed between the gas and aerosol phase for the volatile inorganics, instead transport is explicitly modeled. Comparison between the

model predictions and experimentally determined electrolyte activities show satisfactory agreement except for  $\text{H}_2\text{SO}_4$ , but since most  $\text{H}_2\text{SO}_4$  is neutralized by  $\text{NH}_3$  in atmospheric aerosols  $\text{H}_2\text{SO}_4$  usually comprises a small portion of total aerosol mass.

Predictions of AIM have been improved over those of previous equilibrium models. First the distribution of  $\text{NH}_4\text{NO}_3$  between the gas and aerosol phases is based on more up-to-date thermodynamic data in AIM. Second, water may comprise a significant fraction of aerosol mass even under conditions of low r.h., so accurate prediction of aerosol water content is important. We have derived expressions for the temperature dependence of the single-component deliquescence point and proven that the deliquescence point in a multicomponent aerosol is lower than the single-component points. A common misconception is that multicomponent aerosols deliquesce at the lowest single-component deliquescence point. Pilinis *et al.* (1989) attempt to explain the non-zero water content that has been observed in aerosols below the lowest single-component deliquescence point by suggesting that the aerosol is composed of a supersaturated metastable solution instead of a stable one in equilibrium. Although there is experimental evidence that metastable states exist (Rood *et al.*, 1987), we have shown that non-zero water content at low relative humidities can be explained using equilibrium thermodynamic assumptions alone.

Urban airshed models that predict total aerosol mass or aerosol size distribution have assumed thermodynamic equilibrium between the gas and aerosol phase for the volatile inorganic components (Russell *et al.*, 1983; Hogo *et al.*, 1985; Pilinis and Seinfeld, 1988). We have shown in previous work (Wexler and Seinfeld, 1990) that thermodynamic equilibrium is not sufficient for determining the aerosol mass of volatile inorganics. In this paper we describe the development and testing of an aerosol inorganics model that assumes (1) thermodynamic equilibrium within the aerosol and between water in the gas and aerosol phases; and (2) transport of inorganics between the gas and aerosol phases. In subsequent work this aerosol model will be included in an urban airshed model and its predictions compared with gas and aerosol phase measurements taken during SCAQS.

*Acknowledgement*—This work was supported by the State of California Air Resources Board Agreement A932-054.

#### REFERENCES

- Acheson D. T. (1965) Vapor pressure of saturated aqueous salt solutions. In *Humidity and Moisture* (edited by Wexler A.), Vol. 3, pp. 521–530. Reinhold, New York.
- Adams J. R. and Merz A. R. (1929) Hygroscopicity of fertilizer materials and mixtures. *Indust. Eng. Chem.* **21**, 305–310.
- Akerlof G. (1926) Investigations of sulfate solutions. Experimental methods and results on cells without liquid junction. *J. Am. Chem. Soc.* **48**, 1160–1177.
- Allen A. G., Harrison R. M. and Erisman J. (1989) Field measurements of the dissociation of ammonium nitrate and ammonium chloride aerosols. *Atmospheric Environment* **23**, 1591–1599.
- Bassett M. and Seinfeld J. H. (1983) Atmospheric equilibrium model of sulfate and nitrate aerosols. *Atmospheric Environment* **17**, 2237–2252.
- Bassett M. E. and Seinfeld J. H. (1984) Atmospheric equilibrium model of sulfate and nitrate aerosols—II. Particle size analysis. *Atmospheric Environment* **18**, 1163–1170.
- Baxter G. P. and Lansing J. E. (1920) The aqueous pressure of some hydrated crystals. Oxalic acid, strontium chloride and sodium sulfate. *J. Am. Chem. Soc.* **42**, 419–426.
- Bezboruah C. P., Convington A. K. and Robinson R. A. (1970) Excess gibbs energies of aqueous mixtures of alkali metal chlorides and nitrates. *J. Chem. Thermodyn.* **2**, 431–437.
- Butler J. N., Hsu P. T. and Synnott J. C. (1967) Activity coefficient measurements in aqueous sodium chloride-sodium sulfate electrolytes using sodium amalgam electrodes. *J. phys. Chem.* **71**, 910–913.
- Carr D. S. and Harris B. L. (1949) Solutions for maintaining constant relative humidity. *Indust. Eng. Chem.* **41**, 2014–2015.
- Chen C.-C., Britt H. I., Boston J. F. and Evans L. B. (1982) Local composition model for excess gibbs energy of electrolyte systems. *AIChE J.* **28**, 588–596.
- Chen C.-C. and Evans L. B. (1986) A local composition model for the excess gibbs energy of aqueous electrolyte systems. *AIChE J.* **32**, 444–454.
- Cohen M. D., Flagan R. C. and Seinfeld J. H. (1987) Studies of concentrated electrolyte solutions using the electrodynamic balance. 2. Water activities for mixed-electrolyte solutions. *J. phys. Chem.* **91**, 4575–4582.
- Csontos E. (1956) Equilibrium relative humidity of saturated solutions of some crystalline compounds. *Agrokema Talajtan* **5**, 425–432.
- Denbigh K. (1981) *The Principles of Chemical Equilibrium*. Cambridge University Press, Cambridge.
- Dingemans P. (1941) Die dampfspannung von gestättigten  $\text{NH}_4\text{NO}_3$ -lösungen. *Rec. Trav. Chim.* **60**, 317–321.
- Dingemans P. and Dijkgraaf L. L. (1948) The vapour pressure of saturated solutions of sodium nitrate in water. *Rec. Trav. Chim.* **67**, 231–234.
- Edgar G. and Swan W. O. (1922) The factors determining the hygroscopic properties of soluble substances. I. The vapor pressures of saturated solutions. *J. Am. Chem. Soc.* **44**, 570–577.
- Gmelins (1966) *Gmelins Handbuch der Anorganischen Chemie, Natrium Ergänzungsband Lieferung 3*. Verlag Chemie, Weinheim.
- Goldberg R. N. (1981) Evaluated activity and osmotic coefficients for aqueous solutions: thirty-six uni-bivalent electrolytes. *J. phys. Chem. Ref. Data* **10**, 671–764.
- Gray H. A., Cass G. R., Huntzicker J. J., Heyerdahl E. K. and Rau J. A. (1986) Characteristics of atmospheric organic and elemental carbon particle concentrations in Los Angeles. *Envir. Sci. Technol.* **20**, 580–589.
- Haghtalab A. and Vera J. H. (1988) A nonrandom factor model for the excess gibbs energy of electrolyte solutions. *AIChE J.* **34**, 803–813.
- Hamer W. J. and Wu Y.-C. (1972) Osmotic coefficients and mean activity coefficients of uni-univalent electrolytes in water at 25 C. *J. phys. Chem. Ref. Data* **1**, 1047–1099.
- Hanel G. and Zankl B. (1979) Aerosol size and relative humidity: water uptake by mixtures of salts. *Tellus* **31**, 478–486.
- Harned H. S. and Owen B. B. (1958) *The Physical Chemistry of Electrolyte Solutions*. Reinhold, New York.
- Harned H. S. and Robinson R. A. (1968) Multicomponent electrolyte solutions. In *The International Encyclopedia of*

- Physical Chemistry and Chemical Physics Topic 15. Equilibrium Properties of Electrolyte Solutions* (edited by Robinson R. A.), Vol. 2. Pergamon Press, Oxford.
- Hedlin C. P. and Trofimenkoff F. N. (1965) Relative humidities over saturated solutions of nine salts in the temperature range from 0 to 90 F. In *Humidity and Moisture* (edited by Wexler A.), Vol. 3, pp. 519–520. Reinhold, New York.
- Heintzenberg J. (1989) Fine particles in the global troposphere. *Tellus* **41B**, 149–160.
- Hogo H., Seigneur C. and Yocke M. A. (1985) Technical description of a photochemical air quality model with extensions to calculate aerosol dynamics and visibility. Draft SCAQMD STAR Project, Working Paper 1.
- Jacob D. J., Waldman J. M., Munger J. W. and Hoffman M. R. (1985) Chemical composition of fogwater collected along the California coast. *Envir. Sci. Technol.* **19**, 730–736.
- JANAF (1971) Thermochemical tables. *NSRDS-NBS* 37.
- Karapet'yants M. Kh. and Karapet'yants M. L. (1970) *Thermodynamic Constants of Inorganic and Organic Compounds*. Humphrey Science, Ann Arbor.
- Kirgintsev A. N. and Luk'yanov A. V. (1963) Isopiestic investigation of ternary solutions. I. *Russ. J. phys. Chem.* **37**, 1501–1502.
- Kirgintsev A. N. and Luk'yanov A. V. (1964) Isopiestic investigation of ternary solutions. III. Sodium chloride–sodium nitrate–water, sodium chloride–sodium bromide–water, and ammonium chloride–ammonium bromide–water. *Russ. J. phys. Chem.* **38**, 867–869.
- Kirgintsev A. N. and Luk'yanov A. V. (1965) Isopiestic investigation of ternary solutions. VI. Aqueous ternary solutions containing sodium nitrate with the nitrates of lithium, potassium, ammonium, rubidium, and caesium, respectively. *Russ. J. phys. Chem.* **39**, 653–655.
- Kirgintsev A. N. and Trushnikova L. N. (1968) Isopiestic method of determining the composition of solid phases in three-component systems. *Russ. J. Inorg. Chem.* **13**, 600–601.
- Kusik C. L. and Meissner H. P. (1978) Electrolyte activity coefficients in inorganic processing. *AIChE Symp. Series* **173**, **74**, 14–20.
- Lanier R. D. (1965) Activity coefficients of sodium chloride in aqueous three-component solutions by cation-sensitive glass electrodes. *J. phys. Chem.* **69**, 3992–3998.
- Leopold H. G. and Johnston J. (1927) The vapor pressure of the saturated aqueous solution of certain salts. *J. Am. Chem. Soc.* **49**, 1974–1988.
- Lietzke M. H., Hupf H. B. and Stroughton R. W. (1965) Electromotive force studies in aqueous solutions at elevated temperatures. VI. The thermodynamic properties of HCl–NaCl mixtures. *J. phys. Chem.* **69**, 2395–2399.
- Liu Y., Harvey A. H. and Prausnitz J. M. (1989) Thermodynamics of concentrated electrolyte solutions. *Chem. Eng. Comm.* **77**, 43–66.
- McRae G. J., Goodin W. R. and Seinfeld J. H. (1982) Numerical solution of the atmospheric diffusion equation for chemically reacting flows. *J. comp. Physics* **45**, 1–42.
- Meissner H. P. and Peppas N. A. (1973) Activity coefficients—aqueous solutions of polybasic acids and their salts. *AIChE J.* **19**, 806–809.
- Merz A. R., Fry W. H., Hardesty J. O. and Adams J. R. (1933) Hygroscopicity of fertilizer salts. *Indust. Eng. Chem.* **25**, 136–137.
- O'Brien F. E. M. (1948) The control of humidity by saturated salt solutions. *J. sci. Instrum.* **25**, 73–76.
- Parker V. B., Wagman D. D. and Garvin D. (1976) Selected thermochemical data compatible with the CODATA recommendations. *NBSIR*, 75–968.
- Pilinis C. and Seinfeld J. H. (1987) Continued development of a general equilibrium model for inorganic multicomponent atmospheric aerosols. *Atmospheric Environment* **21**, 2453–2466.
- Pilinis C. and Seinfeld J. H. (1988) Development and evaluation of an Eulerian photo-chemical gas–aerosol model. *Atmospheric Environment* **22**, 1985–2001.
- Pilinis C., Seinfeld J. H. and Grosjean D. (1989) Water content of atmospheric aerosols. *Atmospheric Environment* **23**, 1601–1606.
- Pio C. A. and Harrison R. M. (1987) The equilibrium of ammonium chloride aerosol with gaseous hydrochloric acid and ammonia under tropospheric conditions. *Atmospheric Environment* **21**, 1243–1246.
- Pitzer K. S. (1979) Theory: ion interaction approach. In *Activity Coefficients in Electrolyte Solutions* (edited by Pytkowicz R. M.), Vol. 1, pp. 157–208. CRC Press, Boca Raton, FL.
- Pitzer K. S. (1986) Theoretical considerations of solubility with emphasis on mixed aqueous electrolytes. *Pure appl. Chem.* **58**, 1599–1610.
- Prideaux E. B. R. (1920) The deliquescence and drying of ammonium and alkali nitrates and a theory of the absorption of water vapour by mixed salts. *J. Soc. Chem. Ind.* **39**, 182T–185T.
- Prutton C. F., Brosheer J. C. and Maron S. H. (1935) The system  $\text{NH}_4\text{Cl}-\text{NH}_4\text{NO}_3-\text{H}_2\text{O}$  at 0.4, 25, and 50°. *J. Am. Chem. Soc.* **57**, 1656–1657.
- Robinson R. A. and Stokes R. H. (1959) *Electrolyte Solutions*. Butterworths, London.
- Robinson R. A., Roy R. N. and Bates R. G. (1974) The system  $\text{H}_2\text{O}-\text{HCl}-\text{NH}_4\text{Cl}$  at 25°C: a study of Harned's rule. *J. sol. Chem.* **3**, 837–846.
- Rockland L. B. (1960) Saturated salt solutions for static control of relative humidity between 5 and 40°C. *Analyt. Chem.* **32**, 1375–1376.
- Rood M. J., Covert D. S. and Larson T. V. (1987) Hygroscopic properties of atmospheric aerosol in Riverside, California. *Tellus* **39B**, 383–397.
- Russell A. G., McRae G. J. and Cass G. R. (1983) Mathematical modeling of the formation and transport of ammonium nitrate aerosol. *Atmospheric Environment* **17**, 949–964.
- Russell A. G. and Cass G. R. (1986) Verification of a mathematical model for aerosol nitrate and nitric acid formation and its use for control measure evaluation. *Atmospheric Environment* **20**, 2011–2025.
- Russell A. G., McCue K. F. and Cass G. R. (1988) Mathematical modeling of the formation of nitrogen-containing air pollutants. I. Evaluation of an Eulerian photochemical model. *Envir. Sci. Technol.* **22**, 263–271.
- Russell D. L. (1970) *Optimization Theory*. Benjamin, New York.
- Saxena P., Hudischewskyj A. B., Seigneur C. and Seinfeld J. H. (1986) A comparative study of equilibrium approaches to the chemical characterization of secondary aerosols. *Atmospheric Environment* **20**, 1471–1483.
- Staples B. R. (1981) Activity and osmotic coefficients of aqueous sulfuric acid at 298.15 K. *J. phys. Chem. Ref. Data* **10**, 779–798.
- Stelson A. W. and Seinfeld J. H. (1982) Relative humidity and temperature dependence of the ammonium nitrate dissociation constant. *Atmospheric Environment* **16**, 983–992.
- Stokes R. H. (1948) The vapor pressures of solutions of sodium and potassium bisulfates at 25°. *J. Am. Chem. Soc.* **70**, 874.
- Stokes R. H. and Robinson R. A. (1966) Interactions in aqueous nonelectrolyte solutions. I. Solute–solvent equilibria. *J. phys. Chem.* **70**, 2126–2130.
- Tang I. N., Munkelwitz H. R. and Davis J. G. (1978) Aerosol growth studies—IV. Phase transformation of mixed salt aerosols in a moist atmosphere. *J. Aerosol Sci.* **9**, 505–511.
- Tang I. N. (1980) Deliquescence properties and particle size change of hygroscopic aerosols. In *Generation of Aerosols* (edited by Willeke K.), pp. 153–167. Ann Arbor Science, Ann Arbor, MI.
- Tani B., Siegel S., Johnson S. A. and Kumar R. (1983) X-ray diffraction investigation of atmospheric aerosols in the

- 0.3–1.0  $\mu\text{m}$  aerodynamic size range. *Atmospheric Environment* **17**, 2277–2283.
- Wagman D. D., Evans W. H., Parker V. B., Harlow I., Bailey S. M. and Schumm R. H. (1968) Selected values of chemical thermodynamic properties; tables for the first thirty-four elements in the standard order of arrangement. *NBS technical note* 270-3.
- Wagman D. D., Evans W. H., Parker V. B., Schumm R. H., Harlow I., Bailey S. M., Churney K. L. and Nuttall R. L. (1982) The NBS tables of chemical thermodynamic properties: selected values for inorganic and  $C_1$  and  $C_2$  organic substances in SI units. *J. phys. Chem. Ref. Data* **11**, Suppl. 2.
- Wexler A. and Hasegawa S. (1954) Relative humidity-temperature relationships of some saturated salt solutions in the temperature range 0 to 50 C. *J. Res. Natl. Bur. Std.* **53**, 19–26.
- Wexler A. S. and Seinfeld J. H. (1990) The distribution of ammonium salts among a size and composition dispersed aerosol. *Atmospheric Environment* **24A**, 1231–1246.
- Wilson R. E. (1921) Some new methods for the determination of the vapor pressure of salt-hydrates. *J. Am. Chem. Soc.* **43**, 704–725.
- Wink W. A. and Sears G. R. (1950) Instrumentation Studies LVII. Equilibrium relative humidities above saturated salt solutions at various temperatures. *TAPPI* **33**, 96A–99A.
- Winkler P. (1973) The growth of atmospheric aerosol particles as a function of the relative humidity—II. An improved concept of mixed nuclei. *Aerosol Sci.* **4**, 373–387.
- Winkler P. (1988) The growth of atmospheric aerosol particles with relative humidity. *Physica Scripta* **37**, 223–230.
- Wishaw B. F. and Stokes R. H. (1954) Activities of aqueous ammonium sulphate solutions at 25°C. *Trans. Faraday Soc.* **50**, 952–954.
- Wu Y. C., Rush R. M. and Scatchard G. (1968) Osmotic and activity coefficients for binary mixtures of sodium chloride, sodium sulfate, magnesium sulfate, and magnesium chloride in water at 25°C. I. Isopiestic measurements on the four systems with common ions. *J. phys. Chem.* **72**, 4048–4053.
- Wu Y. C. and Hamer W. J. (1980) Revised values of the osmotic coefficients and mean activity coefficients of sodium nitrate in water at 25°C. *J. phys. Chem. Ref. Data* **9**, 513–518.
- Young T. R. and Boris J. P. (1977) A numerical technique for solving stiff ordinary differential equations associated with the chemical kinetics of reactive flow problems. *J. phys. Chem.* **81**, 2424–2427.
- Young T. R. (1980) CHEMEQ—a subroutine for solving stiff ordinary differential equations. Naval Research Laboratory Memorandum Report 4091.
- Young T. R. (1983) CHEMEQ—VAX version update to Appendix B of T. R. Young (1980).
- Zdanovskii A. B. (1948) New methods of calculating solubilities of electrolytes in multicomponent systems. *Zhur. Fiz. Khim.* **22**, 1475–1485.
- Zemaitis J. F., Clark D. M., Rafal M. and Scrivner N. C. (1986) *Handbook of Aqueous Electrolyte Thermodynamics*. AIChE, New York.

## ANALYSIS OF AEROSOL AMMONIUM NITRATE: DEPARTURES FROM EQUILIBRIUM DURING SCAQS



ANTHONY S. WEXLER\*

Department of Mechanical Engineering and Environmental Quality Laboratory, California Institute of Technology, Pasadena, CA 91125, U.S.A.

and

JOHN H. SEINFELD

Department of Chemical Engineering, California Institute of Technology, Pasadena, CA 91125, U.S.A.

(First received 14 November 1990 and in final form 14 May 1991)

**Abstract**—The size distribution of the inorganic components of atmospheric aerosols measured during the 1987 Southern California Air Quality Study (SCAQS) are used to investigate the hypothesis that transport limits equilibration of gas- and aerosol-phase ammonium nitrate and influences their size distribution. Estimates of the equilibration time constants at four sites in southern California show a wide range of values; at small values equilibrium is expected whereas at large values departures from equilibrium are expected. An equilibrium indicator is proposed based on the size distributions of aerosol ammonium and nitrate that shows when particles of different size are in mutual equilibrium with respect to ammonium nitrate. Values of the indicator range from unity, demonstrating equilibrium, to less than 0.5, demonstrating that different size particles are not in mutual equilibrium. Comparison of the time constant values to the equilibrium indicator values show a significant correlation, so it is concluded that different size aerosol particles are often not in mutual equilibrium due to transport limitations, supporting the hypothesis. It is concluded that both thermodynamics and mass transport must be considered to predict accurately the size distribution of the volatile inorganics in atmospheric aerosol.

*Key word index:* SCAQS, ammonium nitrate, atmospheric aerosols, thermodynamic equilibrium.

### INTRODUCTION

One of the most intriguing aspects of atmospheric aerosols concerns the behavior of ammonium nitrate. Stelson *et al.* (1979) first suggested that aerosol ammonium nitrate levels could be determined from the equilibrium among ammonia, nitric acid, and aerosol ammonium nitrate. The assumption of thermodynamic equilibrium has been employed to partition the volatile compounds between the gas and aerosol phases (Bassett and Seinfeld, 1983; Russell *et al.*, 1983, 1988; Saxena *et al.*, 1983, 1986; Russell and Cass, 1986) and to predict their aerosol size distribution (Bassett and Seinfeld, 1984; Pilinis *et al.*, 1987; Pilinis and Seinfeld, 1987, 1988). Although the equilibrium assumption has been supported by some ambient data (Doyle *et al.*, 1979; Grosjean, 1982; Hildemann *et al.*, 1984), other data indicate that it may not always hold (Cadle *et al.*, 1982; Tanner, 1982; Allen *et al.*, 1989).

The South Coast Air Basin (SoCAB) of southern California experiences some of the highest aerosol concentrations in the U.S. These aerosols are primarily

composed of elemental carbon, and organic and inorganic compounds. The inorganic compounds are primarily ammonium, sodium, nitrate, sulfate, and chloride, which typically comprise 25–50% of the mass of the aerosol (Gray *et al.*, 1986). During the summer and fall of 1987, extensive measurements were made in the SoCAB of gas- and aerosol-phase concentrations of ammonia and nitric acid and their size distributions (Hering and Blumenthal, 1989; Lawson, 1990) as part of the Southern California Air Quality Study (SCAQS). This study contained the most complete measurement of these quantities and the first carried out at multiple sites concurrently. Briefly, at nine B sites in the SoCAB, the gas- and aerosol-phase concentrations of ammonium and nitric acid were measured with annular denuders contained in the SCAQS sampler (Hering and Blumenthal, 1989). SCAQS sampler data were collected by Aerovironment (Fitz and Zwicker, 1988; Chan and Durkee, 1989) and meteorological data were collected by the California Air Resources Board and the South Coast Air Quality Management District (Chan and Durkee, 1989). At four of these sites, Claremont, downtown Los Angeles, Riverside, and Long Beach, called the B+ sites, size distributions were measured using Berner impactors (Wall *et al.*, 1988). These data

\* Present address: Department of Mechanical Engineering, University of Delaware, Newark, DE 19716, U.S.A.

were collected by the Air and Industrial Hygiene Laboratory of the California Department of Health Services (John *et al.*, 1989a,b, 1990). In this paper we explore the evidence for thermodynamic equilibrium among ammonia, nitric acid, and aerosol ammonium nitrate for the B+ sites during SCAQS.

In previous work we have predicted that under certain atmospheric conditions, the volatile inorganic components of atmospheric aerosol may not be in equilibrium with their gas-phase counterparts due to transport limitations, so that under such conditions mass transport between the gas and aerosol phases may have to be explicitly modeled. We also predicted that even if the aerosol is in equilibrium with the gas phase, the size distribution of the volatile inorganic components of atmospheric aerosols often cannot be uniquely determined from thermodynamic considerations alone, and thus mass transport usually has to be included to determine the size distribution of the volatile inorganic components (Wexler and Seinfeld, 1990). In a subsequent work, we developed a transport model of atmospheric aerosols that assumes the aerosol particles are in internal equilibrium to predict their surface partial pressures of ammonia and nitric acid, and explicitly models transport between the gas and aerosol phases. In that work we compared the predictions of the model to (1) laboratory measurements and (2) the predictions of other aerosol equilibrium models (Wexler and Seinfeld, 1991). The dynamics of the departure from equilibrium has also been examined by Harrison and MacKenzie (1990), who tested their hypothesis of a kinetically limited departure from equilibrium with a model of gas-to-particle transport and surface reaction processes.

Comparison of measured gas-phase ammonia and nitric acid concentrations with those predicted from aerosol composition often indicate departures from equilibrium (Cadle *et al.*, 1982; Tanner, 1982, Allen *et al.*, 1989) without identification of the cause for the observed departure. The purpose of the present study is to analyze the data from the four SCAQS B+ sites, identify departures from equilibrium, and identify how transport limitations contribute to these departures. We first discuss calculation of the time constant that governs equilibration due to transport between the gas and aerosol phases. Then we explore how particles of different size and composition depart from equilibrium with each other. Finally we discuss the implications of our findings to the behavior of atmospheric aerosols.

#### TIME CONSTANT FOR EQUILIBRATION OF $\text{NH}_4\text{NO}_3$

For ammonium nitrate equilibrium to hold, transport between the gas and aerosol phases must be fast compared to the time-scales that characterize changes in the ambient temperature, relative humidity and gas-phase concentrations of ammonia and nitric acid (Wexler and Seinfeld, 1990). There are two distinct

physical processes that lead to equilibration between the gas and aerosol phases, and these processes have different time-scales. In this section we describe the time-scales that govern equilibration between the gas and aerosol phases and evaluate them from data collected during SCAQS.

Let us consider an atmosphere containing gas-phase ammonia and nitric acid and aqueous or solid aerosol particles that contain ammonium nitrate and possibly other salts. If the ambient gas-phase ammonia and nitric acid concentrations exceed those at the particle surface, ammonia and nitric acid diffuse towards and condense on the particles. This diffusive transport between the two phases eventually leads to their equilibration because of depletion of ammonia and nitric acid from the gas phase, and resulting decreases in their gas-phase concentrations.

Transport from the gas to the aerosol phase also increases the amount of aerosol ammonia and nitric acid. These increases in the aerosol mass of ammonium nitrate lead to equilibration if the particle-surface gas-phase concentrations of these species also increase. For instance, if the aerosol mass of water remains constant during condensation of ammonia and nitric acid on an aqueous-phase particle, the aerosol-phase ammonium nitrate molality increases during condensation, which is reflected by an increase in the surface partial pressures. These changes in surface partial pressures then hastens the process of equilibration. However, increases in the aerosol mass of ammonium nitrate do not always lead to increases in the surface partial pressures. For instance, if the aerosol particles are solid, their surface partial pressures of ammonium nitrate are constant, in which case equilibration cannot take place simply as a result of changes in the aerosol mass of ammonium nitrate.

Thus diffusive transport between the gas and aerosol phases eventually leads to their equilibration, and two time-scales govern the approach to equilibrium. One time-scale,  $\tau_\infty$ , characterizes the approach due to changes in the gas-phase concentrations, and the other time-scale,  $\tau_p$ , characterizes the approach due to changes in the aerosol-phase concentrations. These equilibration time-scales are not necessarily the same because during condensation the partial pressures at the particle surface may change slower or faster than the ambient partial pressures.

What is the overall time-scale for equilibration between the gas and aerosol phases? Consider the gas phase and the aerosol phase to be two compartments that may exchange ammonium nitrate. For two coupled compartments, the overall time-scale for equilibration,  $\tau$ , is the harmonic mean of the individual time-scales, which for the current case is  $\tau = (1/\tau_\infty + 1/\tau_p)^{-1}$ . Thus the shorter time-scale governs the equilibration process. If one of the time-scales is infinitely long, such as  $\tau_p$  in the case of a solid aerosol, the overall time-scale is equal to the finite one, in this case  $\tau_\infty$ .

For aerosol particles containing solid ammonium

nitrate,  $\tau_p$  is infinitely long and thus irrelevant to the equilibration process, since a change in the mass of solid aerosol ammonium nitrate does not lead to a change in the surface equilibrium concentration of the vapor-phase species. For aqueous aerosol particles,  $\tau_p$  is also not relevant if ammonium nitrate is osmotically dominant, that is, if the ammonium nitrate concentration greatly exceeds those of the other electrolytes. When a particle is osmotically dominated by ammonium nitrate, condensation of ammonium nitrate on the particle is accompanied by condensation of water to maintain the water activity in the particle equal to the ambient relative humidity. This condensation of water causes the ammonium nitrate molality to remain relatively constant as condensation ensues. Since the molality does not change substantially for these particles, neither does the surface gas-phase concentration. Thus  $\tau_p$  is large or irrelevant for particles osmotically dominated by ammonium nitrate, because the surface concentrations cannot change and equilibrate with the ambient concentrations, and equilibration only takes place when the gas-phase concentrations decline to the point where they are equal to those at the particle surface.

When the ammonium nitrate is osmotically benign, that is, when its aerosol concentration is much less than that of other electrolytes, transport of ammonium nitrate to the particle does not affect the aerosol water content. In this case, changes in aerosol ammonium nitrate concentration are directly reflected as changes in molality, which are then directly reflected as changes in surface partial pressure. Particles osmotically benign with respect to ammonium nitrate, therefore, have shorter equilibration time-scales than those whose water content increases significantly during condensation. For osmotically benign particles, the time-scale changes with the aerosol mass of water. If the aerosol mass of water is large, the aerosol compartment is large, and a significant gas-to-particle conversion is needed to alter the particle ammonium nitrate molality and the surface partial pressures. Thus for osmotically benign particles, a large aerosol water content leads to a long time-scale, and a small aerosol water content is characterized by a short time-scale.

In summary, two time-scales exist for equilibration. Diffusive transport between the gas and aerosol phases changes the amount of ammonia and nitric acid in each phase with the resulting change in ambient concentrations giving the gas-phase equilibration time-scale  $\tau_\infty$ . Change in particle surface concentrations due to changes in aerosol mass of ammonium nitrate from the transport of ammonia and nitric acid between the phases leads to the particle-phase equilibration time-scale  $\tau_p$ .

In general, atmospheric aerosol particles have different sizes and compositions. Consider  $n$  kinds of particles each of uniform size and composition. In this case there are  $n$  time-scales  $\tau_{p,i}$ ,  $i=1, n$ , associated with equilibration of each kind of aerosol particle due

to changes in its surface partial pressures, along with the single time-scale  $\tau_\infty$  associated with equilibration due to changes in the ambient gas-phase concentrations. Just as before, the time-scale  $\tau_\infty$  characterizes the change in ambient concentrations due to the overall transport between the gas and aerosol phases. But in this case there is no single  $\tau_p$ . Instead there are  $n$  different  $\tau_{p,i}$  values which cannot be combined into an appropriate single  $\tau_p$  value.

Since there are numerous time-scales,  $\tau_{p,i}$ , and under typical conditions in the SoCAB, (1) the relative humidity is often low enough to result in solid aerosol particles and (2) there is considerably more aerosol nitrate than sulfate, so the time constants  $\tau_{p,i}$  are usually large compared to  $\tau_\infty$ , we will concentrate our analysis here on the time constant  $\tau_\infty$ . We wish to evaluate  $\tau_\infty$  for the conditions during SCAQS, but to do so we must first express it in terms of the measured quantities. The rate of change of the ambient gas-phase concentration,  $C_\infty$ , of a single species due to its transport between the gas and aerosol phases can be written as

$$\frac{dC_\infty}{dt} = \int_0^\infty n(R_p) J(R_p) dR_p, \quad (1)$$

where  $n(R_p)$  is the number distribution of particles ( $m^{-4}$ ) and  $J(R_p)$  is the flux ( $\text{mol s}^{-1}$ ) of the gas-phase species to or from a single particle of radius  $R_p$  (m). An expression for the single-particle flux is

$$J(R_p) = \frac{4\pi R_p D (C_p - C_\infty)}{(1 + D/\alpha \bar{c} R_p)}, \quad (2)$$

where  $C_p$  is the particle-surface gas-phase concentration,  $D$  is the molecular diffusivity,  $\bar{c}$  is the mean molecular speed, and  $\alpha$  is the particle-surface accommodation coefficient of the condensing species (Wexler and Seinfeld, 1990). We have shown in previous work that, for ammonia and nitric acid condensing on atmospheric particles, the quantity  $D/\bar{c}$  can be approximated by  $\lambda$ , the mean free path of air molecules in air (Wexler and Seinfeld, 1990). Since the time constant  $\tau_\infty$  is defined by  $\tau_\infty^{-1} = 1/C_\infty dC_\infty/dt$ , we can combine this relation with Equations (1) and (2) to obtain:

$$\tau_\infty^{-1} = 4\pi D \int_0^\infty \frac{n(R_p) R_p dR_p}{1 + \frac{\lambda}{\alpha R_p}}. \quad (3)$$

If the particle number distribution is available,  $\tau_\infty$  may be estimated using Equation (3). If the particle mass distribution is available, the number distribution,  $n(R_p)$ , can be related to the mass distribution,  $m(R_p)$ , by  $m(R_p) = 4/3\pi R_p^3 \rho_p n(R_p)$ , where  $\rho_p$  is the particle density, to get

$$\tau_\infty^{-1} = 3D \int_0^\infty \frac{m(R_p) dR_p}{\left(1 + \frac{\lambda}{\alpha R_p}\right) R_p^2 \rho_p}, \quad (4)$$

but since the mass distributions are provided in logarithmic form (John *et al.*, 1989b), the identity  $m(R_p)dR_p = m(\log_{10} R_p)d\log_{10} R_p = m(\log_{10} R_p)dR_p/2.303 R_p$  yields the desired relation:

$$\tau_x^{-1} = \frac{3D}{2.303} \int_0^\infty \frac{m(\log_{10} R_p)dR_p}{\left(1 + \frac{\lambda}{\alpha R_p}\right) R_p^3 \rho_p} \quad (5)$$

Either Equation (3) or (5) can be used to estimate  $\tau_\infty$ , since both number distributions (Chan and Durkee, 1989) and mass distributions of the inorganic species (John *et al.*, 1990) were measured during SCAQS. But both of these size distributions introduce different uncertainties into the estimates of  $\tau_\infty$ . Let us now examine the likely uncertainties caused by using each of these distributions.

As has been shown during SCAQS (McMurry and Stolzenburg, 1989), the aerosol is hygroscopically externally mixed, that is, a fraction of the particles of a given size are hydrophilic and the rest are hydrophobic. Since ammonium nitrate is very hygroscopic, we conclude that ammonium nitrate is not transported to a hydrophobic fraction of the particles and use of the overall number distributions to estimate  $\tau_\infty$  tends to overestimate the surface area available for transport, which results in an underestimate of  $\tau_\infty$  by at most a factor of 2 (McMurry and Stolzenburg, 1989).

Another consideration is that the hygroscopic aerosol particles contain non-ionic components such as elemental carbon and organics. The size distributions reported by John and co-workers (John *et al.*, 1989b) do not include the non-ionic components, so use of these size distributions tend to underestimate  $m$ , thereby overestimating the value of  $\tau_\infty$ . Since both forms of size distribution data are difficult to relate to the calculation of  $\tau_\infty$ , we chose to use the data of John and co-workers (John *et al.*, 1989a,b, 1990) in Equation (5), since it will be used in other calculations in this work. Since the inorganics typically comprise about 1/3 of the total aerosol mass, this choice tends to result in overpredictions of  $\tau_\infty$  by roughly a factor of 3.

To complete the evaluation of Equation (5), we must estimate values for the rest of the parameters on the right-hand side. Of these parameters, the most difficult one to estimate is the accommodation coefficient,  $\alpha$ . The range of accommodation coefficient values for ammonia and nitric acid is probably  $0.001 < \alpha < 1$  depending on the phase state of the particle and on the presence of organic surface-active agents (Gill *et al.*, 1983; Wexler and Seinfeld, 1990), and since the  $\lambda/R_p$  values for these particles are not much less than unity, uncertainties in  $\alpha$  are reflected as uncertainties in  $\tau_\infty$ . For the calculations here, we have assumed  $\alpha = 0.1$  which may tend to underpredict the value of  $\tau_\infty$ , since  $\alpha$  may be 1 or 2 orders of magnitude smaller than 0.1. Due to the large uncertainty in  $\alpha$ , it is not appropriate to compare the calculated values of

$\tau_\infty$  to the values of other time-scales of atmospheric relevance. Instead we will seek correlations between the values of  $\tau_\infty$  and the values of other indicators of equilibrium. As long as the value of the accommodation coefficient  $\alpha$  is constant, such correlations represent a valid approach to analyzing atmospheric data. In subsequent sections we will be concerned only with the relative values of  $\tau_\infty$ .

Tables 1–5 show the values of the time constant,  $\tau_\infty$ , calculated with Equation (5) and assuming  $D = 0.1 \text{ cm}^2 \text{ s}^{-1}$ ,  $\lambda = 0.065 \text{ } \mu\text{m}$ ,  $\rho_p = 1.3 \text{ gm cm}^{-3}$ , and  $\alpha = 0.1$ . The values of  $\tau_\infty$  are generally in the range of 1–15 min, and since the inorganic aerosol measurements during SCAQS had sampling times in excess of 3 h, it would appear that a departure from equilibrium may not be discernible. But if our estimates of

Table 1. Indicators of ammonium nitrate equilibrium for Claremont, CA

Date (1987)	Hour	$\tau_\infty$ (h)	$C_{an}$	$D_{p,Na}$ ( $\mu\text{m}$ )
19.06	08	0.04	0.84	3.2
19.06	12	0.05	0.84	2.3
19.06	16	0.07	0.73	2.3
19.06	21	0.05	0.78	2.4
24.06	08	0.03	0.85	15.0
24.06	12	0.05	0.80	5.5
24.06	16	0.05	0.63	5.0
24.06	21	0.06	0.82	4.5
25.06	08	0.04	0.83	13.2
25.06	12	0.03	0.84	15.0
25.06	16	0.07	0.75	3.1
25.06	21	0.07	0.72	6.8
13.07	08	0.05	0.78	15.0
13.07	12	0.05	0.78	15.0
13.07	16	0.07	0.66	5.9
13.07	21	0.16	0.68	3.9
14.07	08	0.05	0.83	7.6
14.07	12	0.06	0.79	15.0
14.07	16	0.06	0.53	15.0
14.07	21	0.07	0.75	8.6
15.07	08	0.05	0.81	15.0
15.07	12	0.07	0.76	15.0
15.07	16	0.06	0.77	15.0
15.07	21	0.06	0.87	15.0
27.08	08	0.05	0.78	8.8
27.08	12	0.03	0.84	15.0
27.08	16	0.07	0.76	3.6
27.08	21	0.09	0.73	3.5
28.08	08	0.05	0.79	6.1
28.08	12	0.04	0.85	5.1
28.08	16	0.04	0.73	3.4
28.08	21	0.05	0.78	4.0
29.08	08	0.02	0.84	15.0
29.08	12	0.03	0.85	15.0
29.08	16	0.04	0.73	15.0
29.08	21	0.04	0.75	15.0
02.09	08	0.15	0.42	5.1
02.09	12	0.06	0.70	15.0
02.09	16	0.15	0.59	1.7
02.09	21	0.11	0.71	2.6
03.09	08	0.05	0.77	6.3
03.09	12	0.03	0.81	10.3
03.09	16	0.10	0.67	2.1
03.09	21	0.11	0.76	2.5

Ammonium nitrate during SCAQS

Table 2. Indicators of ammonium nitrate equilibrium for Long Beach, CA in the summer

Date (1987)	Hour	$\tau_{\infty}$ (h)	$C_{an}$	$D_{p,Na}$ ( $\mu\text{m}$ )
19.06	08	0.05	0.57	1.5
19.06	12	0.14	—	—
19.06	16	0.11	0.52	1.6
19.06	21	0.11	0.56	2.1
24.06	08	0.07	0.65	2.6
24.06	12	0.14	0.57	2.0
24.06	16	0.11	0.67	2.0
24.06	21	0.06	0.71	2.5
25.06	08	0.12	0.56	2.2
25.06	12	0.18	0.61	1.6
25.06	16	0.32	0.63	1.8
25.06	21	0.14	0.81	7.2
13.07	08	0.05	0.81	4.6
13.07	12	0.08	0.72	4.1
13.07	16	0.10	0.46	3.7
13.07	21	0.15	0.54	3.1
14.07	08	0.11	0.45	4.3
14.07	12	0.08	0.45	5.1
14.07	16	0.08	0.43	4.5
14.07	21	0.15	0.56	4.2
15.07	08	0.08	0.52	4.8
15.07	12	0.24	0.45	4.1
15.07	16	0.24	0.66	3.2
15.07	21	0.24	0.27	9.8
27.08	08	0.05	0.80	3.0
27.08	12	0.07	0.70	2.4
27.08	16	0.15	0.60	1.9
27.08	21	0.10	0.65	2.8
28.08	08	0.03	0.76	4.7
28.08	12	0.04	0.59	4.6
28.08	16	0.09	0.52	2.5
28.08	21	0.09	0.62	2.9
29.08	08	0.04	0.66	3.7
29.08	12	0.09	0.47	3.5
29.08	16	0.13	0.51	2.3
29.08	21	0.14	0.67	2.2
02.09	08	0.01	0.72	1.7
02.09	12	0.02	0.79	3.1
02.09	16	0.07	0.55	1.7
02.09	21	0.06	0.63	1.8
03.09	08	0.09	0.24	15.0
03.09	12	0.12	0.52	1.6
03.09	16	0.18	0.49	1.4
03.09	21	0.20	0.51	1.5

Table 3. Indicators of ammonium nitrate equilibrium for Riverside, CA

Date (1987)	Hour	$\tau_{\infty}$ (h)	$C_{an}$	$D_{p,Na}$ ( $\mu\text{m}$ )
19.06	08	0.03	0.83	3.4
19.06	12	0.02	0.91	2.3
19.06	16	0.04	0.79	4.1
19.06	21	0.04	0.71	3.2
24.06	08	0.02	0.78	15.0
24.06	12	0.01	0.93	15.0
24.06	16	0.03	0.77	15.0
24.06	21	0.02	0.79	8.4
25.06	08	0.02	0.87	15.0
25.06	12	0.01	0.92	15.0
25.06	16	0.05	0.85	5.5
25.06	21	0.03	0.81	5.7
13.07	08	0.02	0.87	15.0
13.07	12	0.02	0.92	15.0
13.07	16	0.02	0.89	15.0
13.07	21	0.06	0.77	7.7
14.07	08	0.04	0.83	8.2
14.07	12	0.02	0.92	15.0
14.07	16	0.03	0.88	15.0
14.07	21	0.03	0.86	15.0
15.07	08	0.02	0.88	15.0
15.07	12	0.02	0.91	15.0
15.07	16	0.03	0.93	15.0
15.07	21	0.03	0.89	15.0
27.08	08	0.01	0.81	15.0
27.08	12	0.01	0.94	15.0
27.08	16	0.02	0.89	15.0
27.08	21	0.02	0.82	5.9
28.08	08	0.02	0.79	15.0
28.08	12	0.01	0.93	15.0
28.08	16	0.02	0.89	15.0
28.08	21	0.01	0.88	15.0
29.08	08	0.01	0.89	15.0
29.08	12	0.02	0.93	15.0
29.08	16	0.02	0.90	15.0
29.08	21	0.02	0.79	15.0
02.09	08	0.12	0.39	4.1
02.09	12	0.26	0.08	15.0
02.09	16	0.22	0.32	15.0
02.09	21	0.03	0.84	5.0
03.09	08	0.04	0.74	4.0
03.09	12	0.02	0.86	15.0
03.09	16	0.04	0.85	4.8
03.09	21	0.05	0.81	3.1

the time constants are too short due to our choice of an accommodation coefficient of 0.1, we may be able to observe a departure from equilibrium. The values of  $\tau_{\infty}$  in Tables 1–5 will be compared to various indicators of equilibrium in subsequent sections.

**A PROPOSED INDICATOR FOR DEPARTURE FROM EQUILIBRIUM**

Accurate measurements of the aerosol-phase ammonium nitrate concentration and the gas-phase ammonia and nitric acid concentrations in the atmosphere are difficult even when sampling times in excess of a few hours are employed. Furthermore, a comparison of the measured ammonia, nitric acid,

and ammonium concentrations to those predicted by equilibrium calculations often leads to serious disagreement, with the source of disagreement unidentifiable from the comparison alone. Transport limitations provide one possible explanation for these departures from equilibrium. As we have shown, the time-scales for equilibration between the gas and aerosol phases may range from a few seconds to over a day under conditions that often occur in, for instance, the SoCAB. Thus we seek an indicator of departure from equilibrium, and correlations between this indicator and the estimated time constants for ammonium nitrate equilibration. Observation of such a correlation adds support to the hypothesis that transport limits equilibration between gas- and aerosol-phase ammonium and nitric acid. In this section we derive

Table 4. Indicators of ammonium nitrate equilibrium for downtown Los Angeles, CA

Date (1987)	Hour	$\tau_\infty$ (h)	$C_{an}$	$D_{p,Na}$ ( $\mu\text{m}$ )
11.11	08	0.17	—	—
11.11	12	0.12	0.33	4.3
11.11	16	0.05	0.72	14.0
11.11	21	0.11	0.74	7.9
12.11	08	0.07	0.71	15.0
12.11	12	0.02	0.97	15.0
12.11	16	0.02	0.94	15.0
12.11	21	0.05	0.88	12.8
13.11	08	0.02	0.95	15.0
13.11	12	0.02	0.91	15.0
13.11	16	0.04	0.74	14.9
13.11	21	0.10	0.82	4.9
03.12	08	0.02	0.98	15.0
03.12	12	0.02	0.95	15.0
03.12	16	0.01	0.92	15.0
03.12	21	0.03	0.92	15.0
10.12	08	0.06	0.87	15.0
10.12	12	0.03	0.93	15.0
10.12	16	0.03	0.87	15.0
10.12	21	0.04	0.89	15.0
11.12	08	0.03	0.93	15.0
11.12	12	0.01	0.93	15.0
11.12	16	0.01	0.93	15.0
11.12	21	0.02	0.93	15.0

Table 5. Indicators of ammonium nitrate equilibrium for Long Beach, CA in the winter

Date (1987)	Hour	$\tau_\infty$ (h)	$C_{an}$	$D_{p,Na}$ ( $\mu\text{m}$ )
11.11	08	0.07	0.89	15.0
11.11	12	0.05	0.92	15.0
11.11	16	0.04	0.83	15.0
11.11	21	0.05	0.80	15.0
12.11	08	0.03	0.90	15.0
12.11	12	0.02	0.89	15.0
12.11	16	0.02	0.92	15.0
12.11	21	0.03	0.88	9.9
13.11	08	0.01	0.89	15.0
13.11	12	0.08	0.67	4.3
13.11	16	0.13	0.61	2.2
13.11	21	0.12	0.69	2.9
03.12	08	0.00	0.94	15.0
03.12	12	0.01	0.92	15.0
03.12	16	0.00	0.91	15.0
03.12	21	0.01	0.90	15.0
10.12	08	0.01	0.95	15.0
10.12	12	0.01	0.94	15.0
10.12	16	0.02	0.79	15.0
10.12	21	0.05	0.87	6.1
11.12	08	0.02	0.97	15.0
11.12	12	0.01	0.93	15.0
11.12	16	0.01	0.94	15.0
11.12	21	0.01	0.94	15.0

the equations that describe an indicator, and in subsequent sections illustrate correlations between the indicator and the time constant.

We begin by considering aqueous-phase aerosols that contain ammonium, nitrate, possibly other

strong electrolytes, and other substances which we assume to be inert. Now consider two populations of these aerosol particles that are in equilibrium with gas-phase ammonia and nitric acid such that these two populations of particles contain  $M_{a,i}$  moles of ammonium and  $M_{n,i}$  moles of nitrate in a solution of  $W_i$  kilograms of water for particle compositions,  $i=1, 2$ . If these two populations of particles are in equilibrium with gas-phase ammonia and nitric acid then

$$PPP_m = K_{an} \gamma_{an}^2 \frac{M_{a,1} M_{n,1}}{W_1^2} = K_{an} \gamma_{an}^2 \frac{M_{a,2} M_{n,2}}{W_2^2}, \quad (6)$$

where  $K_{an}$  is the equilibrium constant for aqueous ammonium nitrate and  $\gamma_{an}$  is the activity coefficient of ammonium nitrate.  $\gamma_{an}$  is a slowly varying function of the ionic strength, and since for atmospheric aerosols the ionic strength is primarily governed by the relative humidity and less so by the composition, we assume that the activity coefficients for the two types of particles are approximately the same.

The water content of the aerosol is usually estimated with the ZSR relationship (Zdanovskii, 1948; Stokes and Robinson, 1966; Hanel and Zankl, 1979; Cohen *et al.*, 1987; Pilinis and Seinfeld, 1987)

$$W_i = \sum_j \frac{M_{i,j}}{m_{0,j}(\text{r.h.})}, \quad (7)$$

where  $m_{0,j}(\text{r.h.})$  is the molality of species  $j$  that gives a solution of water activity r.h. and  $M_{j,i}$  are the moles of aerosol electrolyte  $j$  per  $\text{m}^3$  air in particles of composition  $i$ .

In the SoCAB it is often observed that the strong electrolyte portion of the aerosol is mostly comprised of ammonium, nitrate, and sulfate in inland locations. At coastal locations the aerosol may also contain substantial portions of sodium and to a lesser extent chloride. For now then let us assume that the aerosol is composed primarily of ammonium, nitrate, and sulfate, and that by charge balance

$$M_{a,i} \approx M_{n,i} + 2M_{s,i}, \quad (8)$$

where  $M_{s,i}$  is the number of moles of sulfate in the aerosol of composition  $i$ . Combining Equations (6)–(8) to eliminate  $M_{s,i}$  gives

$$\frac{PPP_m}{\gamma_{an}^2 K_{an}} = \frac{M_{a,i}/M_{n,i}}{\left\{ \frac{1}{m_{0,n}} + \frac{1}{2m_{0,s}} \left( \frac{M_{a,i}}{M_{n,i}} - 1 \right) \right\}^2}. \quad (9)$$

Thus for an aqueous  $\text{NH}_4\text{NO}_3$ – $(\text{NH}_4)_2\text{SO}_4$  aerosol, the ratio  $M_{a,i}/M_{n,i}$  is uniquely determined by the ammonium nitrate partial pressure product. If we look at the composition of particles of different size that are primarily composed of ammonium, nitrate, and sulfate, these particles should all have the same ratio  $M_{a,i}/M_{n,i}$  if they are in equilibrium with gas-phase ammonia and nitric acid.

Equation (9) has important implications for field measurements. When these measurements are performed, numerous aerosol particles are collected to form a sample, and this sample is then analyzed for its chemical composition. If the chemical composition of the sample is then assumed to represent the chemical composition of each particle, an equilibrium calculation can be done and the measured gas-phase concentrations of ammonia and nitric acid can be compared to those predicted from the chemical composition of the aerosol (Doyle *et al.*, 1979; Tanner, 1982; Grosjean, 1982; Hildemann *et al.*, 1984). But if each aerosol particle is in equilibrium with gas-phase ammonia and nitric acid, will the chemical composition of the sample also be in equilibrium? One of the conclusions that can be drawn from Equation (9) is that the sample will be in equilibrium with gas-phase ammonia and nitric acid if it is aqueous and the dissolved electrolytes are primarily ammonium nitrate and ammonium sulfate.

If we now add one more degree of freedom, by allowing the aerosol to contain, say sodium, the next most prevalent ion in Los Angeles aerosols, then the ratio  $M_{a,i}/M_{n,i}$  may differ for aerosols of different composition, depending on the mole fraction of sodium. At most locations in the SoCAB, sodium does not comprise a large portion of the ionic components of atmospheric aerosol (Eldering *et al.*, 1991), so at these locations the ratio  $M_{a,i}/M_{n,i}$  is well determined by the partial pressure product alone. At coastal locations with an on-shore wind, sodium chloride aerosol generated in sea spray may be advected inland invalidating the assumptions behind Equation (9). In a subsequent section we examine the validity of the assumptions behind Equation (9) during SCAQS.

Let us return to the ammonium nitrate-ammonium sulfate aqueous-phase aerosol in equilibrium with respect to gas-phase ammonia and nitric acid. For a size distributed aerosol, the ratio  $M_{a,i}/M_{n,i}$  must be the same for any size aerosol particle and thus for aerosol particles of all sizes to obey Equation (9) the normalized size distributions of aerosol ammonium and nitrate must be the same. In order to obtain a quantitative measure of the degree of overlap of the ammonium and nitrate size distributions, let us define a coincidence factor,  $C'_{an}$ , as

$$C'_{an} = 1 - \frac{1}{2} \int_0^{\infty} \left| \frac{M_n(D_p)}{M_n^t} - \frac{M_a(D_p)}{M_a^t} \right| dD_p, \quad (10)$$

where  $M_i(D_p)$  and  $M_i^t = \int_0^{\infty} M_i(D_p) dD_p$  are the molar size distribution and total number of moles of nitrate,  $i=n$ , and ammonium,  $i=a$ , and  $D_p$  is the aerosol diameter.  $C'_{an}$  is zero when the normalized size distributions do not overlap and unity when they coincide perfectly.

If the aerosol is predominantly comprised of ammonium, nitrate, and sulfate, and if transport and kinetic constraints limit the equilibration of gas- and aerosol-phase ammonium nitrate, a correlation

should exist in the atmosphere between the time constant for equilibration,  $\tau_{\infty}$ , and the coincidence factor,  $C'_{an}$ . In the next section we estimate the coincidence factors from the size-distributed aerosol composition measurements taken during SCAQS, and compare these to the estimated time constant values calculated in the previous section.

#### COINCIDENCE OF THE NITRATE AND AMMONIUM SIZE DISTRIBUTIONS

In the previous section we proposed an indicator for departure from equilibrium for an ammonium nitrate-ammonium sulfate size-distributed aerosol. In the SoCAB such pure aerosols do not typically exist and other ions such as sodium may alter the equilibrium partial pressure product. Under conditions where a significant fraction of sodium exists Equation (10) will not hold, so an alternative is sought. Since it has been observed in the SoCAB that sodium generally occurs in larger aerosol particles whereas ammonium, nitrate, and sulfate occur in somewhat smaller particles, we can choose that the integral in Equation (10) be performed only over the smaller particles

$$C_{an} = 1 - \frac{1}{2} \int_{0.05}^{D_{p,Na}} \left| \frac{M_n(D_p)}{M_n^t} - \frac{M_a(D_p)}{M_a^t} \right| dD_p, \quad (11)$$

where  $C_{an}$  is the coincidence factor in the size range of  $0.05 \mu\text{m}$  to  $D_{p,Na}$ , and  $0 \leq C_{an} \leq 1$ .  $D_{p,Na}$  is the size of particle below which the number of moles of sodium is less than one-tenth the number of moles of ammonium.

$$\int_{0.05}^{D_{p,Na}} M_a(D_p) dD_p > 10 \int_{0.05}^{D_{p,Na}} M_{Na}(D_p) dD_p, \quad (12)$$

where  $M_{Na}(D_p)$  is the molar size distribution of sodium. The values of  $D_{p,Na}$  calculated with Equation (12) are listed in Tables 1-5. For both winter sites and for Rubidoux in the summer, the values of  $D_{p,Na}$  are usually  $15 \mu\text{m}$ , the maximum value, indicating very little sodium in these samples. At Long Beach during the summer measurements, sodium comprised a substantial molar fraction of the larger particles. On average, Claremont shows intermediate sodium quantities.

Using the values of  $D_{p,Na}$  in Tables 1-5, Equation (11) can be evaluated for each of the measurements. These coincidence factors are also listed in Tables 1-5. We see that although there are many coincidence factors that approach unity, indicating  $\text{NH}_4\text{NO}_3$  equilibrium, there are also a substantial number of lower values that do not.

Is there a correlation between the values of  $\tau_{\infty}$  and the coincidence factors? Figures 1-5 show the ammonium-nitrate coincidence factor plotted against the equilibration time-scale  $\tau_{\infty}$  for each of the sites.

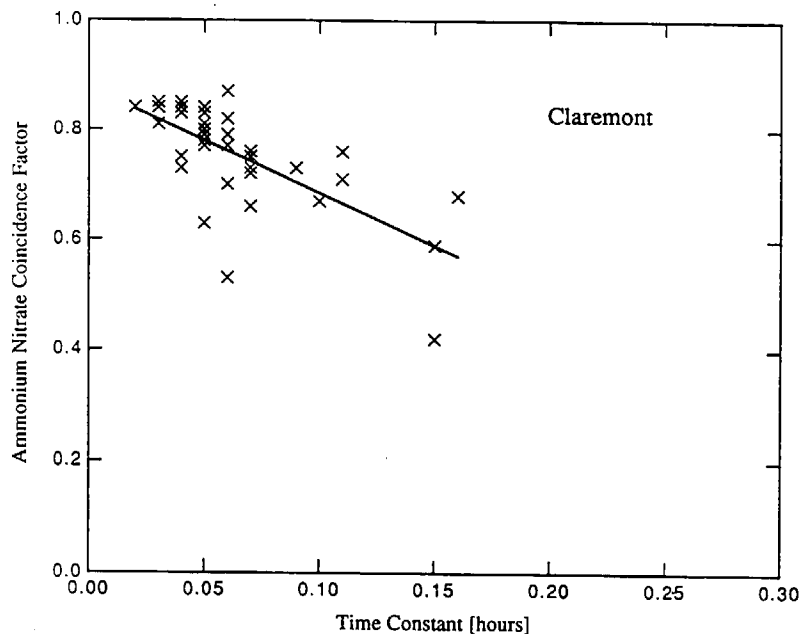


Fig. 1. The ammonium nitrate coincidence factor as a function of the equilibration time-scale  $\tau_{\infty}$  for Claremont, CA.

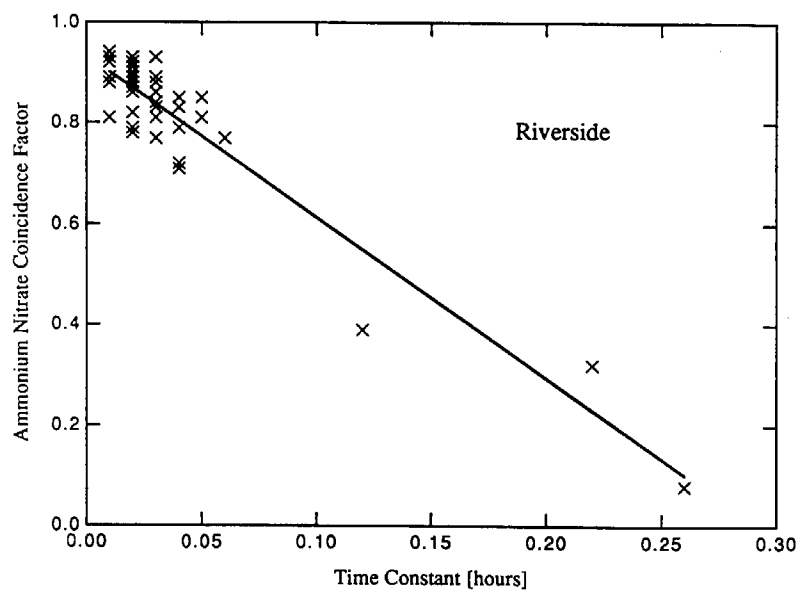


Fig. 2. The ammonium nitrate coincidence factor as a function of the equilibration time-scale  $\tau_{\infty}$  for Riverside, CA.

The lines are the linear best fits to the data. For all sites, when the estimated values of  $\tau_{\infty}$  were short, the coincidence factors were high, and when they were long the coincidence factors were small. What are some of the implications of this finding?

*When do ammonium and nitrate have different size distributions?*

The estimated values of  $\tau_{\infty}$  shown in column 2 of Tables 1-5 are all less than about 15 min and values

greater than about 5 min correspond to the smallest coincidence factors. This 5 min value does not necessarily indicate when equilibrium may be expected to hold, since in estimating  $\tau_{\infty}$  an accommodation coefficient value of  $0.1 \mu\text{m}$  was assumed; the actual value may be 1 or 2 orders of magnitude larger depending on the effect of surface active organic compounds (Wexler and Seinfeld, 1990). Thus 5 min is likely to be the minimum value of  $\tau_{\infty}$  when lack of equilibrium is important, but it may be much longer.

Ammonium nitrate during SCAQS

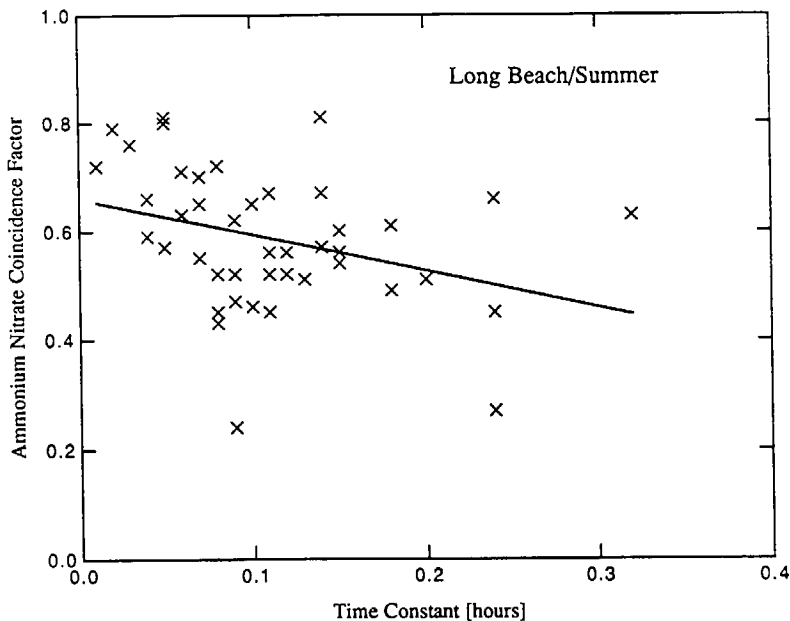


Fig. 3. The ammonium nitrate coincidence factor as a function of the equilibration time-scale  $\tau_{\infty}$  for Long Beach, CA in the summer.

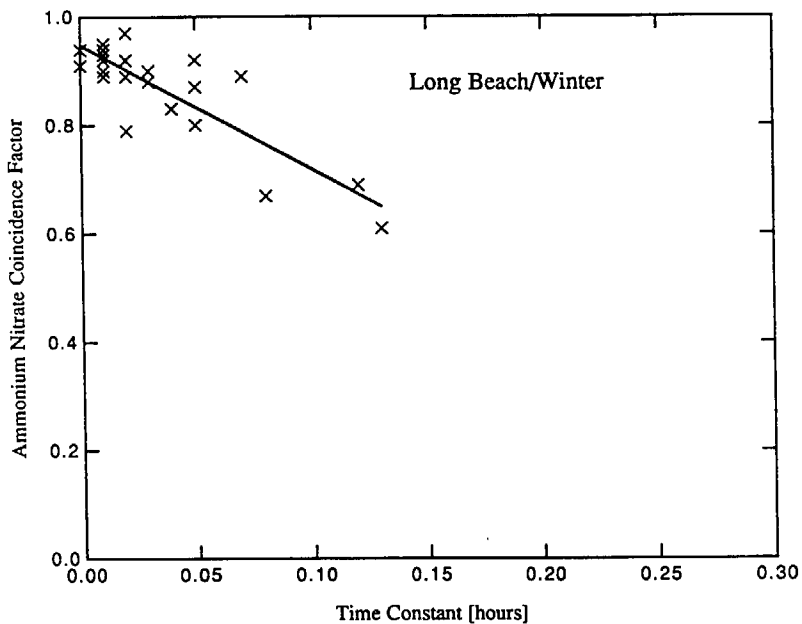


Fig. 4. The ammonium nitrate coincidence factor as a function of the equilibration time-scale  $\tau_{\infty}$  for Long Beach, CA in the winter.

Furthermore, the appropriate time-scales for equilibration of aerosol particles of different composition are  $\tau_{p,i}$ , not  $\tau_{\infty}$ . The time constant,  $\tau_{\infty}$ , governs equilibration due to changes in the ambient concentrations. The time constants  $\tau_{p,i}$  were not explicitly considered

here and govern equilibration due to changes in the ammonium nitrate particle-surface partial pressure product. Although equilibration between particles of different ammonium nitrate ratios occurs over times proportional to the  $\tau_{p,i}$ , these time constants can be

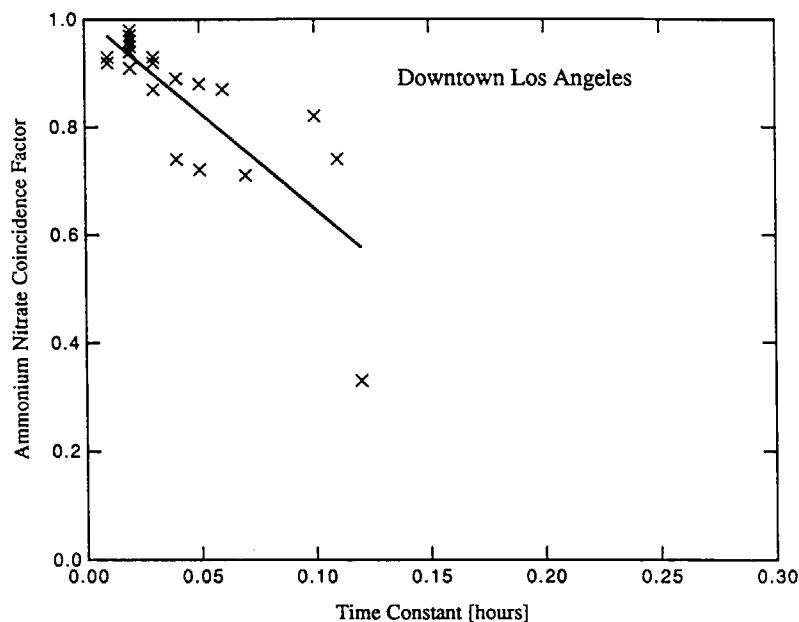


Fig. 5. The ammonium nitrate coincidence factor as a function of the equilibration time-scale  $\tau_{\infty}$  for downtown Los Angeles, CA.

related to  $\tau_{\infty}$  for an osmotically benign, monodisperse aerosol of uniform composition by

$$\tau_p \approx \frac{W}{K} \tau_{\infty}, \quad (13)$$

where  $W$  is the aerosol water content and  $K$  is the equilibrium constant between the gas and aqueous form of the components (Wexler and Seinfeld, 1990). Thus,  $\tau_{\infty}$  and  $\tau_p$  may vary in a similar fashion, but they are of different magnitudes.

We postulated (1) that under warm, heavily polluted conditions indicative of inland Los Angeles regions, the aerosol is more likely to be in equilibrium with the gas phase; and (2) that under cooler, less polluted conditions indicative of a more coastal Los Angeles climate, the aerosol is less likely to be in equilibrium with the gas phase (Wexler and Seinfeld, 1990). In the summer, the two inland locations, Riverside and Claremont, show a much higher coincidence factor than the coastal location, Long Beach, although there is not a significant difference between the coincidence factors at the winter sites, Long Beach and downtown Los Angeles. The inland locations were predicted to have shorter values of  $\tau_{\infty}$  since there the mean aerosol size is smaller and the aerosol mass loading is higher, both of which provide a larger surface for transport to and from the aerosol phase. The coastal locations were predicted to have longer  $\tau_{\infty}$  values because there the mean aerosol size is larger and the aerosol mass small, both of which lead to a smaller surface area for transport. The data appear to support these earlier postulates.

*Why do ammonium and nitrate have different size distributions?*

As we discussed earlier, ammonium and nitrate appear to reside in different size distributions under conditions of long equilibration time constants,  $\tau_{\infty}$ . The question now arises as to the physical mechanisms that are responsible for the appearance of these species in different size particles.

It has been proposed that the Kelvin effect may be an explanation for the observation that nitrate tends to appear in the larger particles and sulfate in the smaller particles under typical conditions in Los Angeles (Bassett and Seinfeld, 1984). We postulated that the Kelvin effect probably provides a minimal influence on the size distribution of ammonium nitrate (Wexler and Seinfeld, 1990). Under conditions when the  $\tau_{\infty}$  is short, the aerosols of various sizes and compositions are able to equilibrate with each other. If the Kelvin effect were significant, ammonium and nitric acid would preferably condense on larger particles, and the non-volatile sulfate would remain in smaller particles. But if the ionic components of the aerosol are primarily ammonium, nitrate, and sulfate then from Equation (11) we have

$$\frac{M_{a,i}}{M_{n,i}} \approx 1 + 2 \frac{M_{s,i}}{M_{n,i}} \quad (14)$$

and we see that the ratio  $M_{a,i}/M_{n,i}$  would be different for the large and small particles, and the observed coincidence factor would be small. What is observed though are high coincidence factors for short values of

$\tau_p$ , and thus the Kelvin effect does not appear to influence significantly the size distribution of ammonium nitrate in the atmosphere.

Another mechanism that may distribute ammonium and nitrate differently by size due to differences in the distribution of nitrate and sulfate is transport from the gas to aerosol phase. The single particle mass transport is given in Equation (2). Taking the ratio of this expression with itself for different size particles gives

$$\frac{J(R_{p,1})}{J(R_{p,2})} = \frac{R_{p,1}\alpha + Kn_2}{R_{p,2}\alpha + Kn_1} \quad (15)$$

Thus we see that the accommodation coefficient is the species-dependent quantity that may influence the size distribution of a condensing species. Since nitrate usually appears in larger particles, and sulfate in smaller particles this implies that the accommodation coefficient for nitric acid must be less than that for sulfuric acid. The accommodation coefficients of highly soluble species on pure water are typically close to unity. Under atmospheric conditions the accommodation coefficients are typically lower due to surface active organics (Gill *et al.*, 1983), and these surface active agents probably inhibit the accommodation of nitric and sulfuric acids to a similar degree. Thus different accommodation coefficients may explain the different distributions, but only if the sulfuric acid accommodation coefficient is significantly higher than that of nitric acid.

Another possible explanation for the different size distributions of nitrate and sulfate is heterogeneous sulfate formation, which has been proposed as a mechanism for sulfate formation in aqueous-phase particles (Hering and Friedlander, 1982). Most likely  $SO_2$  oxidation is reaction-limited in aerosol particles, that is, other physical processes such as transport and mixing are fast compared with the speed of the  $SO_2$  oxidation reaction (Schwartz, 1988), so heterogeneously formed sulfate should be size distributed proportional to the volume, or third, moment of the size distribution.

Sulfate and nitrate formed in the gas phase condense on aerosol particles according to Equation (2), so their distribution lies between the first and second moment of the aerosol size distribution, and we term this distribution the transport moment. Condensed sulfate or nitrate is size distributed according to the first moment for large particles with high accommodation coefficient and to the second moment for small particles, or particles with a low accommodation coefficient.

If heterogeneous sulfate formation is significant in the atmosphere, the sulfate should be present in the larger particles since its formation is proportional to the volume moment, and the nitrate should be present in the smaller particles since its formation is proportional to the transport moment (Hering and Friedlander, 1982; Seinfeld and Bassett, 1984). This is counter

to the observation that the nitrate is usually observed in the larger particles and the sulfate in the smaller, which does not preclude heterogeneous formation of sulfate, but does lead to the conclusion that any heterogeneous sulfate formation is sufficiently small that it does not appear to influence its size distribution with respect to nitrate.

The volatility of nitrate may also affect its size distribution with respect to sulfate. Since the vapor pressure of sulfate is negligible, any sulfuric acid formed in the gas phase indiscriminantly condenses in a distribution proportional to the transport moment, subsequently increasing particle pH. This increased pH tends to increase the vapor pressure of volatile nitric acid, driving it to condense in particles where the sulfate does not prefer to condense. Since the transport moment tends to favor condensation of sulfate on smaller particles, this is a possible explanation for the observed lack of coincidence of the nitrate and sulfate, and the presence of nitrate in the larger size particles.

Is the relation between time-scale and coincidence consistent with this proposal? Starting with a neutral-pH size-distributed aerosol, when the time-scales are long, gas-phase sulfuric and nitric acid initially condense on the particles according to the transport moment, but as the particle acidity increases the nitrate is effectively blocked from further condensation and instead tends to condense where the pH is higher. As the aerosol ages, the time-scales typically decrease due to larger atmospheric aerosol loading, which gives an opportunity for the larger particles rich in volatile nitrate to equilibrate with the smaller particles that are poor in nitrate.

Some of the wind trajectories in the Los Angeles basin carry pollutants over dairy feedlots that are large sources of ammonia. These ammonia rich masses eventually reach the Riverside area heavily laden with aerosol due to the high ammonia concentration. Since ammonia tends to neutralize aerosol pH, aerosols collected in Riverside should have a higher level of coincidence than Claremont, which is a site with similar meteorologic conditions, but without the large source of ammonia downwind. Figures 1 and 2 show the Claremont and Riverside data. Although the coincidence factors are higher for Riverside, the values of  $\tau_\infty$  are correspondingly smaller, such that the best fit lines have nearly the same slope and intercept. Thus, we cannot conclude from these data that sulfate condensing in smaller particles drives nitrate to the larger particles.

We have examined a number of possible mechanisms why sulfate appears in smaller particles and nitrate in larger ones. The data lead one to conclude that the Kelvin effect is not responsible, since under equilibrium conditions the size distributions tend to coincide. Aqueous-phase oxidation of sulfite does not seem to be the explanation since this process would lead to more sulfate in larger particles, counter to many observations including those during SCAQS.

Different accommodation coefficients for nitric and sulfuric acid may explain the distributions, but the accommodation coefficients of the two species must be significantly different to produce the observed distributions. Finally, acidification of aerosol particles due to sulfate condensation in smaller particles, may force the nitrate to condense in the larger and more neutral particles.

*Aerosol particles are not in equilibrium with each other*

It is clear from Figs 1–5 that the aerosol during SCAQS had a wide range of coincidence factors and that the degree of coincidence correlates with the estimated time constant  $\tau_{\infty}$ . The lack of coincidence between the ammonium and nitrate size distributions indicates that the surface partial pressures of ammonia and nitric acid are different for particles of different size, and that these particles are not in equilibrium with each other. Since there is a strong correlation between this lack of equilibrium and the estimated values of  $\tau_{\infty}$ , we can conclude that, as predicted in earlier work, transport limitations cause the lack of equilibrium (Wexler and Seinfeld, 1990).

What does this correlation between  $C_{an}$  and  $\tau_{\infty}$  say about equilibrium between the gas and aerosol phases? If the time constant for equilibration of the gas phase,  $\tau_{\infty}$ , is shorter than the time constants for equilibration of the aerosol phase,  $\tau_{p,i}$ , the gas-phase ammonium nitrate will tend to reach equilibrium with the aerosol before aerosol particles of different sizes equilibrate with each other. Once the gas phase has reached equilibrium with the aerosol phase, ammonium nitrate evaporates from particles with higher surface partial pressures and condenses on those with lower surface partial pressures. The gas phase acts as a conduit, passing ammonium nitrate among particles, while its ammonium nitrate concentration remains steady. Thus, even if aerosol particles are not in equilibrium with each other, the gas-phase concentration of ammonium nitrate may be in equilibrium with the transport-averaged aerosol surface partial pressures of ammonium nitrate, and therefore, the degree of equilibrium among aerosol particles does not indicate, one way or the other, equilibrium between the gas and aerosol phases.

**IMPLICATIONS FOR AEROSOL MODELING:  
EQUILIBRIUM OR NOT?**

The major hypothesis investigated in this work is that transport on a time-scale proportional to  $\tau_{\infty}$  limits equilibration between gas- and aerosol-phase ammonium nitrate. To investigate the validity of this hypothesis we showed that ammonium nitrate–ammonium sulfate aerosols must have a coincidence factor of unity for all the aerosol particles to be in mutual ammonium nitrate equilibrium, and that lower coincidence factors indicate departures from equilibrium. We demonstrated that a significant cor-

relation existed during SCAQS between the calculated coincidence factors and the estimated time constants. Thus we conclude that transport limitations are a significant factor in the observed departures from equilibrium, but because there is still substantial scatter in the data, we cannot conclude that transport limitations are the sole cause for these observed departures.

The analysis we have just performed has a number of implications regarding the development of atmospheric aerosol models. The first regards models designed to predict the total mass of particulate matter (e.g. Russell *et al.*, 1983, 1986, 1988). These models assume that (1) the volatile inorganic aerosol species are in equilibrium with their gas-phase counterparts, and (2) the gas-phase ammonia and nitric acid concentrations in equilibrium with the overall PM10 aerosol composition are the same as those in equilibrium with the full size distribution of particles. We have shown that a mixture of ammonium nitrate–ammonium sulfate aerosol particles has the same equilibrium surface partial pressures of ammonia and nitric acid as individual particles, so that modeling the total PM10 content of the aerosol yields the same equilibrium gas-phase concentrations of ammonium and nitric acid as would have been predicted by modeling the complete size distribution of the aerosol.

The second implication of this work concerns prediction of the size distribution of the volatile inorganic species. In previous work we showed that, even at equilibrium, transport between the gas and aerosol phases governs the size distribution of ammonium nitrate for solid particles of aqueous particles osmotically dominated by ammonium nitrate (Wexler and Seinfeld, 1990). In this work we demonstrate that during SCAQS different size particles were not in mutual equilibrium with respect to ammonium nitrate and that the lack of equilibrium correlates well with the magnitude of the time constant,  $\tau_{\infty}$ . Since a significant percentage of the samples showed departure from mutual equilibrium, a full transport and equilibrium representation of the aerosol must be employed to accurately predict the size distribution of the volatile inorganics.

*Acknowledgement*—This work was supported by the State of California Air Resources Board Agreement A932-054.

**REFERENCES**

- Allen A. G., Harrison R. M. and Erisman J. (1989) Field measurements of the dissociation of ammonium nitrate and ammonium chloride aerosols. *Atmospheric Environment* **23**, 1591–1599.
- Bassett M. and Seinfeld J. H. (1983) Atmospheric equilibrium model of sulfate and nitrate aerosols. *Atmospheric Environment* **17**, 2237–2252.
- Bassett M. E. and Seinfeld J. H. (1984) Atmospheric equilibrium model of sulfate and nitrate aerosols—II. Particle size analysis. *Atmospheric Environment* **18**, 1163–1170.

- Cadle S. H., Countess R. J. and Kelly N. A. (1982) Nitric acid and ammonia in urban and rural locations. *Atmospheric Environment* **16**, 2501–2506.
- Chan M. and Durkee K. (1989) Southern California Air Quality Study B-site operations. California Air Resources Board A5-196-32.
- Cohen M. D., Flagan R. C. and Seinfeld J. H. (1987) Studies of concentrated electrolyte solutions using the electrodynamic balance. 2. Water activities for mixed-electrolyte solutions. *J. phys. Chem.* **91**, 4575–4582.
- Doyle G. J., Tuazon E. C., Graham R. A., Mischke T. M., Winer A. M. and Pitts J. N. (1979) Simultaneous concentrations of ammonia and nitric acid in a polluted atmosphere and their equilibrium relationship to particulate ammonium nitrate. *Envir. Sci. Technol.* **13**, 1416–1419.
- Eldering A., Solomon P. A., Salmon L. G., Fall T. and Cass G. R. (1991) Hydrochloric acid: a regional perspective on concentrations and formation in the atmosphere of southern California. *Atmospheric Environment* **25A**, 2091–2102.
- Fitz D. and Zwicker J. (1988) Design and testing of the SCAQS sampler for the SCAQS study, 1987. California Air Resources Board A6-077-32.
- Gill P. S., Graedel T. E. and Weschler C. J. (1983) Organic films on atmospheric aerosol particles, fog droplets, cloud droplets, raindrops, and snowflakes. *Rev. Geophys. Space Phys.* **21**, 903–920.
- Gray H. A., Cass G. R., Huntziger J. J., Heyerdahl E. K. and Rau J. A. (1986) Characteristics of atmospheric organic and elemental carbon particle concentrations in Los Angeles. *Envir. Sci. Technol.* **20**, 580–589.
- Grosjean D. (1982) The stability of particulate nitrate in the Los Angeles atmosphere. *Sci. Total Envir.* **25**, 263–275.
- Hanel G. and Zankl B. (1979) Aerosol size and relative humidity: water uptake by mixtures of salts. *Tellus* **31**, 478–486.
- Harrison R. M. and MacKenzie A. R. (1990) A numerical simulation of kinetic constraints upon achievement of the ammonium nitrate dissociation equilibrium in the troposphere. *Atmospheric Environment* **24A**, 91–102.
- Hering S. V. and Friedlander S. K. (1982) Origins of aerosol sulfur size distributions in the Los Angeles basin. *Atmospheric Environment* **16**, 2647–2656.
- Hering S. V. and Blumenthal D. L. (1989) Southern California Air Quality Study (SCAQS) description of measurement activities, final report. California Air Resources Board A5-157-32.
- Hildemann L. M., Russell A. G. and Cass G. R. (1984) Ammonia and nitric acid concentrations in equilibrium with atmospheric aerosols: experiment vs theory. *Atmospheric Environment* **18**, 1737–1750.
- John W., Wall S. M., Ondo J. L. and Winklmayr W. (1989a) Acidic size distributions during SCAQS. California Air Resources Board A6-112-32.
- John W., Wall S. M., Ondo J. L. and Winklmayr W. (1989b) Acidic aerosol size distributions during SCAQS. Compilation of data tables and graphs. California Air Resources Board A6-112-32.
- John W., Wall S. M., Ondo J. L. and Winklmayr W. (1990) Modes in the size distributions of atmospheric inorganic aerosol. *Atmospheric Environment* **24A**, 2349–2359.
- Lawson D. R. (1990) The Southern California Air Quality Study. *J. Air Waste Mngmt Ass.* **40**, 156–165.
- McMurry P. H. and Stolzenburg M. R. (1989) On the sensitivity of particle size to relative humidity for Los Angeles aerosols. *Atmospheric Environment* **23**, 497–507.
- Pilinis C. and Seinfeld J. H. (1987) Continued development of a general equilibrium model for inorganic multicomponent atmospheric aerosols. *Atmospheric Environment* **21**, 2453–2466.
- Pilinis C., Seinfeld J. H. and Seigneur C. (1987) Mathematical modeling of the dynamics of multicomponent atmospheric aerosols. *Atmospheric Environment* **21**, 943–955.
- Pilinis C. and Seinfeld J. H. (1988) Development and evaluation of an Eulerian photochemical gas-aerosol model. *Atmospheric Environment* **22**, 1985–2001.
- Russell A. G., McRae G. J. and Cass G. R. (1983) Mathematical modeling of the formation and transport of ammonium nitrate aerosol. *Atmospheric Environment* **17**, 949–964.
- Russell A. G. and Cass G. R. (1986) Verification of a mathematical model for aerosol nitrate and nitric acid formation and its use for control measure evaluation. *Atmospheric Environment* **20**, 2011–2025.
- Russell A. G., McCue K. F. and Cass G. R. (1988) Mathematical modeling of the formation of nitrogen-containing air pollutants. 1. Evaluation of an Eulerian photochemical model. *Envir. Sci. Technol.* **22**, 263–271.
- Saxena P., Seigneur C. and Peterson T. W. (1983) Modeling of multiphase atmospheric aerosols. *Atmospheric Environment* **17**, 1315–1329.
- Saxena P., Hudischewskyj A. B., Seigneur C. and Seinfeld J. H. (1986) A comparative study of equilibrium approaches to the chemical characterization of secondary aerosols. *Atmospheric Environment* **20**, 1471–1483.
- Schwartz S. E. (1988) Mass-transport limitation to the rate of in-cloud oxidation of SO<sub>2</sub>: re-examination in the light of new data. *Atmospheric Environment* **22**, 2491–2499.
- Stelson A. W., Friedlander S. K. and Seinfeld J. H. (1979) A note of the equilibrium relationship between ammonia and nitric acid and particulate ammonium nitrate. *Atmospheric Environment* **13**, 369–371.
- Stokes R. H. and Robinson R. A. (1966) Interactions in aqueous nonelectrolyte solutions. I. Solute-solvent equilibria. *J. phys. Chem.* **70**, 2126–2130.
- Tanner R. L. (1982) An ambient experimental study of phase equilibrium in the atmospheric system: aerosol H<sup>+</sup>, NH<sub>4</sub><sup>+</sup>, SO<sub>4</sub><sup>2-</sup>, NO<sub>3</sub><sup>-</sup> - NH<sub>3</sub>(g), HNO<sub>3</sub>(g). *Atmospheric Environment* **16**, 2935–2942.
- Wall S. M., John W. and Ondo J. L. (1988) Measurement of aerosol size distributions for nitrate and major ionic species. *Atmospheric Environment* **22**, 1649–1656.
- Wexler A. S. and Seinfeld J. H. (1990) The distribution of ammonium salts among a size and composition dispersed aerosol. *Atmospheric Environment* **24A**, 1231–1246.
- Wexler A. S. and Seinfeld J. H. (1991) Second-generation inorganic aerosol model. *Atmospheric Environment* **25A**, 2731–2748.
- Zdanovskii A. B. (1948) New methods of calculating solubilities of electrolytes in multicomponent systems. *Zhur. Fiz. Khim.* **22**, 1475–1485.